Available online at www.sciencedirect.com
ScienceDirect
BBRC
ELSEVIER
Biochemical and Biophysical Research Communications 351 (2006) 540–546
www.elsevier.com/locate/ybbrc

A ubiquitin E3 ligase Efp is up-regulated by interferons and conjugated with ISG15

Norie Nakasato [a,b], Kazuhiro Ikeda [a], Tomohiko Urano [a,c], Kuniko Horie-Inoue [a], Satoru Takeda [b], Satoshi Inoue [a,c,*]

[a] Division of Gene Regulation and Signal Transduction, Research Center for Genomic Medicine, Saitama Medical University, Saitama, Japan
[b] Department of Obstetrics and Gynecology, Saitama Medical Center, Saitama Medical University, Saitama, Japan
[c] Department of Geriatric Medicine, Graduate School of Medicine, The University of Tokyo, Tokyo, Japan

Received 11 October 2006
Available online 18 October 2006

Abstract

Interferon (IFN) regulates various target genes that mediate important roles in immune responses such as antiviral state. Protein ISG15-conjugation (ISGylation) is implicated in the IFN-induced antiviral response. Here we demonstrate that Efp mRNA as well as protein expression could be up-regulated by Type I IFN in HeLa cells and HepG2 cells. Luciferase assay reveals that the first intron of Efp gene contains a functional interferon-stimulated response element (ISRE) and electrophoretic mobility shift assay shows that the ISRE binds to signal transducer and activator of transcription 1 (STAT1). Chromatin immunoprecipitation assays have shown that the ISRE recruits STAT1 *in vivo* IFN-dependently. Moreover, we demonstrate that Efp protein could be conjugated with not only ubiquitin but also ISG15. These data suggest that Efp is an IFN-responsive gene that potentially mediates IFN actions, involved in ISGylation and ubiquitination of proteins including Efp itself.
© 2006 Elsevier Inc. All rights reserved.

Keywords: Estrogen-responsive finger protein (Efp); Interferon; ISG15; Interferon-stimulated response element (ISRE); Signal transducer and activator of transcription 1 (STAT1)

Interferons (IFNs) have an important role in immune system to defend against viral infections. Type I IFN (IFN-α and -β) is produced by virus infected cells and then binds to receptors on the cell surface to activate a transcription factor complex, interferon-stimulated gene factor-3 (ISGF3), which is composed of signal transducer and activator of transcription 1 (STAT1), STAT2, and interferon regulatory factor 9 (IRF9) [1]. ISGF3 binds to IFN-stimulated response elements (ISREs) and induces expression of various target genes that function in antiviral state [2].

The interferon-stimulated gene 15 (ISG15) has been originally identified as type I IFN-stimulated gene encoding a 15-kDa protein [3]. ISG15 protein contains two conserved ubiquitin-like domains and is conjugated to target proteins, or ISGylated together with E1, E2, and E3 enzymes through the system similar to ubiquitination [4]. Based on the findings that ISG15 expression and protein ISGylation were highly induced upon viral infection [5,6], the ISGylation system is considered as a novel pathway that transduces the antiviral response in IFN-stimulated cells. Indeed, it was reported that ISG15 can inhibit release of human immunodeficiency virus type 1 (HIV-1) virions [7] and attenuate Sindbis virus infection [8]. However, since ISG15 knockout mice showed that ISG15 had no effect on infection of certain viruses [9], the precise mechanism and regulation of ISGylation remains to be resolved.

We previously identified and demonstrated that estrogen-responsive finger protein Efp is an ubiquitin E3 ligase that ubiquitinates the 14-3-3σ protein, a negative regulator of the cell cycle progression [10,11]. Recently, Efp has been found as an ISG15 E3 ligase [12]. Efp belongs to the protein

* Corresponding author. Fax: +81 42 985 7209.
E-mail address: INOUE-GER@h.u-tokyo.ac.jp (S. Inoue).

0006-291X/$ - see front matter © 2006 Elsevier Inc. All rights reserved.
doi:10.1016/j.bbrc.2006.10.061

family of tripartite motif (TRIM), which is composed of RING, B-box, and coiled coil domains. Recent evidence suggests that TRIM family proteins have antiviral properties. TRIM19/promyelocytic leukemia (PML), which has been identified as a fusion protein with retinoic acid receptor α (RARα) in promyelocytic leukemia, is well documented to have a potential role against virus infections [13,14]. TRIM5 is a host cell factor responsible for the antiretroviral activities, previously described as Lv1 and Ref1 [15,16]. Taken together, these findings lead us to the notion that the TRIM family represents a new and widespread class of antiviral proteins involved in innate immunity [17].

Here we demonstrate that Efp expression is enhanced by IFNs. Luciferase assay reveals that Efp promoter/enhancer is activated by IFNs through a functional ISRE that is located in the first intron. This ISRE binds with one of the ISGF3 components STAT1 *in vitro* and recruits STAT1 *in vivo* IFN-dependently. Moreover, we have shown that Efp could be conjugated with not only ubiquitin, but also ISG15.

Materials and methods

Cell culture. HeLa, HepG2, and 293T cells were purchased from American Type Culture Collection (Manassas, VA). Cells were maintained in Dulbecco's modified Eagle's medium (DMEM) supplemented with 10% fetal calf serum (FCS) at 37 °C in 5% CO_2 and a humidified atmosphere.

Quantitative PCR. HeLa cells and HepG2 cells were treated with 500 U/ml IFN-α, IFN-β, IFN-γ (PeproTech EC) or vehicle (PBS) for 6 and 24 h in the presence or absence of cycloheximide (CHX) (1 μg/ml) (Nacalai Tesque, Kyoto, JAPAN). Real-time quantitative RT-PCR (qPCR) was performed as described previously [18], using 36B4 for normalization. The sequences of primers are as follows: Efp forward primer, 5′-GTGACCACGGCTTTGTCATCT-3′; Efp reverse primer, 5′-TAAAGTCCACCCTGAACTTATACATCAG-3′; ISG15 forward primer, 5′-TGGCGGGCAACGAATT-3′; ISG15 reverse primer, 5′-GGGTGATCTGCGCCTTCA-3′; UBE1L forward primer, 5′-TGATGTTTGAGAAGGATGATGACA-3′; UBE1L reverse primer, 5′-CCGGTGGAATCCCGTAGTT-3′; UBCH8 forward primer, 5′-GGAACCTGTCCAGCGATGAT-3′; UBCH8 reverse primer, 5′-TCAGGTGGTAGGGAGGTTGGT-3′; 36B4 forward primer, 5′-CCACGCTGCTGAACATGCT-3′; 36B4 reverse primer, 5′-GATGCTGCCATTGTCGAACA-3′.

Cloning of promoter region of Efp gene containing ISRE, luciferase assay, and chloramphenicol acetyl transferase (CAT) assay. An 1559 bp length of a putative ISRE-containing genomic DNA fragment (−173 to +1386 bp, where the translation initiation site stands for nucleotide +1) [19] and its 1415 bp deletion mutant lacking the ISRE sequence were amplified by PCR and cloned into pGL3-basic vector (Efp-Luc and EfpΔISRE-Luc), respectively. Luciferase assay was performed using HeLa cells transfected with 0.1 μg of each luciferase reporter together with 0.02 μg pRL-TK (Promega) as described previously [20]. Twelve hours after transfection, cells were treated with 500 U/ml IFN-β or vehicle for 24 h and luciferase activities were determined. Data are expressed as means ± SD of three independent experiments performed in triplicate. CAT assay was performed in HeLa cells treated with 500 U/ml IFN-β or vehicle, using reporter plasmids, pCAThe-173 and pCAThe-1625, as previously described [19].

Electrophoretic mobility shift assay (EMSA). EMSA was performed as described previously [19]. Nuclear extract from HeLa cells treated with IFN-β for 24 h was prepared using NP-40 lysis buffer. Annealed oligonucleotides 5′-GATTTAGTTTCATTTTACTGTTGA-3′ corresponding to the ISRE in Efp intron 1 were labeled using [γ-^{32}P]ATP (Amersham Biosciences) using a MEGA label kit (Takara Bio, Tokyo, JAPAN). Ten micrograms of nuclear protein, a ^{32}P-labeled double-stranded probe (20,000 counts/min), and 3 μl of 5× binding buffer [19] were mixed in a total volume of 15 μl. In competition assays, 10-fold or 50-fold amounts of unlabeled oligonucleotides of ISRE or mutated ISRE (GATTTAGTGGAATTTTACTGTTGA) were added simultaneously to the radio-labeled probe. For neutralization experiments, anti-human STAT1 antibody (E-23, Santa Cruz Biotechnology) or non-immune IgG was incubated with the nuclear extracts for 20 min before the addition of the probes.

Western blotting. Western blotting was performed as described previously [20]. Lysates from HeLa cells and HepG2 cells treated with 500 U/ml IFN-α, IFN-β or IFN-γ for 24 or 36 h were resolved by 10% denaturing SDS–polyacrylamide gel electrophoresis. Blotted membranes were incubated with Efp antibody [11], followed by a reaction with anti-rabbit Ig (Amersham Biosciences) and the enhanced chemiluminescence system (Amersham Biosciences).

Chromatin immunoprecipitation assay (ChIP). ChIP assay was performed as described previously [18]. HeLa cells were treated with 500 U/ml IFN-β or vehicle for 24 h. Lysates corresponding to 2×10^7 cells were incubated with 2 μg of anti-STAT1 antibody (E-23, Santa Cruz Biotechnology) or acetylated histone H3 (Upstate). Precipitated DNA fragments were quantified by quantitative real-time PCR. The sequences of ISRE and GAPDH primers are as follows: ISRE forward primer, 5′-TCCCTCACGAAGTCCTGGTGGCA-3′, ISRE reverse primer, 5′-AGGTCAGGCTAAGTTCATTTCTC-3′, GAPDH forward primer, 5′-GGTGGTCTCCTCTGACTTCAACA-3′, GAPDH reverse primer, 5′-GTGGTCGTTGAGGGCAATG-3′. Fold enrichment of STAT1 or acetylated H3 in IFN-β-treated cells was quantified by $\Delta\Delta C_T$ method [18].

Immunoprecipitation. cDNAs of human ISG15, ubiquitin, and Efp were amplified by PCR with specific primers and subcloned into pcDNA3 (Invitrogen) or pCI-NEO (Promega) to generate mammalian expression plasmids. To analyze ISGylation and ubiquitination of Efp protein, 293T cells were transiently transfected with S-tagged Efp together with FLAG-tagged ubiquitin or ISG15. After cultured for 48 h, cells were lysed in 1% Triton X-100 buffer (50 mM Hepes, 150 mM NaCl, 10% glycerol, 1% Triton X-100, 1.5 mM $MgCl_2$, 1 mM EGTA, 100 mM NaF, 10 μg/ml aprotinin, 10 μg/ml leupeptin, and 1 mM phenylmethylsulfonyl fluoride). For immunoprecipitation, cell lysate was mixed with anti-FLAG M2 affinity gel (Sigma) and FLAG-tagged proteins were eluted with 3× FLAG peptide after washing. The elutant was immunodetected by anti-S monoclonal antibody (Novagen).

Results

Induction of Efp mRNA and protein by IFNs

To examine whether Efp expression is modulated by IFNs, HeLa, and HepG2 cells were treated with IFNs or vehicle and Efp mRNA expression was quantified using qPCR (Fig. 1A). The results showed that type I IFN (IFN-α and -β) up-regulated Efp mRNA levels by 4- to 8-fold over vehicle treatment after 6 and 24 h in HeLa cells whereas type II IFN (IFN-γ) did not. Similarly, Efp mRNA was induced by type I IFN but not by IFN-γ in HepG2 cells. These IFN-induced mRNA expression could also be observed by the addition of cycloheximide, indicating that IFN could up-regulate Efp mRNA expression independent of *de novo* protein synthesis. Next, we assessed endogenous Efp protein expression in HeLa and HepG2 cells by Western blot analysis. The up-regulation of Efp protein was observed at 24 and 36 h after treatment with IFN-α and β in both HeLa and HepG2 cells (Fig. 1B), consistent with the IFN-induced expression of Efp mRNA.

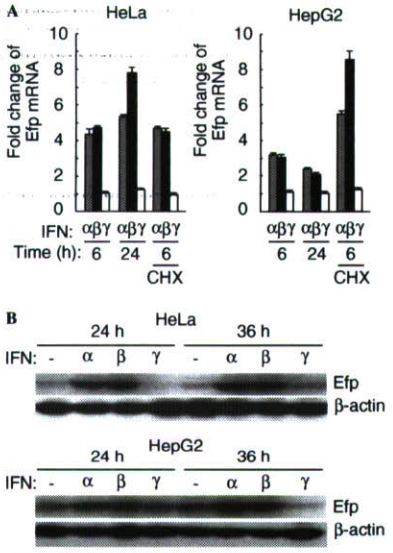

Fig. 1. IFN-induced expression of Efp. (A) IFN-induced expression of Efp mRNA. HeLa and HepG2 cells were treated with the indicated IFNs (500 U/ml each) or the vehicle (PBS) for the indicated times in the presence or the absence of cycloheximide (1 μg/ml). Real-time quantitative PCR (qPCR) was performed using cDNAs generated from total RNA. Experiments were repeated three times and the results are represented as means ± SD. (B) IFN-induced expression of Efp protein. HeLa cells and HepG2 cells were treated with IFNs or vehicle for 24 and 36 h. Cell lysates were immunodetected by anti-Efp antibody [11].

Functional ISRE in the first intron of human Efp gene

It is known that type I IFN stimulates gene transcription through IFN-stimulated response elements (ISRE, Fig. 2A) [21]. Computational analysis was performed to search for ISREs in the Efp gene locus and its 5-kb upstream or downstream regions. Only one putative ISRE sequence was found in the first intron of the gene (Fig. 2A). We have previously shown that the 5′-flanking region of the Efp gene had a basal transcriptional promoter activity; this 5′-region of Efp contains an E-box element that could bind USF-1 at positions −110 to −105 bp, and another positive regulatory region containing two GC-boxes locates just upstream to the E-box [19]. We checked IFN responsiveness of two CAT reporter constructs pCAThe-173 and pCAThe-1625, which possesses the basal promoter region and 1625-bp 5′-flanking region of Efp gene, respectively. IFN-β treatment scarcely changed the transcription activities of pCAThe-173 and pCAThe-1625 compared with vehicle treatment (1.06 ± 0.10- and 1.12 ± 0.19-fold, respectively). These results suggest that this 5′-upstream region without the ISRE sequence could not respond to IFN-β. Then, we generated two luciferase reporter plasmids, Efp-Luc and EfpΔISRE-Luc. Efp-Luc contained the 1559-bp genomic DNA fragment of Efp gene at positions −173 to +1386 bp, while EfpΔISRE-Luc included a 1415-bp fragment lacking the ISRE sequence from Efp-Luc (Fig. 2B). Luciferase activity of Efp-Luc but not EfpΔISRE-Luc in HeLa cells was increased by INF-β treatment. The IFN responsiveness of the ISRE sequence was further examined using SV40 promoter-driven luciferase vectors containing the intact ISRE or its mutated sequence (Fig. 2C). Our data indicate that this bioinformatically identified ISRE is indeed functional and would contribute to the IFN responsiveness of human Efp promoter in HeLa cells.

STAT1 binds to the ISRE of Efp intron 1

To examine the possible trans-acting factors that bind to the ISRE, we performed electrophoretic mobility shift assay. Nuclear extracts of HeLa cells treated with or without IFN-β were incubated with a ^{32}P-labeled ISRE oligonucleotide in the presence or absence of competitive oligonucleotides (Fig. 3A). A single DNA–protein complex was detected and the amount of this complex was clearly increased when the cells were stimulated with IFN-β. The DNA–protein interaction was competed by a 10- and 50-fold excess of unlabeled ISRE oligonucleotide over the radiolabeled probe, whereas no competition of DNA–protein binding was observed by the addition of the mutated ISRE oligonucleotide. Since it is known that type I IFN activates STAT1 and STAT2, which are components of the ISRE-recognizing ISGF3 complex [2], we investigated whether STAT1 modulates the signal of DNA–protein complex (Fig. 3B). The addition of anti-STAT1 antibody to IFN-treated nuclear extracts diminished the signals of DNA–protein complex in a dose-dependent manner. Because control IgG treatment had no effect on the complex signal, the data indicate that STAT1 would play a role in the complex formation that binds to the ISRE in Efp intron 1. Next, to examine *in vivo* binding of STAT1 to the ISRE of Efp intron 1, we performed ChIP assays using specific antibodies against STAT1 or acetylated histone H3 (acH3) in HeLa cells treated with IFN-β or vehicle (Fig. 3C). The result showed that IFN-β increased STAT1 recruitment on this ISRE by approximately 6-fold compared to vehicle. It is also notable that acH3 was enriched at the ISRE after IFN-β treatment, suggesting that IFN-β may accelerate chromatin acetylation around this locus. These results indicate that STAT1 is an IFN-responsive trans-acting factor of ISRE in Efp intron 1.

Efp protein modification mediated by IFN-induced ISGylation components

Next, we studied the regulation of ISGylation components, ISG15, UBE1L (E1 enzyme), and UBCH8 (E2 enzyme) in HeLa cells. These expressions were measured by qPCR using cDNAs from HeLa cells treated with either

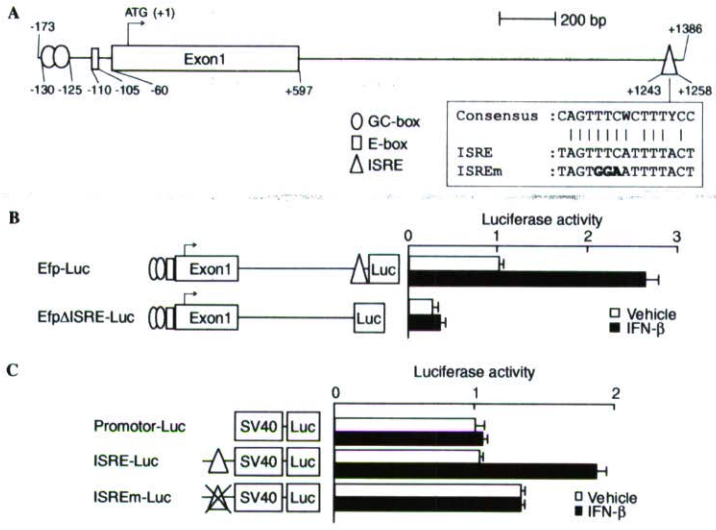

Fig. 2. Functional IFN-stimulated response element (ISRE) in human Efp intron 1. (A) Schematic representation of 5′-flanking region, exon 1, and intron 1 of human Efp gene, and comparison of ISRE sequences with consensus element. E-box, GC-box [19], and ISRE sequences are shown by the box, circles, and a triangle on the map, respectively. In consensus ISRE sequences, W and Y stand for A/T and C/T, respectively. (B,C) Promoter analysis of human Efp gene. The structures of the Efp-promoter luciferase reporter of plasmids are shown schematically (left) and their relative luciferase activities are shown to the right of each construct. The cross represents the mutation in ISRE (ISREm). HeLa cells were plated at a density of 1×10^4 cells per well on 24-well plates and transfected with 0.1 μg of Efp-Luc, EfpΔISRE-Luc, Promoter-Luc, ISRE-Luc or ISREm-Luc together with 0.02 μg of pRL-TK. Plasmids in (C) were generated using a luciferase reporter vector containing a SV40 promoter. Cells were treated with 500 U/ml IFN-β or vehicle for 24 h, and luciferase assay was performed. Data are expressed as means ± SD of three independent experiments performed in triplicate.

IFNs or vehicle for 6 and 24 h (Fig. 4A). ISG15 was only responsive to type I IFN, whereas UBE1L and UBCH8 were markedly induced by both type I and type II IFNs in HeLa cells. Together with the results of Efp (Fig. 1A) that is assumed as an E3 ligase for ISGylation [12], the expression of ISGylation components could be up-regulated by type I IFN, and to a lesser extent by type II IFN. Then, we analyzed Efp protein modification with ISG15 and ubiquitin as E3 ligases, which often exhibit self-conjugation [22,23]. As shown in Fig. 4B, a broad signal with smeared, retarded migration corresponding to poly-ubiquitinated Efp was detected. In addition, a band consistent with the molecular weight of Efp conjugated with a single ISG15 molecule was detected. These results suggest that Efp is an E3 ligase for both ISGylation and ubiquitination, which also exerts its own protein modification.

Discussion

In the present study, we demonstrated that IFN stimulates Efp mRNA and protein expression in human culture cells. Promoter analysis revealed that an ISRE located in the first intron activated the Efp transcriptional activity in an IFN-dependent manner. *In vitro* and *in vivo* binding of STAT1 to this intronic ISRE was shown by EMSA and ChIP analysis, respectively, in an IFN-dependent manner. These results strongly suggest that Efp expression is transcriptionally regulated by STAT1, which could be activated by IFN stimulation. We have previously revealed that the proximal promoter of Efp is activated by estrogen receptor that binds to the estrogen-responsive element in 3′-untranslated region [19,24]. Thus, the gene regulatory region of Efp is capable of responding to both IFN and estrogen stimuli.

Efp is a member of TRIM family proteins which are particularly implicated in antiviral responses [17]. For example, TRIM19/PML has been considered to be involved in resistance to virus infections such as HIV, vesicular stomatitis virus, and influenza A virus [13,14]. Staf50/TRIM22 down-regulates HIV-1 long-terminal repeat-directed transcription, indicating that TRIM22 may have a negative effect on HIV replication cycle [25]. Moreover, TRIM5 proteins from rhesus and African green monkey restrict HIV-1 replication at an early step in reverse transcription prior to nuclear import [16]. Human, rhesus, and African green monkey TRIM5 has been shown to restrict N-tropic murine leukemia virus (N-MLV) [15]. Among these TRIMs, IFN-regulated expression of TRIM5, TRIM19, and TRIM22 has been shown [13,20,25]. Some other TRIMs including TRIM21/SSA1,

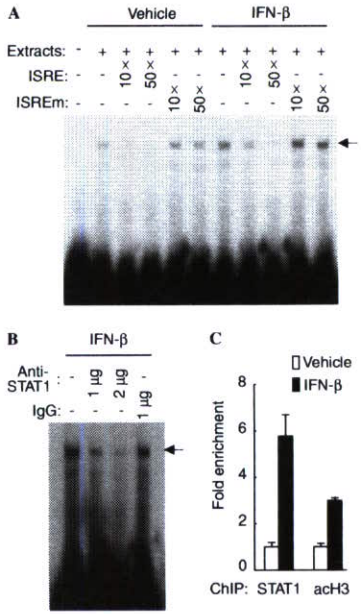

Fig. 3. Recruitment of STAT1 onto the intronic ISRE of human Efp gene. (A) EMSA of the ISRE sequence of Efp gene. ^{32}P-labeled ISRE oligonucleotides were incubated with 5 μg of HeLa cell nuclear extracts treated with or without 500 U/ml IFN-β for 24 h. A 10- or 50-fold excess of unlabeled ISRE/ISREm oligonucleotides was added for competition. (B) Antibody interference with the complex bound to the ISRE oligonucleotide. Anti-STAT1 antibody or non-immune IgG was used in the EMSA prior to addition of ^{32}P-labeled ISRE. Arrows in panels A and B indicate the identical protein–DNA complex containing STAT1. (C) ChIP assay was performed using HeLa cells treated with 500 U/ml IFN-β or vehicle for 24 h using STAT1 or acetylated histone H3 specific antibodies. Protein-crosslinked genomic DNAs were isolated from the cells, and ChIP-enriched or control input DNAs were used as templates for quantitative PCR specific for the ISRE sequence of Efp intron 1 or the coding region of GAPDH as a negative control. Results were normalized by input DNAs and are represented as fold enrichment in IFN-β-treated cells relative to the values in vehicle-treated cells.

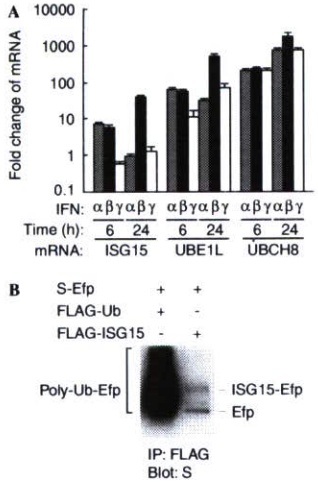

Fig. 4. ISG15-conjugation of Efp protein by IFN-induced ISGylation components. (A) IFN-induced mRNA expression of ISG15, UBE1L (E1), and UBCH8 (E2). HeLa cells were treated with the indicated IFNs (500 U/ml each) or the vehicle for 6 or 24 h. qPCR was performed using cDNAs generated from total RNA. Experiments were repeated three times and the results are represented as means ± SD. (B) ISGylation and ubiquitination of Efp protein. 293T cell extracts transiently transfected with Flag-tagged Efp (Flag-Efp), Flag-tagged ubiquitin (Flag-Ub), and Flag-tagged ISG15 (Flag-ISG15) were subjected to immunoprecipitation with anti-Flag antibody and, subsequently, to Western blot analysis probed with anti-S antibody. Signals for poly-Ub-Efp, ISG15-Efp, and Efp are indicated.

TRIM6/long-formed IFP, and TRIM34/short-formed IFP were also found to be regulated by IFNs [26]. Thus, the TRIM family may play a widespread and evolutionarily conserved role in innate immunity against viral infection.

Coimmunoprecipitation experiments showed that Efp protein could be modulated by both ISG15 and ubiquitin, suggesting that Efp might function as an E3 ligase for self-ISGylation and self-ubiquitination. Dual E3 ligase activities of Efp in ISG15- and ubiquitin-conjugation have been recently revealed [11,12]. ISGylation is carried out through sequential enzyme reactions resembling ubiquitination. Regarding ISGylation, E1 (UBE1L), E2 (UBCH8 and UBCH6), and E3 (Herc5 and Efp) enzymes are identified so far [4,27–30]. We also showed that other ISGylation components including ISG15, UBE1L (E1), and UBCH8 (E2) were among the IFN response genes in HeLa cells, in consistency with recent evidence [31,32]. With regard to the interaction between ISGylation and ubiquitination, there are reports that ISGylation competes with ubiquitination. For example, ISGylation of UBC13 disrupts its ability to form thioester bond with ubiquitin [33], and ISG15 conjugation to UBCH6 and UBCH8 suppresses their ubiquitin E2 enzyme activities [27,28]. Such interference is a possible mechanism for the inhibition of HIV-1 virion release because IFN-induced ISG15 inhibits the ubiquitination of HIV-1 Gag and vacuolar protein-sorting protein Tsg101 and disrupts the interaction between them [7]. Moreover, ISG15 expression may protect mice from Sindbis virus infection through an unclear mechanism [8]. It is tempting to speculate that IFN-stimulated Efp could modulate protein ISGylation and ubiquitination contributing together to antiviral response.

In addition, ISG15 may play a role in reproduction system since expression of ISG15 and ISG15-conjugated proteins are found in uterus during pregnancy and ISG15 expression is induced by type I IFN-τ secreted from conceptus in ruminants [34,35]. Elevation of ISG15 expression is also detected in some tumors where an antagonistic role of ISG15 is suggested in regulating the ubiquitin-mediated protein turnover [36]. Efp is expressed predominantly in reproductive tissues and is demonstrated to be necessary for estrogen-dependent growth in uterus [37,38]. Furthermore, Efp is up-regulated in some breast cancer tissues [24,39] and plays a crucial role in tumor growth where the ubiquitin E3 ligase activity of Efp is involved in the ubiquitin–proteasomal degradation of 14-3-3σ protein [11]. Thus, Efp may modulate target protein functions as a dual ISG15 and ubiquitin E3 ligase to mediate integrated signals between IFN and estrogen in reproductive tissues and cancer.

Acknowledgments

We thank T. Hishinuma and K. Chida for their technical assistance. This work was supported in part by Grants-in-Aid from the Ministry of Health, Labor and Welfare; from the Japan Society for the Promotion of Science; from The Promotion and Mutual Aid Corporation for Private Schools of Japan. This work was supported in part by grants of the Genome Network Project and the DECODE from the Ministry of Education, Culture, Sports, Science and Technology of Japan.

References

[1] C.M. Horvath, G.R. Stark, I.M. Kerr, J.E. Darnell Jr., Interactions between STAT and non-STAT proteins in the interferon-stimulated gene factor 3 transcription complex, Mol. Cell. Biol. 16 (1996) 6957–6964.
[2] T. Decker, S. Stockinger, M. Karaghiosoff, M. Müller, P. Kovarik, IFNs and STATs in innate immunity to microorganisms, J. Clin. Invest. 109 (2002) 1271–1277.
[3] D.C. Blomstrom, D. Fahey, R. Kutny, B.D. Korant, E. Knight Jr., Molecular characterization of the IFN-induced 15-kDa protein: molecular cloning and nucleotide and amino acid sequence, J. Biol. Chem. 261 (1986) 8811–8816.
[4] O. Staub, Ubiquitylation and isgylation: overlapping enzymatic cascades do the job, Sci. STKE 10 (2004) 43.
[5] K.R. Loeb, A.L. Haas, The interferon-inducible 15-kDa ubiquitin homolog conjugates to intracellular proteins, J. Biol. Chem. 267 (1992) 7806–7813.
[6] K.J. Ritchie, C.S. Hahn, K.I. Kim, M. Yan, D. Rosario, L. Li, J.C. de la Torre, D.E. Zhang, Role of ISG15 protease UBP43 (USP18) in innate immunity to viral infection, Nat. Med. 10 (2004) 1374–1378.
[7] A. Okumura, G. Lu, I. Pitha-Rowe, P.M. Pitha, Innate antiviral response targets HIV-1 release by the induction of ubiquitin-like protein ISG15, Proc. Natl. Acad. Sci. USA 103 (2006) 1440–1445.
[8] D.J. Lenschow, N.V. Giannakopoulos, L.J. Gunn, C. Johnston, A.K. O'Guin, R.E. Schmidt, B. Levine, H.W. Virgin IV, Identification of interferon-stimulated gene 15 as an antiviral molecule during Sindbis virus infection in vivo, J. Viol. 79 (2005) 13974–13983.
[9] A. Osiak, O. Utermohlen, S. Niendorf, I. Horak, K. Knobeloch, ISG15, an interferon-stimulated ubiquitin-like protein, is not essential for STAT1 signaling and responses against Vesicular Stomatitis and Lymphocytic Choriomeningitis Virus, Mol. Cell. Biol. 25 (2005) 6338–6345.
[10] S. Inoue, A. Orimo, T. Hosoi, S. Kondo, H. Toyoshima, T. Kondo, A. Ikegami, Y. Ouchi, H. Orimo, M. Muramatsu, Genomic binding-site cloning reveals an estrogen-responsive gene that encodes a RING finger protein, Proc. Natl. Acad. Sci. USA 90 (1993) 11117–11121.
[11] T. Urano, T. Saito, T. Tsukui, M. Fujita, T. Hosoi, M. Muramatsu, Y. Ouchi, S. Inoue, Efp targets 14-3-3σ for proteolysis and promotes breast tumour growth, Nature 417 (2002) 871–875.
[12] W. Zou, D.E. Zhang, The interferon-inducible ubiquitin-protein isopeptide ligase (E3) EFP also functions as an ISG15 E3 ligase, J. Biol. Chem. 281 (2006) 3989–3994.
[13] M.K. Chelbi-Alix, F. Quignon, L. PELICANO, M.H.M. Koken, H. DE THE, Resistance to virus infection conferred by the IFN-induced promyelocytic leukemia protein, J. Viol. 72 (1998) 1043–1051.
[14] P. Turelli, V. Doucas, E. Craig, B. Mangeat, N. Klages, R. Evans, G. Kalpana, D. Trono, Cytoplasmic recruitment of IN11 and PML on incoming HIV preintegration complexes: interference with early steps of viral replication, Mol. Cell 7 (2001) 1245–1254.
[15] Z. Keckesova, L.M.J. Ylinen, G.J. Towers, The human and African green monkey TRIM5α genes encode Ref1 and Lv1 retroviral restriction factor activities, Proc. Natl. Acad. Sci. USA 101 (2004) 10780–10785.
[16] M. Stremlau, C.M. Owens, M.J. Perron, M. Kiessling, P. Autissier, J. Sodroski, The cytoplasmic body component TRIM5α restricts HIV-1 infection in Old World monkeys, Nature 427 (2004) 848–853.
[17] S. Nisole, J.P. Stoye, A. Saïb, Trim family proteins: retroviral restriction and antiviral defense, Nat. Rev. Microbiol. 3 (2005) 799–808.
[18] K. Horie-Inoue, H. Bono, Y. Okazaki, S. Inoue, Identification and functional analysis of consensus androgen response elements in human prostate cancer cells, Biochem. Biophys. Res. Commun. 325 (2004) 1312–1317.
[19] K. Ikeda, S. Inoue, A. Orimo, M. Sano, T. Watanabe, K. Tsutsumi, M. Muramatsu, Multiple regulatory elements and binding proteins of the 5′-flanking region of the human estrogen-responsive finger protein (efp) gene, Biochem. Biophys. Res. Commun. 236 (1997) 765–771.
[20] K. Asaoka, K. Ikeda, T. Hishinuma, K. Horie-Inoue, S. Takeda, S. Inoue, A retrovirus restriction factor TRIM5α is transcriptionally regulated by IFNs, Biochem. Biophys. Res. Commun. 338 (2005) 1950–1956.
[21] N. Tanaka, T. Taniguchi, The interferon regulatory factors and oncogenesis, Semin. Cancer Biol. 10 (2000) 73–81.
[22] A.M. Burger, Y. Gao, Y. Amemiya, H.J. Kahn, R. Kitching, Y. Yang, P. Sun, S.A. Narod, W.M. Hanna, A.K. Seth, A novel RING-type ubiquitin ligase breast cancer-associated gene 2 correlates with outcome in invasive breast cancer, Cancer Res. 65 (2005) 10401–10412.
[23] Y. Jenkins, V. Markovtsov, W. Lang, P. Sharma, D. Pearsall, J. Warner, C. Franci, B. Huang, J. Huang, G.C. Yam, J.P. Vistan, E. Pali, J. Vialard, M. Janicot, J.B. Lorens, D.G. Payan, Y. Hitoshi, Critical role of the ubiquitin ligase activity of UHRF1, a nuclear RING finger protein, in tumor cell growth, Mol. Biol. Cell 16 (2005) 5621–5629.
[24] K. Ikeda, A. Orimo, Y. Higashi, M. Muramatsu, S. Inoue, Efp as a primary estrogen-responsive gene in human breast cancer, FEBS Lett. 472 (2000) 9–13.
[25] C. Tissot, N. Mechti, Molecular cloning of a new interferon-induced factor that represses human immunodeficiency virus type 1 long terminal repeat expression, J. Biol. Chem. 270 (1995) 14891–14898.
[26] A. Orimo, N. Tominaga, K. Yoshimura, Y. Yamauchi, M. Nomura, M. Sato, Y. Nogi, M. Suzuki, H. Suzuki, K. Ikeda, S. Inoue, M. Muramatsu, Molecular cloning of ring finger protein 21 (RNF21)/interferon-responsive finger protein (ifp1), which possesses two RING-B box-coiled coil domains in tandem, Genomics 69 (2000) 143–149.
[27] C. Zhao, S.L. Beaudenon, M.L. Kelley, M. Brett Waddell, W. Yuan, B.A. Schulman, J.M. Huibregtse, R.M. Krug, The UbcH8 ubiquitin E2 enzyme is also the E2 enzyme for ISG15, an IFN-α/β-induced ubiquitin-like protein, Proc. Natl. Acad. Sci. USA 101 (2004) 7578–7582.
[28] T. Takeuchi, S. Iwahara, Y. Saeki, H. Sasajima, H. Yokosawa, Link between the ubiquitination system and the ISG15 conjugation system: ISG15 conjugation to the UbcH6 ubiquitin E2 enzyme, J. Biochem. (Tokyo) 138 (2005) 711–719.

[29] A. Dastur, S. Beaudenon, M. Kelley, R.M. Krug, J.M. Huibregtse, Herc5, an interferon-induced HECT E3 enzyme, is required for conjugation of ISG15 in human cells, J. Biol. Chem. 281 (2006) 4334–4338.
[30] T. Takeuchi, S. Inoue, H. Yokosawa, Identification and Herc5-mediated ISGylation of novel target proteins, Biochem. Biophys. Res. Commun. 348 (2006) 473–477.
[31] T.A. Nyman, S. Matikainen, T. Sareneva, I. Julkunen, N. Kalkkinen, Proteome analysis reveals ubiquitin-conjugating enzymes to be a new family of interferon-α-regulated genes, Eur. J. Biochem. 267 (2000) 4011–4019.
[32] J.J.Y. Wong, Y.F. Pung, N.S.K. Sze, K.C. Chin, HERC5 is an IFN-induced HECT-type E3 protein ligase that mediates type I IFN-induced ISGylation of protein targets, Proc. Natl. Acad. Sci. USA 103 (2006) 10735–10740.
[33] T. Takeuchi, H. Yokosawa, ISG15 modification of Ubc13 suppresses its ubiquitin-conjugating activity, Biochem. Biophys. Res. Commun. 336 (2005) 9–13.
[34] M.M. Joyce, F.J. White, R.C. Burghardt, J.J. Muniz, T.E. Spencer, F.W. Bazer, G.A. Johnson, Interferon stimulated gene 15 conjugates to endometrial cytosolic proteins and is expressed at the uterine-placental interface throughout pregnancy in sheep, Endocrinology 146 (2005) 675–684.
[35] L.A. Rempel, B.R. Francis, K.J. Austin, T.R. Hansen, Isolation and sequence of an interferon-τ-inducible, pregnancy- and bovine interferon-stimulated gene product 15 (ISG15) specific, bovine ubiquitin-activating E1-like (UBE1L) enzyme, Biol. Reprod. 72 (2005) 365–372.
[36] S.D. Desai, A.L. Haas, L.M. Wood, Y.C. Tsai, S. Pestka, E.H. Rubin, A. Saleem, A. Nur-E-Kamal, L.F. Liu, Elevated expression of ISG15 in tumor cells interferes with the ubiquitin/26S proteasome pathway, Cancer Res. 66 (2006) 921–928.
[37] A. Orimo, S. Inoue, K. Ikeda, S. Noji, M. Muramatsu, Molecular cloning, structure, and expression of mouse estrogen-responsive finger protein Efp: co-localization with estrogen receptor mRNA in target organs, J. Biol. Chem. 270 (1995) 24406–24413.
[38] A. Orimo, S. Inoue, O. Minowa, N. Tominaga, Y. Tomioka, M. Sato, J. Kuno, H. Hiroi, Y. Shimizu, M. Suzuki, T. Noda, M. Muramatsu, Underdeveloped uterus and reduced estrogen responsiveness in mice with disruption of the estrogen-responsive finger protein gene, which is a direct target of estrogen receptor α, Proc. Natl. Acad. Sci. USA 96 (1999) 12027–12032.
[39] T. Suzuki, T. Urano, T. Tsukui, K. Horie-Inoue, T. Moriya, T. Ishida, M. Muramatsu, Y. Ouchi, H. Sasano, S. Inoue, Estrogen-responsive finger protein as a new potential biomarker for breast cancer, Clin. Cancer Res. 11 (2005) 6148–6154.

Available online at www.sciencedirect.com
ScienceDirect
ELSEVIER
Biochemical and Biophysical Research Communications 348 (2006) 473–477
BBRC
www.elsevier.com/locate/ybbrc

Identification and Herc5-mediated ISGylation of novel target proteins ☆

Tomoharu Takeuchi [a], Satoshi Inoue [b], Hideyoshi Yokosawa [a,*]

[a] Department of Biochemistry, Graduate School of Pharmaceutical Sciences, Hokkaido University, Sapporo 060-0812, Japan
[b] Department of Geriatric Medicine, Graduate School of Medicine, The University of Tokyo, 7-3-1 Hongo, Bunkyo-ku, Tokyo 113-8655, Japan

Received 5 July 2006
Available online 28 July 2006

Abstract

ISG15, a protein containing two ubiquitin-like domains, is an interferon-stimulated gene product that functions in antiviral response and is conjugated to various cellular proteins (ISGylation) upon interferon stimulation. ISGylation occurs via a pathway similar to the pathway for ubiquitination that requires the sequential action of E1/E2/E3: the E1 (UBE1L), E2 (UbcH8), and E3 (Efp/Herc5) enzymes for ISGylation have been hitherto identified. In this study, we identified six novel candidate target proteins for ISGylation by a proteomic approach. Four candidate target proteins were demonstrated to be ISGylated in UBE1L- and UbcH8-dependent manners, and ISGylation of the respective target proteins was stimulated by Herc5. In addition, Herc5 was capable of binding with the respective target proteins. Thus, these results suggest that Herc5 functions as a general E3 ligase for protein ISGylation.
© 2006 Elsevier Inc. All rights reserved.

Keywords: ISG15; Interferon; Ubiquitin; Herc5

Type I interferon functions in cellular antiviral response via induction of genes called interferon-stimulated genes (ISGs) [1]. Recently, ISG15, one of the ISGs, was found to function as an antiviral protein against Sindbis virus and HIV-1 [2,3] although the molecular mechanism remains unknown. ISG15 contains two ubiquitin-like domains and belongs to the ubiquitin-like protein family. The expression of ISG15 is induced by interferon stimulation and ISG15 is conjugated to various cellular proteins (ISGylation) in a manner similar to ubiquitination that is catalyzed by the sequential action of E1 (ubiquitin-activating enzyme), E2 (ubiquitin-conjugating enzyme), and E3 (ubiquitin ligase) [4,5]. Target proteins modified with ISG15 [6–8], the E1 (UBE1L) and E2 (UbcH8) enzymes functioning in ISGylation [9–11], and a de-ISGylating enzyme (UBP43) [12] have been identified, but biological consequences of ISGylation have been studied in only a few cases [13–15]. Recently, Efp and Herc5 have been reported to function as E3 ligases for ISGylation [16,17], but there seems to be a difference in function between Efp and Herc5 because Herc5, but not Efp, influences the ISGylation status of whole cellular proteins [16,17].

In this study, we identified six novel candidate target proteins for ISGylation and confirmed that four identified proteins, XPD (ERCC2), STK38, RGS3 isoform 1, and α-tubulin, are actually ISGylated in UBE1L- and UbcH8-dependent manners. In addition, we found that Herc5 is capable of binding with and stimulating ISGylation of the respective novel target proteins.

Materials and methods

Cell culture and transfection. HeLa cells were cultured in Dulbecco's modified Eagle's medium (Sigma) supplemented with 10% heat-inactivated calf serum (Hyclone). Transfection was performed according to the standard calcium precipitation protocol.

☆ *Abbreviations:* ISG, interferon-stimulated gene; E1, ubiquitin-activating enzyme; E2, ubiquitin-conjugating enzyme; E3, ubiquitin ligase; XP, xeroderma pigmentosum; ERCC, excision-repair, complementing defective, in Chinese hamster; STK, serine/threonine kinase; RGS, regulator of G protein signaling; PP, protein phosphatase; Efp, estrogen-responsive finger protein; Herc, HECT domain and RCC1-like domain containing protein.

* Corresponding author. Fax: +81 11 706 4900.
E-mail address: yoko@pharm.hokudai.ac.jp (H. Yokosawa).

0006-291X/$ - see front matter © 2006 Elsevier Inc. All rights reserved.
doi:10.1016/j.bbrc.2006.07.076

Plasmid construction. The mammalian expression plasmids of ISG15, UBE1L, and UbcH8 were generated as described previously [15]. The open-reading frames of human XPD (ERCC2), STK38, RGS3 isoform 1, α-tubulin, and Herc5 were amplified by PCR. All constructs were verified by DNA sequencing. To generate the expression plasmids, the PCR fragments were subcloned into pCI-neo-3Flag and pCI-neo-2S vectors that had been generated by inserting oligonucleotides encoding three repeats of Flag-tag sequence and two repeats of S-peptide sequence, respectively, into the pCI-neo mammalian expression vector (Promega). To generate the expression plasmid of Efp, the open-reading frame of human Efp was cut from the Myc-Efp plasmid that had been constructed as described previously [18] and was subcloned into the pCI-neo-2S vector.

Isolation of ISGylated proteins. HeLa cells that had been transiently transfected with Flag-tagged ISG15, S-tagged UBE1L, and S-tagged UbcH8 expression plasmids and cultured for 36 h were washed with ice-cold phosphate-buffered saline and lysed with RIPA buffer containing 50 mM Tris–HCl, pH 7.5, 150 mM NaCl, 0.1% SDS, 0.5% sodium deoxycholate, 1% Nonidet P-40, 1 mM DTT, and 5 mM *N*-ethylmaleimide. The cell lysate was sonicated for 3 s and the debris was removed by centrifugation. The resulting supernatant was incubated with anti-Flag M2 antibody-immobilized agarose (Sigma), and the resulting immunoprecipitate was washed three times with RIPA buffer, followed by washing three times with a buffer containing 20 mM Tris–HCl, pH 7.5, 500 mM NaCl, 0.2% Nonidet P-40, and 10% glycerol. The materials bound to the beads were eluted with 3× Flag peptide (Sigma) (200 μg/ml) and subjected to acetone precipitation.

SDS–PAGE and Western blotting. Isolated ISGylated proteins were separated by SDS–PAGE and stained with Coomassie brilliant blue. Western blotting was performed as described previously [13].

Peptide mass fingerprinting. Peptide mass fingerprinting was performed as described previously [19] except for the use of MS-fit (http://prospector.ucsf.edu/ucsfhtml4.0/msfit.htm) for analysis of peptide mass fingerprints. Protein classification was made by searching the OMIM™ database (http://www.ncbi.nlm.nih.gov/entrez/query.fcgi?db=OMIM).

Immunoprecipitation and affinity purification. To analyze ISGylation, HeLa cells that had been transiently transfected with indicated plasmids and cultured for 24 h were lysed with buffer A containing 50 mM Tris–HCl, pH 7.5, 150 mM NaCl, 0.1% SDS, 0.5% sodium deoxycholate, 1% Nonidet P-40, 1 mM phenylmethylsulfonyl fluoride, and 5 mM *N*-ethylmaleimide, and the supernatant of the cell lysate was subjected to immunoprecipitation using anti-Flag tag antibody-immobilized agarose beads. The resulting immunoprecipitate was washed five times with buffer A and subjected to Western blotting. To analyze the binding capacity of Herc5 or Efp, HeLa cells that had been transiently transfected with indicated plasmids and cultured for 24 h were lysed with buffer B containing 20 mM Tris–HCl, pH 7.5, 150 mM NaCl, 0.2% Nonidet P-40, 10% glycerol, and 1 mM phenylmethylsulfonyl fluoride, and the supernatant of the cell lysate was subjected to affinity purification using S-protein-immobilized agarose beads (Novagen). The resulting precipitate was washed three times with buffer B and subjected to Western blotting.

Results and discussion

Identification of proteins modified with ISG15

To determine the physiological meanings of ISGylation, it is necessary to identify proteins that are modified with ISG15. We carried out a proteomic analysis of ISGylated proteins. Flag-tagged ISG15, S-tagged UBE1L, and S-tagged UbcH8 were expressed in HeLa cells, and ISGylated proteins were isolated from the cell extract by immunoprecipitation with anti-Flag tag antibody-immobilized agarose beads and subsequent elution with 3× Flag peptide. The isolated proteins were separated by SDS–PAGE and stained with Coomassie brilliant blue

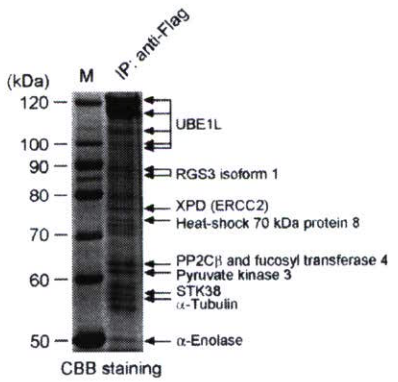

Fig. 1. Identification of proteins ISGylated. The extract of HeLa cells that had expressed Flag-tagged ISG15 together with S-tagged UBE1L and S-tagged UbcH8 was subjected to immunoprecipitation (IP) with anti-Flag tag antibody-immobilized agarose beads, and isolated ISGylated proteins were separated by SDS–PAGE and stained with Coomassie brilliant blue (CBB). The bands identified by peptide mass fingerprinting are indicated by arrows. M, molecular mass markers.

(Fig. 1). The separated protein bands were subjected to peptide mass fingerprinting and 10 candidate target proteins for ISGylation were identified (Table 1). Among them, six proteins are novel candidate target proteins that have not been reported.

To confirm the above results of peptide mass fingerprinting, we cloned four novel candidate target proteins for ISGylation, XPD (ERCC2), STK38, RGS3 isoform 1, and α-tubulin. The respective Flag-tagged candidate target proteins were expressed together with T7-tagged ISG15, S-tagged UBE1L, and S-tagged UbcH8 in HeLa cells, and the extracts of transfected cells were subjected to immunoprecipitation using anti-Flag tag antibody-immobilized agarose beads and then to Western blotting with anti-Flag tag and anti-T7 tag antibodies (Fig. 2). In either case, two bands with slower mobilities (open arrowheads) than that of the original one (a closed arrowhead) were

Table 1
Candidate target proteins for ISGylation identified in this study

Name	Function
XPD (ERCC2)[a]	DNA repair helicase
STK38[a]	Serine/threonine kinase
RGS3 isoform 1[a]	GTPase-activating protein
α-Tubulin[a]	Cytoskeleton
PP2Cβ[a]	Serine/threonine phosphatase
Fucosyl transferase 4[a]	Fucosyl transferase
UBE1L[b]	E1 for ISGylation
Heat-shock 70 kDa protein 8[b]	Chaperone
Pyruvate kinase 3[b]	Phosphotransferase
α-Enolase[b]	Phosphopyruvate hydratase

[a] Newly identified in this study.
[b] Previously reported [7,8].

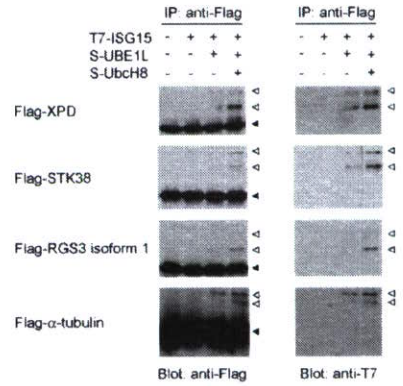

Fig. 2. Four candidate target proteins, XPD (ERCC2), STK38, RGS3 isoform 1, and α-tubulin, are ISGylated in UBE1L- and UbcH8-dependent manners. The extract of HeLa cells that had expressed the respective Flag-tagged candidate proteins together with T7-tagged ISG15, S-tagged UBE1L, and S-tagged UbcH8 as indicated was subjected to immunoprecipitation (IP) with anti-Flag tag antibody-immobilized agarose beads. The resulting immunoprecipitate was subjected to Western blotting with anti-Flag tag and anti-T7 tag antibodies. ISGylated forms of the candidate proteins are indicated by open arrowheads and the original forms are indicated by closed arrowheads.

detected in the presence of both UBE1L and UbcH8 by immunoblotting with anti-Flag tag antibody (left panel), and the bands with the same slower mobilities were also detected by immunoblotting with anti-T7 tag antibody (right panel). These results suggest that XPD (ERCC2), STK38, RGS3 isoform 1, and α-tubulin are actually ISGylated.

Herc5 stimulates ISGylation of novel target proteins

Efp and Herc5 have been reported to be E3 ligases for ISGylation [16,17], although they also function as ubiquitin E3 ligases [18,20]. We carried out experiments to determine which E3 ligase stimulates ISGylation of four target proteins newly identified in this study, XPD (ERCC2), STK38, RGS3 isoform 1, and α-tubulin. First, we constructed mammalian expression plasmids of Efp and Herc5 and expressed them together with T7-tagged ISG15, S-tagged UBE1L, and S-tagged UbcH8 in HeLa cells. The extracts of transfected cells were subjected to Western blotting with anti-T7 tag and anti-S peptide antibodies (Fig. 3). Consistent with previous reports [16,17], Herc5, but not Efp, stimulated ISGylation of the whole cellular proteins. Next, the above four Flag-tagged target proteins were expressed together with T7-tagged ISG15, S-tagged UBE1L, S-tagged UbcH8, and S-tagged Herc5 or Efp in HeLa cells, and the extracts of transfected cells were subjected to immunoprecipitation using anti-Flag tag antibody-immobilized agarose beads and then to Western blotting with anti-Flag tag and anti-T7 tag antibodies

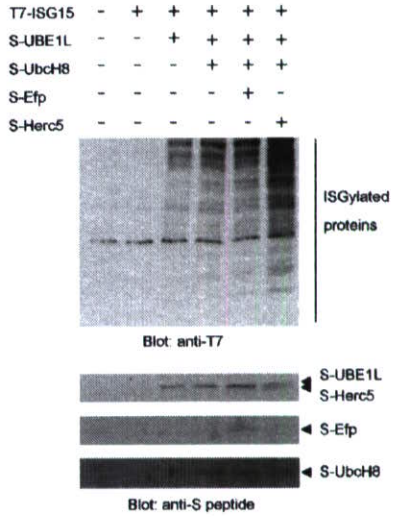

Fig. 3. Herc5 stimulates ISGylation of the whole cellular proteins. The extract of HeLa cells that had been transiently transfected with indicated plasmids was subjected to Western blotting with anti-T7 tag and anti-S peptide antibodies.

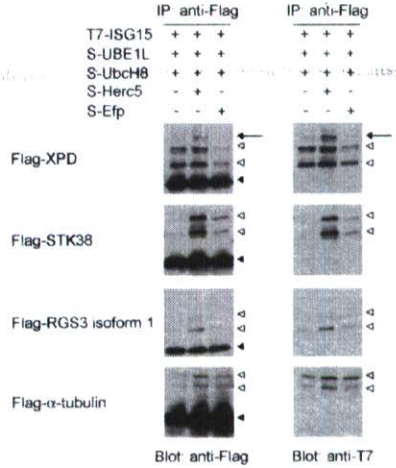

Fig. 4. Effects of co-expressions of Herc5 and Efp on ISGylation of four target proteins, XPD (ERCC2), STK38, RGS3 isoform 1, and α-tubulin. The extracts of HeLa cells that had been transiently transfected with indicated plasmids were subjected to immunoprecipitation (IP) with anti-Flag tag antibody-immobilized beads and then to Western blotting with anti-Flag tag and anti-T7 tag antibodies. ISGylated forms of the target proteins are indicated by open arrowheads and the original forms are indicated by closed arrowheads. An additional band due to ISGylated XPD (ERCC2) is indicated by an arrow.

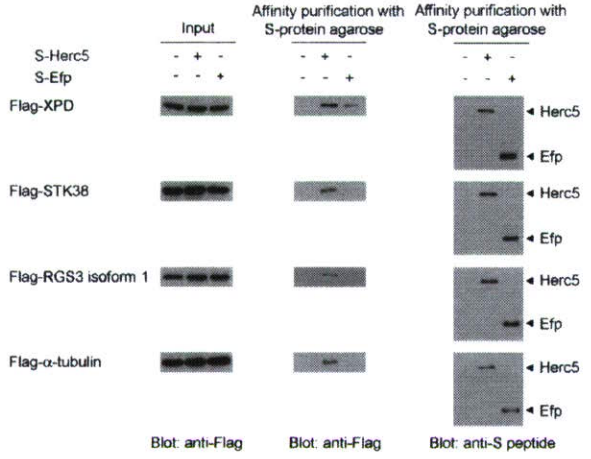

Fig. 5. Herc5 is capable of binding with four target proteins, XPD (ERCC2), STK38, RGS3 isoform 1, and α-tubulin. The extract of HeLa cells that had expressed the respective Flag-tagged target proteins together with S-tagged Herc5 or Efp as indicated was subjected to affinity purification using S-protein-immobilized agarose beads and then to Western blotting with anti-Flag tag and anti-S peptide antibodies.

(Fig. 4). ISGylation of STK38 or RGS3 isoform 1 was strongly stimulated by co-expression of Herc5 and very weakly by Efp (see two bands indicated by open arrowheads in either case). In the case of XPD (ERCC2), an additional band due to an ISGylated form was detected when Herc5, but not Efp, was co-expressed (see one band indicated by an arrow). On the other hand, ISGylation of α-tubulin was stimulated by Efp as well as by Herc5 (see two bands indicated by open arrowheads). These results suggest that Herc5 functions as an E3 ligase for ISGylation of all four target proteins.

Herc5 is capable of binding with novel target proteins for ISGylation

It is well known that the ubiquitin E3 ligase recognizes or binds with target proteins for ubiquitination [4]. We next determined whether Herc5 is capable of binding with four target proteins, XPD (ERCC2), STK38, RGS3 isoform 1, and α-tubulin. The respective Flag-tagged target proteins were expressed together with S-tagged Herc5 or Efp in HeLa cells, and the extracts of transfected cells were subjected to affinity purification using S-protein-immobilized agarose beads and then to Western blotting with anti-Flag tag and anti-S peptide antibodies (Fig. 5). Herc5 was found to bind with each of the four target proteins, while Efp was found to bind weakly only with XPD (ERCC2).

In conclusion, we identified six novel target proteins for ISGylation and found that ISGylation of XPD (ERCC2), STK38, RGS3 isoform 1, and α-tubulin is catalyzed by three enzymes, UBE1L, UbcH8, and Herc5. These results agree well with results of a previous study showing that Herc5 is an accelerator of a broad range of ISG15 conjugation [17]. The construction of an *in vitro* ISGylation system containing recombinant Herc5 together with ISG15, UBE1L, and UbcH8 will verify the speculation that Herc5 functions as a general E3 ligase for protein ISGylation.

Acknowledgments

This study was supported in part by Grants-in-Aid for scientific research from the Ministry of Education, Culture, Sports, Science and Technology of Japan.

References

[1] D.V. Kalvakolanu, Alternate interferon signaling pathways, Pharmacol. Ther. 100 (2003) 1–29.
[2] D.J. Lenschow, N.V. Giannakopoulos, L.J. Gunn, C. Johnston, A.K. O'Guin, R.E. Schmidt, B. Levine, H.W. Virgin, Identification of interferon-stimulated gene 15 as an antiviral molecule during Sindbis virus infection in vivo, J. Virol. 79 (2005) 13974–13983.
[3] A. Okumura, G. Lu, I. Pitha-Rowe, P.M. Pitha, Innate antiviral response targets HIV-1 release by the induction of ubiquitin-like protein ISG15, Proc. Natl. Acad. Sci. USA 103 (2006) 1440–1445.
[4] C.M. Pickart, Mechanisms underlying ubiquitination, Annu. Rev. Biochem. 70 (2001) 503–533.
[5] C.T. Dao, D.E. Zhang, ISG15: a ubiquitin-like enigma, Front. Biosci. 10 (2005) 2701–2722.
[6] M.P. Malakhov, K.I. Kim, O.A. Malakhova, B.S. Jacobs, E.C. Borden, D.E. Zhang, High-throughput immunoblotting. Ubiquitin-like protein ISG15 modifies key regulators of signal transduction, J. Biol. Chem. 278 (2003) 16608–16613.
[7] C. Zhao, C. Denison, J.M. Huibregtse, S. Gygi, R.M. Krug, Human ISG15 conjugation targets both IFN-induced and constitutively expressed proteins functioning in diverse cellular pathways, Proc. Natl. Acad. Sci. USA 102 (2005) 10200–10205.
[8] N.V. Giannakopoulos, J.K. Luo, V. Papov, W. Zou, D.J. Lenschow, B.S. Jacobs, E.C. Borden, J. Li, H.W. Virgin, D.E. Zhang, Proteomic identification of proteins conjugated to ISG15 in mouse and human cells, Biochem. Biophys. Res. Commun. 336 (2005) 496–506.
[9] W. Yuan, R.M. Krug, Influenza B virus NS1 protein inhibits conjugation of the interferon (IFN)-induced ubiquitin-like ISG15 protein, EMBO J. 20 (2001) 362–371.
[10] C. Zhao, S.L. Beaudenon, M.L. Kelley, M.B. Waddell, W. Yuan, B.A. Schulman, J.M. Huibregtse, R.M. Krug, The UbcH8 ubiquitin E2 enzyme is also the E2 enzyme for ISG15, an IFN-α/β-induced ubiquitin-like protein, Proc. Natl. Acad. Sci. USA 101 (2004) 7578–7582.
[11] K.I. Kim, N.V. Giannakopoulos, H.W. Virgin, D.E. Zhang, Interferon-inducible ubiquitin E2, Ubc8, is a conjugating enzyme for protein ISGylation, Mol. Cell. Biol. 24 (2004) 9592–9600.
[12] M.P. Malakhov, O.A. Malakhova, K.I. Kim, K.J. Ritchie, D.E. Zhang, UBP43 (USP18) specifically removes ISG15 from conjugated proteins, J. Biol. Chem. 277 (2002) 9976–9981.
[13] T. Takeuchi, H. Yokosawa, ISG15 modification of Ubc13 suppresses its ubiquitin-conjugating activity, Biochem. Biophys. Res. Commun. 336 (2005) 9–13.
[14] W. Zou, V. Papov, O. Malakhova, K.I. Kim, C. Dao, J. Li, D.E. Zhang, ISG15 modification of ubiquitin E2 Ubc13 disrupts its ability to form thioester bond with ubiquitin, Biochem. Biophys. Res. Commun. 336 (2005) 61–68.
[15] T. Takeuchi, S. Iwahara, Y. Saeki, H. Sasajima, H. Yokosawa, Link between the ubiquitin conjugation system and the ISG15 conjugation system: ISG15 conjugation to the UbcH6 ubiquitin E2 enzyme, J. Biochem. (Tokyo) 138 (2005) 711–719.
[16] W. Zou, D.E. Zhang, The interferon-inducible ubiquitin-protein isopeptide ligase (E3) EFP also functions as an ISG15 E3 ligase, J. Biol. Chem. 281 (2006) 3989–3994.
[17] A. Dastur, S. Beaudenon, M. Kelley, R.M. Krug, J.M. Huibregtse, Herc5, an interferon-induced HECT E3 enzyme, is required for conjugation of ISG15 in human cells, J. Biol. Chem. 281 (2006) 4334–4338.
[18] T. Urano, T. Saito, T. Tsukui, M. Fujita, T. Hosoi, M. Muramatsu, Y. Ouchi, S. Inoue, Efp targets 14-3-3 sigma for proteolysis and promotes breast tumour growth, Nature 417 (2002) 871–875.
[19] M. Yamakami, T. Yoshimori, H. Yokosawa, Tom1, a VHS domain-containing protein, interacts with tollip, ubiquitin, and clathrin, J. Biol. Chem. 278 (2003) 52865–52872.
[20] R. Kroismayr, U. Baranyi, C. Stehlik, A. Dorfleutner, B.R. Binder, J. Lipp, HERC5, a HECT E3 ubiquitin ligase tightly regulated in LPS activated endothelial cells, J. Cell. Sci. 117 (2004) 4749–4756.

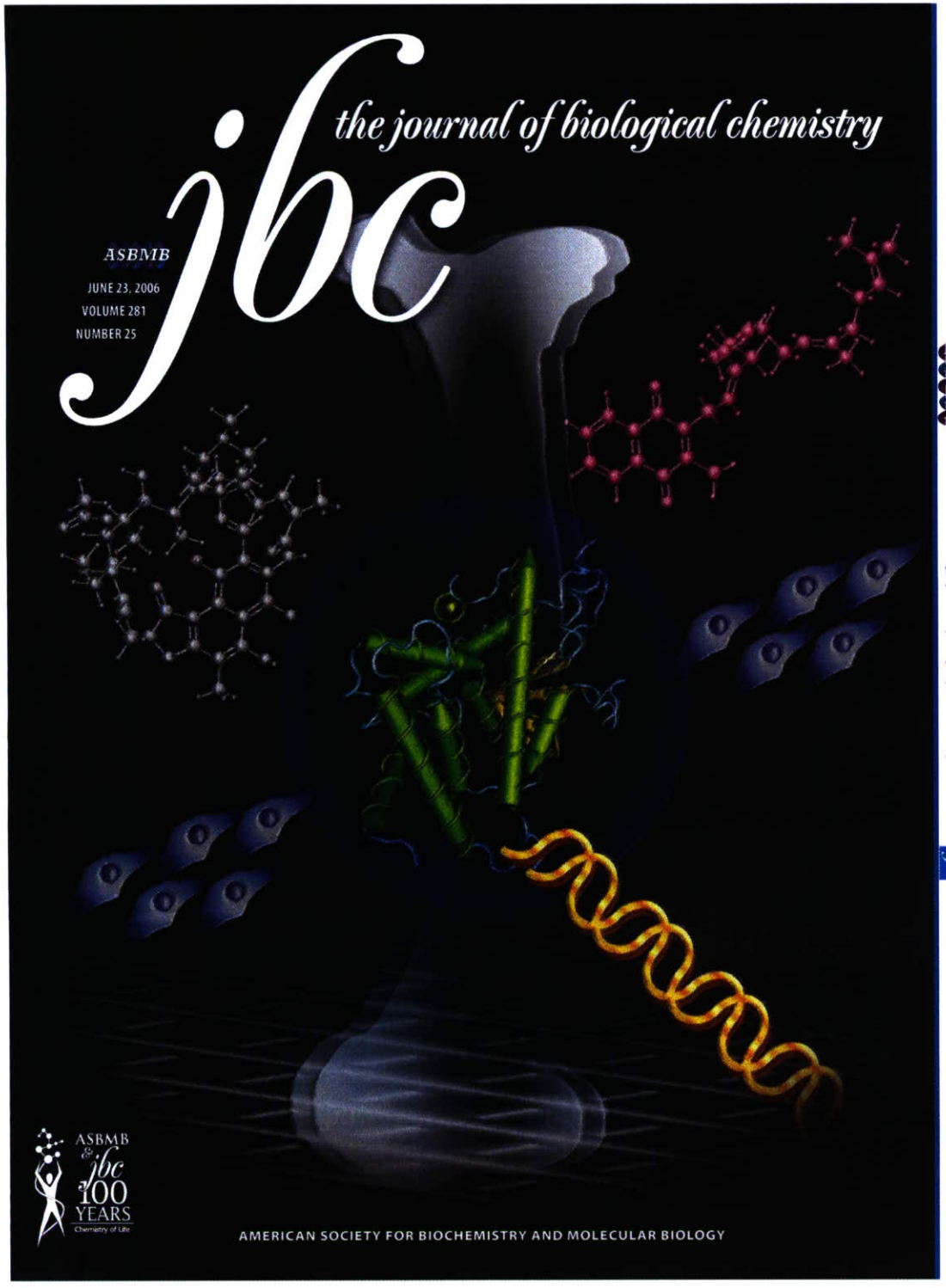

THE JOURNAL OF BIOLOGICAL CHEMISTRY VOL. 281, NO. 25, pp. 16927–16934, June 23, 2006
© 2006 by The American Society for Biochemistry and Molecular Biology, Inc. Printed in the U.S.A.

Steroid and Xenobiotic Receptor SXR Mediates Vitamin K_2-activated Transcription of Extracellular Matrix-related Genes and Collagen Accumulation in Osteoblastic Cells*♦

Received for publication, January 30, 2006, and in revised form, March 28, 2006 Published, JBC Papers in Press, April 10, 2006, DOI 10.1074/jbc.M600896200

Tomoe Ichikawa‡, Kuniko Horie-Inoue‡, Kazuhiro Ikeda‡, Bruce Blumberg§, and Satoshi Inoue‡¶1

From the ‡Division of Gene Regulation and Signal Transduction, Research Center for Genomic Medicine, Saitama Medical School, Saitama 350-1241, Japan, the §Department of Developmental and Cell Biology, University of California, Irvine, California 92697-2300, and the ¶Department of Geriatric Medicine, Graduate School of Medicine, The University of Tokyo, Tokyo 113-8655, Japan

Vitamin K_2 is a critical nutrient required for blood coagulation. It also plays a key role in bone homeostasis and is a clinically effective therapeutic agent for osteoporosis. We previously demonstrated that vitamin K_2 is a transcriptional regulator of bone marker genes in osteoblastic cells and that it may potentiate bone formation by activating the steroid and xenobiotic receptor, SXR. To explore the SXR-mediated vitamin K_2 signaling network in bone homeostasis, we identified genes up-regulated by both vitamin K_2 and the prototypical SXR ligand, rifampicin, in osteoblastic cells using oligonucleotide microarray analysis and quantitative reverse transcription-PCR. Fourteen genes were up-regulated by both ligands. Among these, tsukushi, matrilin-2, and CD14 antigen were shown to be primary SXR target genes. Moreover, collagen accumulation in osteoblastic MG63 cells was enhanced by vitamin K_2 treatment. Gain- and loss-of-function analyses showed that the small leucine-rich proteoglycan, tsukushi, contributes to vitamin K_2-mediated enhancement of collagen accumulation. Our results suggest a new function for vitamin K_2 in bone formation as a transcriptional regulator of extracellular matrix-related genes, that are involved in the collagen assembly.

Vitamin K is an important cofactor in blood coagulation and also known as a potent stimulator of the bone building process. Vitamin K is a family of structurally similar, fat-soluble, 2-methyl-1,4-naphthoquinones, including phylloquinone (K_1), menaquinones (K_2), and menadione (K_3). Vitamin K_1 and vitamin K_2 are natural vitamin Ks. The former is found in plants, whereas the latter is mainly derived from animal sources and produced by intestinal bacteria. *In vitro* studies showed that vitamin K_2 is far more active than K_1 in both promoting bone formation and reducing bone loss (1–5). Human studies have demonstrated that vitamin K_2 is an effective treatment for osteoporosis and preventing fractures (6, 7). Menaquinone-4 (MK-4),[2] the most common form of vitamin K_2 containing four isoprene units, is frequently prescribed for osteoporosis in Japan.

One of the major known functions of vitamin K is the posttranslational modification of vitamin K-dependent proteins containing γ-carboxyglutamic acid (Gla) residues, most of which are related to coagulation (as reviewed in Ref. 8). In vitamin K-dependent carboxylation reactions, the reduced form of vitamin K de-protonates glutamate via the γ-glutamyl carboxylase and the reduced vitamin K is converted to vitamin K epoxide. Two such vitamin K-dependent proteins were identified in bone: osteocalcin and matrix Gla protein (MGP). Osteocalcin is a bone protein only synthesized in osteoblasts and odontoblasts. It serves as a good biochemical marker of the metabolic turnover of bone because the osteocalcin lacking Gla residues cannot bind to hydroxyapatite, one of the major components of bone matrix (9). Levels of undercarboxylated osteocalcin increase during aging and significantly correlates with fracture risk (10). Therefore, vitamin K-modified osteocalcin plays an important role in bone homeostasis. In contrast to osteocalcin, MGP is predominantly expressed in chondrocytes and vascular smooth muscle cells. *Mgp*-deficient mice exhibited inappropriate calcification of various cartilages as well as arterial walls, indicating that MGP is a modulator of extracellular matrix mineralization (11, 12). Despite structural similarities between osteocalcin and MGP, these two Gla proteins exhibit different functions. These findings suggest that vitamin K plays a significant role in bone homeostasis, although the precise mechanisms through which bone Gla proteins regulate homeostasis are complex.

During the 60-year history of vitamin K research, most of the attention has been paid to the actions of vitamin K on γ-carboxylation. We recently identified a novel mechanism of vitamin K functions via transcriptional regulation in osteoblastic cells (13). Both vitamin K_2 and the known SXR ligands rifampicin (RIF) and hyperforin up-regulated expression of the prototypical SXR target gene *CYP3A4* and bone markers such as alkaline phosphatase (*ALP*) and *MGP* (13). Our findings suggested an important role for vitamin K_2-dependent transcriptional regulation in bone homeostasis. Until now, the contribution of distinct vitamin K_2 and SXR target genes to these mechanisms remained to be studied.

In the present study, we searched for SXR target genes induced by vitamin K_2 and RIF in osteoblastic MG63 cells using microarray analysis. Several genes were identified that are up-regulated by both agonists. We focused here on the osteoblastogenic functions of extracellular matrix-related genes as SXR targets in response to vitamin K_2 treatment. Furthermore, we showed that the novel SXR target, tsukushi (*TSK*), plays a role in collagen accumulation in MG63 cells. Our findings indicate that vitamin K_2 activates SXR to regulate the transcription of extracellular matrix-related genes that may contribute to collagen assembly.

* This work was supported in part by grants-in-aid from the Ministry of Health, Labor and Welfare and from the Japan Society for the Promotion of Science and by a grant of the Genome Network Project from the Ministry of Education, Culture, Sports, Science and Technology of Japan and for Development of New Technology from The Promotion and Mutual Aid Corporation for Private Schools of Japan. This work was also supported by National Institutes of Health Grant GM-060572 (to B. B.). The costs of publication of this article were defrayed in part by the payment of page charges. This article must therefore be hereby marked "*advertisement*" in accordance with 18 U.S.C. Section 1734 solely to indicate this fact.

♦ This article was selected as a Paper of the Week.

[1] To whom correspondence should be addressed: Division of Gene Regulation and Signal Transduction, Research Center for Genomic Medicine, Saitama Medical School, 1397-1 Yamane, Hidaka-shi, Saitama 350-1241, Japan. Tel.: 81-42-985-7206; Fax: 81-42-985-7209; E-mail: s_inoue@saitama-med.ac.jp.

[2] The abbreviations used are: MK-4, menaquinone-4; Gla, γ-carboxyglutamic acid; MGP, matrix Gla protein; RIF, rifampicin; FBS, fetal bovine serum; CYP, cytochrome P-450; MES, 4-morpholineethanesulfonic acid; GAPDH, glyceraldehyde-3-phosphate dehydrogenase; siRNA, small interfering RNA.

Downloaded from www.jbc.org at SAITAMA IKA DAIGAKU on November 24, 2006

EXPERIMENTAL PROCEDURES

Cell Culture—MG63 human osteosarcoma cells, 293T, and COS1 cells were grown in Dulbecco's modified Eagle's medium supplement with 10% fetal bovine serum (FBS), 50 units/ml penicillin, and 50 μg/ml streptomycin. Prior to vitamin K_2 treatment, cells were cultured in phenol red-free media containing 10% dextran-charcoal-stripped FBS.

Cloning and Construction of cDNAs—Human SXR (pCDG-SXR), human SXR containing the VP16 activation domain upstream to SXR (VP16-SXR), and tk-$(3A4)_3$-Luc containing three-copy SXR response elements from human cytochrome P-450 (CYP) 3A4 promoter were described previously (14–16). N-terminally FLAG-tagged pcDNA3 (Invitrogen) plasmids containing SXR (pcDNA3-FLAG-SXR) and VP16C-SXR (pcDNA3-FLAG-VP16C-SXR) were generated by PCR using pCDG-SXR and VP16-SXR as templates, respectively, and inserted in-frame to FLAG-tagged pcDNA3 at EcoRI and XhoI sites. VP16C-SXR contained 20 amino acids from the C terminus of VP16 activation domain upstream of SXR. The tsukushi (*TSK*) cDNA was isolated from first-strand cDNA derived from MG63 cells using primers 5′-CACGAATTCGCCACCATGCCGTGGCCCCTGCTG-3′ and 5′-CGACTCGAGCAAGATGGTGGGGCCCCTGGC-3′, inserted in-frame to C-terminally FLAG-tagged pcDNA3 at EcoRI and XhoI sites (pcDNA3-TSK-FLAG). DNA sequences of plasmids were determined by ABI PRIZM 377 Sequencer (Applied Biosystems, Foster City, CA).

Luciferase Assay—Luciferase assay was performed using MG63 cells (2×10^4 cells/well on 24-well plates) transfected with 115 ng of tk-$(3A4)_3$-Luc, 130 ng of pRL-CMV (Promega), and 5 ng of FLAG-pcDNA3 or FLAG-tagged SXR plasmids using the FuGENE 6 reagent (Roche Diagnostics). Twenty-four hours after transfection, cells were treated with 20 μM RIF (Nakalai Tesque, Kyoto, Japan), 20 μM MK-4 (gifted by Eisai Co., Ltd., Tokyo, Japan), or vehicle (0.2% ethanol) for 30 h in fresh media, and luciferase activities were determined by a MicroLumatPlus microplate luminometer (Berthold Technologies) using the dual-luciferase assay system (Promega). Firefly luciferase activity was normalized to *Renilla* luciferase, which was used as a transfection control. The experiments were repeated three times with similar results.

Generation of Stable Cell Lines—MG63 cells were transfected with pcDNA3-FLAG-SXR, pcDNA3-FLAG-VP16C-SXR, pcDNA3-TSK-FLAG, or empty FLAG-tagged pcDNA3 using the FuGENE 6 reagent and selected in 0.5 mg/ml G418. Expression levels of FLAG-SXR, FLAG-VP16C-SXR, and TSK-FLAG proteins were verified by Western blot analysis.

Western Blot Analysis and Immunoprecipitation—Whole cell lysates were prepared using PLC lysis buffer (50 mM Hepes, pH 7.5, 150 mM NaCl, 10% glycerol, 1% Triton X-100, 1.5 mM $MgCl_2$, 1 mM sodium orthovanadate, 10 μg/ml aprotinin, and 10 μg/ml leupeptin). Protein concentrations were analyzed using the BCA protein assay kit (Pierce). Proteins were resolved by SDS-PAGE and electroblotted onto Immobilon-P transfer membrane (Millipore). Membranes were incubated with primary antibodies for 90 min followed by incubation with secondary antibodies for 30 min. After extensive washing, the antibody-antigen complexes were detected using the Western blotting Chemiluminescence Luminol Reagent (Santa Cruz Biotechnology). Antibodies used included anti-PXR (pregnane X receptor)/SXR (N-16 and H-160, Santa Cruz Biotechnology), anti-α-tubulin monoclonal antibody (Zymed Laboratories), anti-FLAG M2 monoclonal antibody (Sigma), and anti-Myc polyclonal antibody (Cell Signaling Technology). For SXR detection in parental MG63 cells, 500 μg of proteins from cell lysates were incubated with anti-SXR antibody (H-160) or normal rabbit IgG (Sigma) at 4 °C overnight. The mixture of cell extracts and antibody was incubated with Protein G-Sepharose beads (Amersham Biosciences) at 4 °C for 2 h, washed four times using PLC lysis buffer. The immunoprecipitated proteins were boiled 5 min in Laemmli sample buffer and separated by SDS-PAGE.

Preparation of cRNA—Total RNA was extracted from MG63 cells stably expressing FLAG-VP16C-SXR treated with vehicle (0.1% ethanol), MK-4 (10 μM), or RIF (10 μM) for 48 h. The methods for preparation of cRNA and subsequent steps leading to hybridization and scanning of the U133A GeneChip Arrays were provided by the manufacturer (Affymetrix). Briefly, poly(A)$^+$ RNA was isolated from 200 μg total RNA of each sample with the Oligotex™-dT30 Super mRNA purification kit (Takara Bio, Kyoto, Japan) and converted into double-stranded cDNA using the cDNA synthesis kit (SuperScript Choice, Invitrogen) with a special oligo$(dT)_{24}$ primer containing a T7 RNA polymerase promoter site added 3′ of the poly(T) tract (Amersham Biosciences). After second-strand synthesis, labeled cRNA was generated from the cDNA sample by an *in vitro* transcription reaction using the bioarray high yield RNA transcript labeling kit (Enzo Life Sciences, Farmingdale, NY) supplemented with biotin-CTP and biotin-UTP (Enzo Life Sciences). The labeled cRNA was purified using RNeasy spin columns (Qiagen). Twenty μg of each cRNA sample was fragmented by mild alkaline treatment, at 94 °C for 35 min in fragmentation buffer (200 mM Tris acetate, pH 8.1, 500 mM potassium acetate, 150 mM magnesium acetate) and then used to prepare 400 μl of master hybridization mix (0.1 mg/ml herring sperm DNA (Promega), 0.5 mg/ml of acetylated bovine serum albumin in hybridization buffer containing 100 mM MES, 1 M [Na^+], 20 mM EDTA, 0.01% Tween 20).

Oligonucleotide Array Hybridization and Scanning—Before hybridization, the cRNA samples were heated to 99 °C for 5 min, equilibrated to 45 °C for 5 min, and clarified by centrifugation (15,000 rpm) at room temperature for 5 min. Aliquots of each sample (10 μg of cRNA in 200 μl of the master mix) were hybridized to U133A GeneChip arrays at 45 °C for 16 h in a rotisserie oven set at 60 rpm. After this, the arrays were washed with non-stringent wash buffer (6 × saline/sodium phosphate/EDTA, 0.01% Tween 20) and stringent wash buffer (100 mM MES/0.1 M [Na^+], 0.01% Tween 20), stained with streptavidin-phycoerythrin (Molecular Probes), washed again, and read using a microarray scanner G2500A (Affymetrix) with the 570-nm long-pass filter. Data analysis was performed by using Affymetrix Microarray Suite software. For comparing arrays, normalization was performed using data from all probe sets.

Reverse Transcription-PCR Analysis—MG63 cells were treated with 10 μM RIF, 10 μM MK-4, or vehicle for indicated times. Total RNA was isolated using the ISOGEN reagent (Nippon Gene, Tokyo, Japan). First strand cDNA was generated from RNase-free DNase I-treated total RNA by using the SuperScript II reverse transcriptase (Invitrogen) and oligo$(dT)_{20}$ primer. For PCR amplification, the primer sequences were: human *TSK*, 5′-CTGAGCGACGTGAACCTTAGC-3′ and 5′-CCTGACTGTGCGTCGTGAAG-3′; human *MATN2*, 5′-ACAGATCCTTTGCCTGTCAGTGT-3′ and 5′-GGTCCCCCAGAGCACAAGA-3′; human *CD14*, 5′-GACTGATGGCGGCTCTCTGT-3′ and 5′-TGTGGGCGTCTCCATTCC-3′; human *CYP3A4*, 5′-TTCAGCCCATCTCCTTTCATATTT-3′ and 5′-CAGTTGGGTGTTGAGGATGGA-3′; human *GAPDH*, 5′-GCCTGCCTGACCAAATGC-3′ and 5′-GTGGTCGTTGAGGGCAATG-3′. mRNAs were quantified by real-time PCR using SYBR green PCR master mix (Applied Biosystems) and the ABI Prism 7000 system (Applied Biosystems) based on SYBR Green I fluorescence. The evaluation of relative differences of PCR product amounts among the treatment groups was carried out by the comparative cycle threshold (C_T) method, using GAPDH as an external control (17).

The experiments were independently repeated at least three times, each performed in triplicate. For cycloheximide treatment, cells were preincubated with the compound (10 μg/ml) 2 h prior to the stimulation by SXR ligands.

RNA Interference—Small interfering RNA (siRNA) duplexes to target human *SXR* and *TSK* were synthesized by Qiagen (Qiagen, Tokyo, Japan). The siRNA target sequences were: *SXR*, 5′-GGCCACTGGCTATCACTTC-3′ (18) and *TSK*, 5′-CCTGCTCACCAGCATCTCA-3′. The siRNA specific to the luciferase gene (Luciferase GL2 Duplex, Dharmacon, Lafayette, CO) and nonspecific control VII (Dharmacon) was used as control. Cells were transfected with siRNA (70 nM) using GeneSilencer reagent (Genlantis, San Diego, CA) for 48 h, and further maintained in the culture medium containing 10% dextran-charcoal-stripped FBS with or without ligand stimulation for indicated times.

Collagen Accumulation Assay by Sirius Red Staining—Cells were cultured until confluence (day 0), and the medium was replaced by the osteoblast differentiation medium (α-minimal essential medium containing 10% FBS, 2 mM glutamine, 50 μg/ml ascorbic acid, and 5 mM β-glycerophosphate) with or without MK-4 (1 μM). Cells were fixed with Bouin's fluid (8.3% formaldehyde and 4.8% acetic acid in saturated aqueous picric acid) for 1 h at room temperature, rinsed with water, and stained with 1 mg/ml of sirius red dye (Direct Red 80) (Sigma) in saturated aqueous picric acid for 1 h. Cells were treated with 0.01 N HCl, and then the stain was extracted by 0.1 N NaOH. The absorbance of the dye solution was measured at 550 nm (19). In experiments with warfarin [3-(α-acetonylbenzyl)-4-hydroxycoumarin, Sigma) treatment, cells at confluence were pretreated with vehicle or warfarin at 5 μM or 25 μM for 1 day, then treated with vehicle or vitamin K_2 (1 μM) for another 3 days in the presence of warfarin (final concentration; 2.5 μM or 12.5 μM). In siRNA treatment experiments, cells were treated with the siRNA twice, 2 days before day 0 and on day 0.

Statistical Analysis—Differences between two groups were analyzed using two-sample, two-tailed Student's *t* test. A *p* value less than 0.05 was considered to be significant. All data are presented in the text and figures as the mean ± S.D.

RESULTS

Construction of SXR Expression Vectors and Generation of Osteoblastic Cells Stably Expressing SXR—Our previous studies showed the direct effect of vitamin K_2 on bone marker expression in osteoblastic cells. Although SXR is endogenously expressed in osteoblastic cells, it has been shown that the expression level is lower than that in cells derived from the intestine. Therefore, to identify vitamin K_2 and SXR target genes in osteoblastic cells, we generated MG63 cells stably expressing SXR. These cells respond more robustly to SXR ligands than do wild type MG63 cells. We constructed two FLAG-tagged expression vectors containing full-length SXR (FLAG-SXR) and SXR fused to the C-terminal portion of the VP16 activation domain (FLAG-VP16C-SXR). Both vitamin K_2 and RIF increased the transcriptional activity of the trimerized SXR response elements derived from the *CYP3A4* promoter in MG63 cells transiently transfected with FLAG-SXR or FLAG-VP16C-SXR (Fig. 1*A*). We also constructed an expression vector fusing SXR to the full-length VP16 activation domain. This construct was constitutively active in the absence of ligand stimulation (data not shown). In contrast, FLAG-VP16C-SXR retained the ligand-dependent activation while it had substantial higher basal transcription level than FLAG-SXR.

For further quantitative analysis of SXR actions in osteoblastic cells, we generated the stable cell lines expressing *SXR* constructs in MG63 cells. For either FLAG-SXR or FLAG-VP16C-SXR, we obtained two MG63 clones each with different expression levels (Fig. 1*B*).

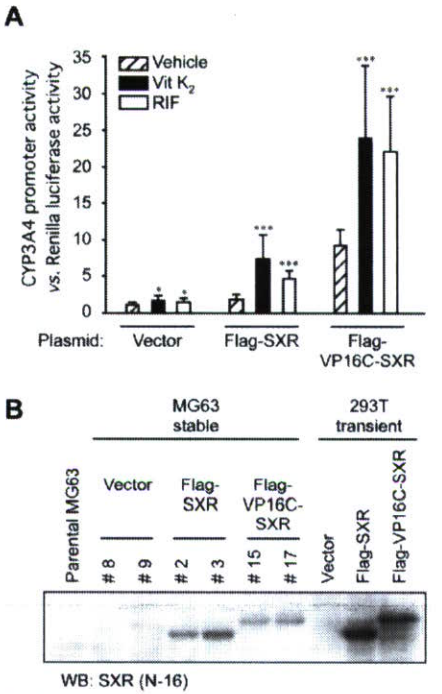

FIGURE 1. **Construction of SXR expression vectors and generation of osteoblastic cells stably expressing SXR.** *A*, activation of *CYP3A4* promoter activity by vitamin K_2 (*Vit K_2*) or RIF treatment. MG63 cells were cotransfected with tk-$(CYP3A4)_3$-Luc, pRL-CMV, and SXR expression vectors (FLAG-SXR and FLAG-VP16C-SXR) or empty vector. Twenty-four hours after transfection, cells were treated with RIF (20 μM), vitamin K_2 (20 μM), or vehicle (0.2% ethanol) for 30 h in fresh media. Firefly luciferase reporter activity was determined and normalized to the *Renilla* luciferase transfection control. Data are expressed as fold induction of luciferase activity by ligands *versus* vehicle in vector-transfected cells. *, $p < 0.05$; ***, $p < 0.001$ (by Student's *t* test). *B*, generation of MG63 cells stably expressing SXR constructs. SXR protein expression in MG63/FLAG-SXR clones #2 and #3 and MG63/FLAG-VP16C-SXR clones #15 and #17 was confirmed by Western blotting (*WB*) using anti-SXR antibody.

Identification of Genes Up-regulated by SXR Ligand in Osteoblastic Cells by GeneChip Analysis—To identify dual up-regulated genes by vitamin K_2 and RIF treatment in osteoblastic cells, we prepared biotin-labeled cRNA samples from MG63 cells expressing FLAG-VP16C-SXR treated with vitamin K_2, RIF, or vehicle. The Affymetrix U133A GeneChip array represents more than 18,000 human transcripts from ~14,000 genes. Analysis of the MG63 samples was performed by hybridizing aliquots of cRNA to the GeneChip arrays. Seventy-seven transcripts were induced 2-fold or greater by vitamin K_2, whereas 100 transcripts were induced by RIF. Eighteen transcripts were up-regulated by both SXR ligands. Therefore, we infer that these are potential SXR target genes.

Table 1 shows the list of 18 transcripts from 14 distinct genes up-regulated by vitamin K_2 and RIF. It is notable that a prototypical SXR-responsive gene ATP-binding cassette subfamily B or multidrug resistance 1 (*MDR1*) (20) was most significantly up-regulated by either vitamin K_2 or RIF. Among these SXR target molecules, we were particularly interested in three genes due to their putative bone-related functions. There were a small leucine-rich proteoglycan named tsukushi

Downloaded from www.jbc.org at SAITAMA IKA DAIGAKU on November 24, 2006

TABLE 1

Dual up-regulated genes by 48-h treatment with vitamin K_2 (10 μM) or RIF (10 μM) in MG63/FLAG-VP16C-SXR cells identified by GeneChip analysis

Gene annotation was determined based on the probe set ID by the Array Finder on the Affymetrix web site.

Probe set ID	Ensemble ID	Gene symbol	Description	-Fold increase over control	
				Vitamin K_2	RIF
209994_s_at	ENSG00000085563	*ABCB1*	ATP-binding cassette, subfamily B (MDR/TAP), member 1	6.06	4.29
209993_at	ENSG00000085563	*ABCB1*	ATP-binding cassette, subfamily B (MDR/TAP), member 1	4.29	4.00
205357_s_at	ENSG00000144891	*AGTR1*	Angiotensin II receptor, type 1	2.83	2.46
212938_at	ENSG00000142156	*COL6A1*	Collagen, type VI, α1	2.64	2.14
201743_at	ENSG00000170458	*CD14*	CD14 antigen	2.46	4.92
209771_x_at	ENSG00000185275	*CD24*	CD24 antigen (small cell lung carcinoma cluster 4 antigen)	2.46	2.30
211839_s_at	ENSG00000184371	*CSF1*	Colony-stimulating factor 1 (macrophage)	2.46	2.30
212937_s_at	ENSG00000142156	*COL6A1*	Collagen, type VI, α1	2.46	2.14
216379_x_at	ENSG00000185275	*CD24*	CD24 antigen (small cell lung carcinoma cluster 4 antigen)	2.46	2.30
202350_s_at	ENSG00000132561	*MATN2*	Matrilin-2	2.30	6.96
203632_s_at	ENSG00000167191	*GPRC5B*	G protein-coupled receptor, family C, group 5, member B	2.30	5.28
211653_x_at	ENSG00000151632	*AKR1C2*	Aldo-keto reductase family 1, member C2	2.30	3.73
218245_at	ENSG00000182704	*TSK*	Likely ortholog of chicken tsukushi	2.30	2.64
218854_at	ENSG00000111817	*SART2*	Squamous cell carcinoma antigen recognized by T cells 2	2.30	5.28
210002_at	ENSG00000141448	*GATA6*	GATA-binding protein 6	2.14	2.14
216594_x_at	ENSG00000187134	*AKR1C1*	Aldo-keto reductase family 1, member C1	2.14	3.73
204151_x_at	ENSG00000187134	*AKR1C1*	Aldo-keto reductase family 1, member C1	2.00	3.48
212268_at	ENSG00000021355	*SERPINB1*	Serine (or cysteine) proteinase inhibitor, clade B (ovalbumin), member 1	2.00	2.83

(*TSK*), an extracellular matrix protein matrilin-2 (*MATN2*), and CD14 antigen.

Ligand-dependent Induction of SXR Target Genes in Osteoblastic Cells—We next validated whether mRNA expression levels for these three genes could be modulated by vitamin K_2 and RIF in MG63 cells ectopically expressing either FLAG-VP16C-SXR or FLAG-SXR using quantitative real-time RT-PCR analysis (Fig. 2). All of the three SXR target genes, *TSK*, *MATN2*, and *CD14*, were up-regulated by SXR ligands. The time-dependent expression profiles of those genes in FLAG-VP16C-SXR and FLAG-SXR-expressing cells were quite similar, although the amplitude of induction was different in these cells. In both cell types, RIF generated stronger induction of mRNA expression than vitamin K_2. Nevertheless, the maximal induction by vitamin K_2 was greater than 2-fold for all three genes in both cell types.

Transcriptional Regulation of SXR Target Genes in Osteoblastic Cells—We next asked whether the induction of SXR target genes was dependent on direct activation of transcription or required ongoing protein synthesis. MG63 cells overexpressing FLAG-SXR were treated with vitamin K_2 or RIF in the presence or absence of cycloheximide. The ligand-dependent up-regulation of the three SXR target genes, including *TSK*, *MATN2*, and *CD14*, was not affected by cycloheximide treatment, indicating that the transcriptional regulation of those genes was independent of protein synthesis (Fig. 3*A*).

To further demonstrate the requirement for SXR in the regulation of *TSK*, *MATN2*, and *CD14*, we investigated the effects of siRNA on the ligand-dependent induction of gene expression. Forty-eight hour treatment with a specific siRNA duplex against SXR (siRNA-SXR), but not with a control siRNA directed against luciferase (siRNA-Luc), reduced the SXR protein level by more than 60% in MG63/SXR clone #3 (Fig. 3*B*). The effectiveness of the SXR-specific siRNA was confirmed as the vitamin K_2-induced up-regulation of CYP3A4 mRNA expression was diminished by the SXR siRNA in MG63/SXR clone #3 (Fig. 3*C*). In that cell system, the SXR siRNA significantly reduced either vitamin K_2- or RIF-activated mRNA expression for *TSK*, *MATN2*, and *CD14* (Fig. 3*D*).

We next examined whether the SXR siRNA duplex reduced the endogenous expression of SXR protein (Fig. 4). The endogenous level of SXR protein in parental MG63 cells was barely detected in Western blot analysis (Fig. 4*A*). Thus, we immunoprecipitated MG63 cell lysates with a polyclonal antibody against the hinge and a part of ligand-binding domain of SXR (H-160) and immunodetected SXR protein by another polyclonal antibody against the SXR N terminus (N-16). The enrichment of SXR protein in immunoprecipitated fraction was also confirmed in COS1 cells transiently transfected with FLAG-SXR (Fig. 4*A*). Based on this evaluation system, we could show that the SXR siRNA reduced the level of endogenous SXR protein in MG63 (Fig. 4*B*).

Since we confirmed that the SXR siRNA duplex was effective to inhibit the endogenous expression of SXR protein, we next analyzed whether the SXR siRNA reduced the expression of the SXR target genes in parental MG63 cells. The SXR siRNA at 14 or 70 nM could significantly reduce endogenous SXR mRNA levels in natural MG63 cells (Fig. 4*C*). The expression of *TSK*, *MATN2*, and *CD14* was all up-regulated by either vitamin K_2 or RIF, indicating that the three genes were *bona fide* SXR targets in parental MG63 cells (Fig. 4*D*). This ligand-dependent induction of all three genes was significantly reduced by the SXR siRNA transfection in parental MG63 cells (Fig. 4*D*).

Vitamin K_2 and TSK Stimulate Collagen Accumulation in Osteoblastic Cells—TSK was recently identified as a bone morphogenic protein-binding protein that belongs to the small leucin-rich proteoglycan family (21), which is implicated as an extracellular matrix component. Because small leucine-rich proteoglycans such as biglycan and decorin are known to interact with matrilin-1 in the cartilage extracellular matrix (22), TSK and matrilin-1-related MATN2 are likely to be involved in the assembly of extracellular matrix, including collagens, in osteoblastic cells.

We next asked whether vitamin K_2 promoted collagen production or stabilized collagen levels. We evaluated collagen amounts by staining cells with a strong anionic dye Sirius red, which reacted with basic groups present in collagens via its sulfonic acid groups. It has been reported that type I and III collagens are well stained by Sirius red (19). Four-day treatment with vitamin K_2 exhibited significantly more intense staining by Sirius red compared with vehicle in MG63 cells under conditions favoring osteoblast differentiation (Fig. 5*A*). We also examined collagen accumulation in murine MC3T3-E1 cells, one of the cell lines with a close-to-normal osteoblast phenotype. Four-day treatment with vitamin K_2 increased collagen accumulation by 15.0% in this cell line. Note that RIF (1 μM) also increased collagen accumulation by 13.6% in MG63 cells after 4-day treatment. Moreover, the vitamin K_2-stimulated collagen accumulation in MG63 cells was not affected by warfarin treatment, suggesting that the γ-carboxylase-dependent vitamin K_2 action may not be involved (Fig. 5*B*).

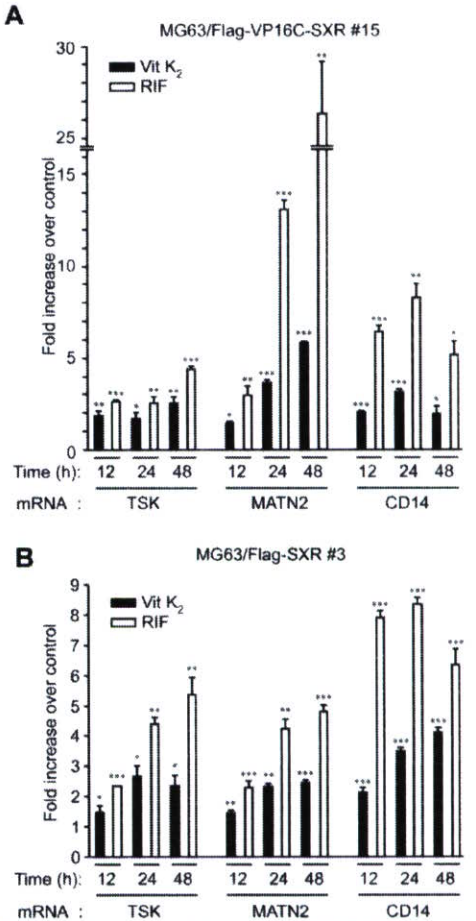

FIGURE 2. **Validation of ligand-induced up-regulation of SXR target genes in osteoblastic cells stably expressing SXR.** MG63/FLAG-VP16C-SXR clone #15 (*A*) and MG63/FLAG-SXR #3 (*B*) cells were treated with vitamin K_2 (*Vit K_2*) (10 μM) or RIF (10 μM) for indicated times. mRNA levels for tsukushi (*TSK*), *MATN2*, and *CD14* were determined by quantitative RT-PCR using *GAPDH* as an external control. Data represent fold induction of mRNA levels by ligands *versus* vehicle. *, $p < 0.05$; **, $p < 0.01$; ***, $p < 0.001$ (by Student's *t* test).

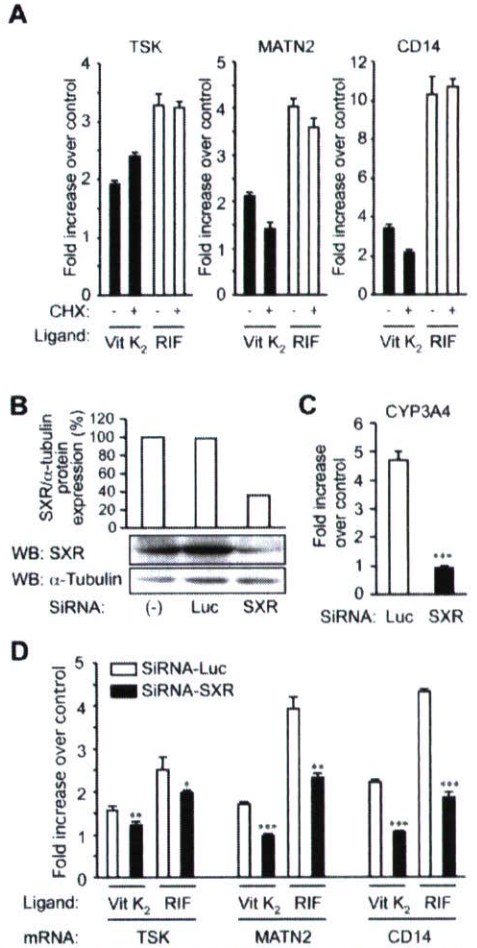

FIGURE 3. **Ligand-induced up-regulation of TSK, MATN2, and CD14 are directly regulated by SXR.** *A*, effects of cycloheximide (*CHX*) on transcription of SXR target genes. MG63/FLAG-SXR #3 cells were pretreated with CHX (10 μg/ml) or vehicle for 2 h, then stimulated by vitamin K_2 (*Vit K_2*) (10 μM) or RIF (10 μM) for 24 h. *B*, reduction of SXR expression by siRNA directed against SXR. MG63/FLAG-SXR cells #3 were transfected with siRNA against luciferase (*Luc*) or SXR (70 nM each) for 48 h. The SXR protein level was analyzed by Western blotting (*WB*). Data in the *upper graph* represent quantified levels of SXR normalized to α-tubulin as determined by NIH image software. *C*, effects of SXR siRNA transfection on vitamin K_2-induced up-regulation of *CYP3A4* mRNA in MG63/FLAG-SXR #3 cells. *D*, effects of SXR siRNA transfection on ligand-induced up-regulation of *TSK*, *MATN2*, and *CD14* mRNA in MG63/FLAG-SXR #3 cells. *, $p < 0.05$; **, $p < 0.01$; ***, $p < 0.001$ (by Student's *t* test).

To determine whether TSK plays a role in the vitamin K_2-stimulated collagen accumulation, MG63 cells stably expressing FLAG-tagged TSK were generated. Two TSK-overexpressing clones were isolated, as confirmed by Western blot analysis (Fig. 5*C*). MG63 clones overexpressing TSK showed significantly enhanced collagen accumulation in 7-day culture under differentiation conditions compared with vector-transfected cells (Fig. 5*D*). During the 7-day culture, the growth of MG63 clones expressing TSK and vector was almost stationary, and there was no significant difference in proliferation between the two groups as determined by the proliferation assay using WST-8 (2-(2-methoxy-4-nitrophenyl)-3-(4-nitrophenyl)-5-(2,4-disulfophenyl)-2*H*-tetrazolium monosodium salt) reagent (Nacalai Tesque, Kyoto, Japan; Ref. 23) (data not shown).

We further investigated whether SXR or TSK loss-of-function affected collagen accumulation in MG63 cells. A siRNA duplex against *TSK* (70 nM) reduced the target mRNA levels by more than 40% in parental MG63 cells, verifying its efficiency (Fig. 6*A*). The *SXR*- and *TSK*-specific siRNA significantly reduced the vitamin K_2-stimulated

Downloaded from www.jbc.org at SAITAMA IKA DAIGAKU on November 24, 2006

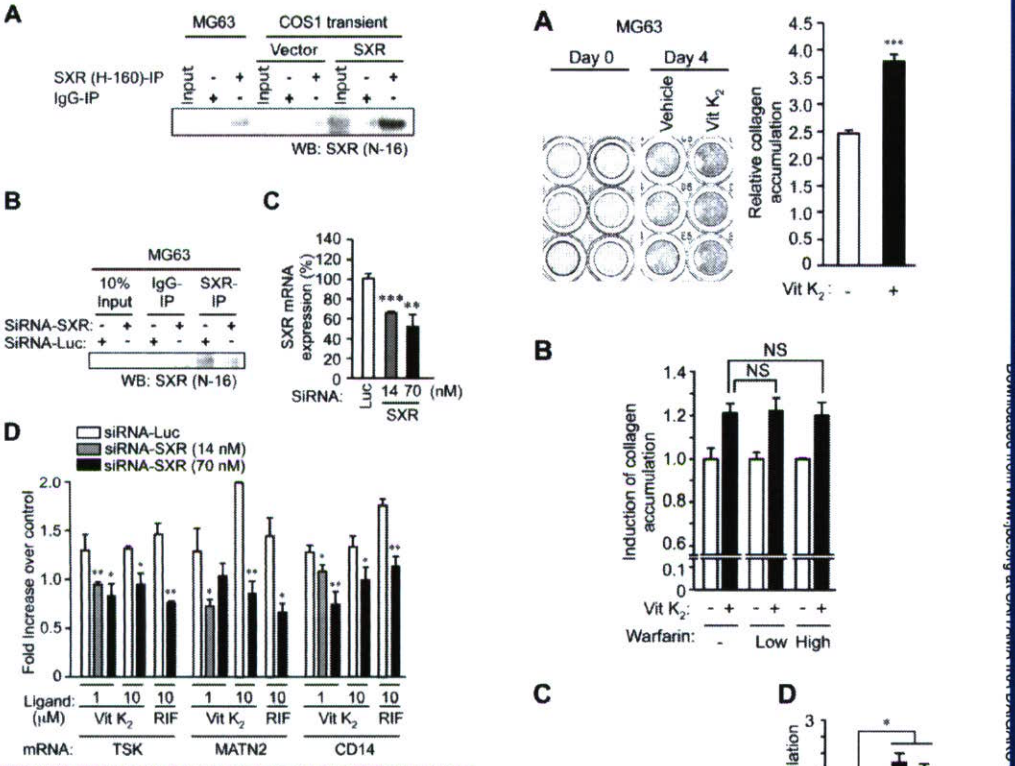

FIGURE 4. ***SXR* siRNA represses ligand-induced up-regulation of SXR target genes in osteoblastic cells.** *A*, detection of endogenous SXR protein enriched by immunoprecipitation (*IP*) in parental MG63 cells. Lysates from MG63 cells and COS1 cells transiently transfected with SXR or empty vector were immunoprecipitated by anti-SXR antibody (H-160), and SXR protein was immunodetected by anti-SXR (N-16) antibody. *B*, reduction of SXR protein level by *SXR* siRNA in MG63 cells. Cells were transfected with *SXR* or luciferase (*Luc*) siRNA for 48 h, and SXR protein level was analyzed as described for *A*. *C*, concentration-dependent effects of *SXR* siRNA on endogenous *SXR* mRNA levels in MG63 cells. Cells were transfected with *SXR* siRNA or control luciferase siRNA at the indicated concentrations for 24 h. *D*, effects of *SXR* siRNA on ligand-induced up-regulation of *TSK*, *MATN2*, and *CD14* mRNA in MG63 cells. After 48-h treatment with siRNA (14 or 70 nM), cells were stimulated with vitamin K_2 (1 or 10 μM) or RIF (10 μM) for 12 h. *, $p < 0.05$; **, $p < 0.01$; ***, $p < 0.001$ (by Student's *t* test). *WB*, Western blotting.

accumulation of collagen in parental MG63 cells compared with luciferase siRNA (Fig. 6, *B* and *C*).

Taken together, our results indicate that vitamin K_2 promotes collagen accumulation in osteoblastic cells via the SXR signaling pathway.

DISCUSSION

In the present study, we identified novel SXR target genes that are up-regulated by both vitamin K_2 and RIF in osteoblastic cells using oligonucleotide microarrays. The effectiveness of vitamin K_2 and RIF treatment was evident by their ability to up-regulate mRNA levels for the well known SXR target gene MDR1. SXR-dependent induction of TSK, MATN2, and CD14 has not been previously reported. Functional analyses indicated that vitamin K_2 can enhance collagen accumulation in osteoblastic cells and that SXR may play a role in the collagen assembly mechanism. Taken together, these results provide important evidence that vitamin K_2 directly activates SXR to promote extracellular matrix formation in osteoblastic cells.

FIGURE 5. **Vitamin K_2 (*Vit K_2*) and TSK expression promote collagen accumulation in osteoblastic cells.** *A*, MG63 cells at confluence were maintained in osteoblast differentiation medium containing ascorbic acid and β-glycerophosphate in the presence or absence of vitamin K_2 (1 μM) for 4 days, and collagen accumulation was analyzed by Sirius red staining (*left panel*). The collagen level was quantified by the absorbance at 550 nm (*right panel*). ***, $p < 0.001$ (by Student's *t* test). *B*, the vitamin K_2-stimulated collagen accumulation was not affected by a γ-carboxylase inhibitor warfarin. Cells at confluence were pretreated with vehicle or warfarin (low, 5 μM; high, 25 μM) for 1 day and incubated with vehicle or vitamin K_2 (1 μM) for another 3 days (warfarin final concentration; low, 2.5 μM; high, 12.5 μM). *NS*, not significant. *C*, generation of MG63 cells stably expressing TSK-FLAG construct. Expression of TSK protein in MG63/TSK-FLAG clones #52 and #68 was immunodetected by anti-FLAG antibody. *D*, TSK overexpression augments collagen accumulation in MG63 cells. Cells at confluence were maintained in the differentiation medium for 7 days, and collagen accumulation was analyzed by Sirius red staining as described for *A*. *, $p < 0.05$ (by Student's *t* test). *WB*, Western blotting.

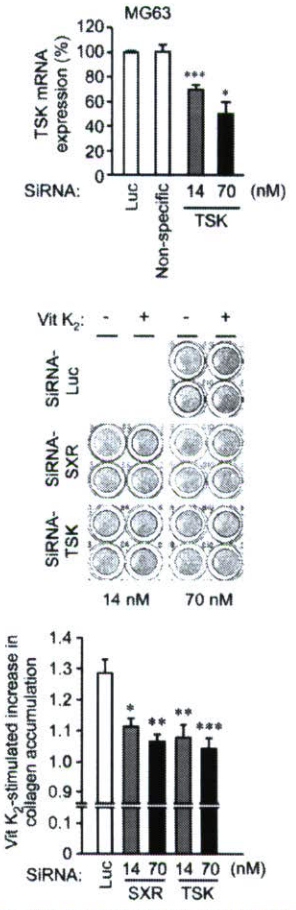

FIGURE 6. **Involvement of SXR and TSK in vitamin K_2 (*Vit K_2*)-mediated collagen accumulation.** *A*, effects of *TSK*-specific siRNA on *TSK* mRNA level in MG63 cells. Cells were transfected with luciferase (*Luc*) siRNA, nonspecific siRNA, or *TSK* siRNA (14 or 70 nM) for 48 h. *B*, *SXR* and *TSK* siRNAs reduce vitamin K_2-mediated collagen accumulation in MG63 cells. Confluent cells in differentiation medium were transfected with siRNA at the indicated concentrations twice every 2 days. Collagen accumulation in 4-day culture in the presence of vitamin K_2 (1 μM) or vehicle was determined by Sirius red staining. *C*, vitamin K_2-stimulated increase in collagen accumulation in *B* was quantified by the absorbance at 550 nm. Each column shows fold induction by vitamin K_2 normalized to that by vehicle and indicated siRNA treatment. *, $p < 0.05$; **, $p < 0.01$; ***, $p < 0.001$ (by Student's *t* test, using the fold induction by vitamin K_2 in Luc siRNA-treated cells as a control).

While vitamin K has been well characterized as a cofactor of γ-carboxylase, we have previously showed that vitamin K_2 could have an anabolic effect on osteoblasts by up-regulating the mRNA levels for bone marker genes through SXR (13). Our present findings that vitamin K_2 promotes extracellular matrix formation by activating SXR to up-regulate the *TSK* mRNA level provides further evidence that vitamin K_2 stimulates bone formation via altering gene expression.

The vitamin K_2-stimulated collagen accumulation through the activation of SXR signaling may be beneficial to decrease bone fractures. Since bone collagen content is reduced in aged and osteoporotic bones (24), the amount and quality of collagen fibrils may be important for maintaining bone strength. Therefore, in addition to its role as an enzymatic cofactor that facilitates γ-carboxylation of bone Gla proteins, vitamin K_2 may serve as a critical factor regulating bone matrix formation.

The identification of new SXR-mediated vitamin K_2 target genes in bone cells has implications for bone homeostasis. Human TSK is an ortholog of chicken TSK, which was recently identified as a bone morphogenic protein-binding protein that plays a role in the development of primitive streak and Hensen's node formation during chick gastrulation (21). TSK, like other small leucine-rich proteoglycans, may play a role in bone formation. Small leucine-rich proteoglycans such as biglycan, decorin, and chondroadherin have been characterized as collagen-binding proteins in bone tissues (25–28). Biglycan-deficient mice exhibit reduced bone mass (29), and biglycan/decorin double-deficient mice show a more severe phenotype of osteoporosis (30).

MATN2 is expressed in various osteoblastic cells as well as mouse primary osteoblasts (31, 32), and it was shown to interact with collagen I (33). The involvement of matrilin proteins together with small leucine-rich proteoglycans in the collagen assembly is exemplified by the complex of matrilin-1 and biglycan/decorin that act as a linkage between the collagen II and collagen VI fibrils (22).

The CD14 antigen is a lipopolysaccharide-binding protein expressed in monocytes where it initiates the innate immune response to bacterial invasion (34). The soluble form of CD14 is an inducer of B-lymphocyte growth and differentiation (35), and B-lymphocyte lineage cells regulate osteoclastogenesis by expressing receptor activator of NF-κB ligand (RANKL) and serving as osteoclast progenitor cells (36). This suggests a role for CD14 in osteoclastogenesis through B-lymphocyte lineage cells. A role for CD14 in bone formation is also suggested by a report showing that the antigen was up-regulated during the differentiation of mouse primary osteoblasts (37). Because osteoclastic resorption and osteoblast formation are coupled in the bone remodeling process, CD14 may play a role as a "coupling factor" between the two functions. In this context, it is interesting that CD24 was identified as an up-regulated gene by both vitamin K_2 and RIF in osteoblastic cells in our microarray analysis because CD24 is also a cell surface antigen predominantly expressed in B-cell lineage cells and it has been implicated in both activation and differentiation of B lymphocytes (38).

In summary, we conclude that SXR mediates vitamin K_2-activated transcription of extracellular matrix-related genes as well as cell surface markers of B-lymphoid lineage cells that may be involved in both osteoblastogenesis and osteoclastogenesis. These results would provide new insight into vitamin K_2 and SXR action on bone homeostasis and osteoporosis treatment and further support the idea that vitamin K_2 acts as a transcriptional mediator of gene expression in bone cells, in addition to its well known role as an enzymatic cofactor.

Acknowledgments—We thank T. Suzuki and R. Nozawa for their technical assistance.

REFERENCES

1. Akedo, Y., Hosoi, T., Inoue, S., Ikegami, A., Mizuno, Y., Kaneki, M., Nakamura, T., Ouchi, Y., and Orimo, H. (1992) *Biochem. Biophys. Res. Commun.* **187,** 814–820
2. Akiyama, Y., Hara, K., Tajima, T., Murota, S., and Morita, I. (1994) *Eur. J. Pharmacol.* **263,** 181–185
3. Hara, K., Akiyama, Y., Nakamura, T., Murota, S., and Morita, I. (1995) *Bone (N.Y.)* **16,** 179–184

Downloaded from www.jbc.org at SAITAMA IKA DAIGAKU on November 24, 2006

4. Koshihara, Y., and Hoshi, K. (1997) *J. Bone Miner. Res.* **12,** 431–438
5. Koshihara, Y., Hoshi, K., Okawara, R., Ishibashi, H., and Yamamoto, S. (2003) *J. Endocrinol.* **176,** 339–348
6. Shiraki, M., Shiraki, Y., Aoki, C., and Miura, M. (2000) *J. Bone Miner. Res.* **15,** 515–521
7. Booth, S. L., Tucker, K. L., Chen, H., Hannan, M. T., Gagnon, D. R., Cupples, L. A., Wilson, P. W., Ordovas, J., Schaefer, E. J., Dawson-Hughes, B., and Kiel, D. P. (2000) *Am. J. Clin. Nutr.* **71,** 1201–1208
8. Plaza, S. M., and Lamson, D. W. (2005) *Altern. Med. Rev.* **10,** 24–35
9. Price, P. A., and Baukol, S. A. (1980) *J. Biol. Chem.* **255,** 11660–11663
10. Vergnaud, P., Garnero, P., Meunier, P. J., Breart, G., Kamihagi, K., and Delmas, P. D. (1997) *J. Clin. Endocrinol. Metab.* **82,** 719–724
11. Luo, G., Ducy, P., McKee, M. D., Pinero, G. J., Loyer, E., Behringer, R. R., and Karsenty, G. (1997) *Nature* **386,** 78–81
12. Murshed, M., Schinke, T., McKee, M. D., and Karsenty, G. (2004) *J. Cell Biol.* **165,** 625–630
13. Tabb, M. M., Sun, A., Zhou, C., Grun, F., Errandi, J., Romero, K., Pham, H., Inoue, S., Mallick, S., Lin, M., Forman, B. M., and Blumberg, B. (2003) *J. Biol. Chem.* **278,** 43919–43927
14. Blumberg, B., Sabbagh, W., Jr., Juguilon, H., Bolado, J., Jr., van Meter, C. M., Ong, E. S., and Evans, R. M. (1998) *Genes Dev.* **12,** 3195–3205
15. Xie, W., Barwick, J. L., Simon, C. M., Pierce, A. M., Safe, S., Blumberg, B., Guzelian, P. S., and Evans, R. M. (2000) *Genes Dev.* **14,** 3014–3023
16. Xie, W., Barwick, J. L., Downes, M., Blumberg, B., Simon, C. M., Nelson, M. C., Neuschwander-Tetri, B. A., Brunt, E. M., Guzelian, P. S., and Evans, R. M. (2000) *Nature* **406,** 435–439
17. Livak, K. J., and Schmittgen, T. D. (2001) *Methods* (*San Diego*) **25,** 402–408
18. Bhalla, S., Ozalp, C., Fang, S., Xiang, L., and Kemper, J. K. (2004) *J. Biol. Chem.* **279,** 45139–45147
19. Tullberg-Reinert, H., and Jundt, G. (1999) *Histochem. Cell Biol.* **112,** 271–276
20. Geick, A., Eichelbaum, M., and Burk, O. (2001) *J. Biol. Chem.* **276,** 14581–14587
21. Ohta, K., Lupo, G., Kuriyama, S., Keynes, R., Holt, C. E., Harris, W. A., Tanaka, H., and Ohnuma, S. (2004) *Dev. Cell* **7,** 347–358
22. Wiberg, C., Klatt, A. R., Wagener, R., Paulsson, M., Bateman, J. F., Heinegard, D., and Morgelin, M. (2003) *J. Biol. Chem.* **278,** 37698–37704
23. Ogushi, T., Takahashi, S., Takeuchi, T., Urano, T., Horie-Inoue, K., Kumagai, J., Kitamura, T., Ouchi, Y., Muramatsu, M., and Inoue, S. (2005) *Cancer Res.* **65,** 3700–3706
24. Bailey, A. J., Wotton, S. F., Sims, T. J., and Thompson, P. W. (1993) *Connect. Tissue Res.* **29,** 119–132
25. Schonherr, E., Witsch-Prehm, P., Harrach, B., Robenek, H., Rauterberg, J., and Kresse, H. (1995) *J. Biol. Chem.* **270,** 2776–2783
26. Mizuno, M., Fujisawa, R., and Kuboki, Y. (1996) *Calcif. Tissue Int.* **59,** 163–167
27. Mansson, B., Wenglen, C., Morgelin, M., Saxne, T., and Heinegard, D. (2001) *J. Biol. Chem.* **276,** 32883–32888
28. Waddington, R. J., Roberts, H. C., Sugars, R. V., and Schonherr, E. (2003) *Eur. Cell Mater.* **6,** 12–21
29. Xu, T., Bianco, P., Fisher, L. W., Longenecker, G., Smith, E., Goldstein, S., Bonadio, J., Boskey, A., Heegaard, A. M., Sommer, B., Satomura, K., Dominguez, P., Zhao, C., Kulkarni, A. B., Robey, P. G., and Young, M. F. (1998) *Nat. Genet.* **20,** 78–82
30. Corsi, A., Xu, T., Chen, X. D., Boyde, A., Liang, J., Mankani, M., Sommer, B., Iozzo, R. V., Eichstetter, I., Robey, P. G., Bianco, P., and Young, M. F. (2002) *J. Bone Miner. Res.* **17,** 1180–1189
31. Deak, F., Piecha, D., Bachrati, C., Paulsson, M., and Kiss, I. (1997) *J. Biol. Chem.* **272,** 9268–9274
32. Piecha, D., Muratoglu, S., Morgelin, M., Hauser, N., Studer, D., Kiss, I., Paulsson, M., and Deak, F. (1999) *J. Biol. Chem.* **274,** 13353–13361
33. Piecha, D., Wiberg, C., Morgelin, M., Reinhardt, D. P., Deak, F., Maurer, P., and Paulsson, M. (2002) *Biochem. J.* **367,** 715–721
34. Wright, S. D., Ramos, R. A., Tobias, P. S., Ulevitch, R. J., and Mathison, J. C. (1990) *Science* **249,** 1431–1433
35. Filipp, D., Alizadeh-Khiavi, K., Richardson, C., Palma, A., Paredes, N., Takeuchi, O., Akira, S., and Julius, M. (2001) *Proc. Natl. Acad. Sci. U. S. A.* **98,** 603–608
36. Manabe, N., Kawaguchi, H., Chikuda, H., Miyaura, C., Inada, M., Nagai, R., Nabeshima, Y., Nakamura, K., Sinclair, A. M., Scheuermann, R. H., and Kuro-o, M. (2001) *J. Immunol.* **167,** 2625–2631
37. Roman-Roman, S., Garcia, T., Jackson, A., Theilhaber, J., Rawadi, G., Connolly, T., Spinella-Jaegle, S., Kawai, S., Courtois, B., Bushnell, S., Auberval, M., Call, K., and Baron, R. (2003) *Bone* (*N.Y.*) **32,** 474–482
38. Kay, R., Rosten, P. M., and Humphries, R. K. (1991) *J. Immunol.* **147,** 1412–1416

Downloaded from www.jbc.org at SAITAMA IKA DAIGAKU on November 24, 2006

nature Vol 446|19 April 2007|doi:10.1038/nature05732

LETTERS

TRIM25 RING-finger E3 ubiquitin ligase is essential for RIG-I-mediated antiviral activity

Michaela U. Gack[1,2], Young C. Shin[1], Chul-Hyun Joo[1,3], Tomohiko Urano[4,5], Chengyu Liang[1], Lijun Sun[6], Osamu Takeuchi[7], Shizuo Akira[7], Zhijian Chen[6], Satoshi Inoue[4,5] & Jae U. Jung[1]

Retinoic-acid-inducible gene-I (RIG-I; also called DDX58) is a cytosolic viral RNA receptor that interacts with MAVS (also called VISA, IPS-1 or Cardif) to induce type I interferon-mediated host protective innate immunity against viral infection[1–6]. Furthermore, members of the tripartite motif (TRIM) protein family, which contain a cluster of a RING-finger domain, a B box/coiled-coil domain and a SPRY domain, are involved in various cellular processes, including cell proliferation and antiviral activity[7]. Here we report that the amino-terminal caspase recruitment domains (CARDs) of RIG-I undergo robust ubiquitination induced by TRIM25 in mammalian cells. The carboxy-terminal SPRY domain of TRIM25 interacts with the N-terminal CARDs of RIG-I; this interaction effectively delivers the Lys 63-linked ubiquitin moiety to the N-terminal CARDs of RIG-I, resulting in a marked increase in RIG-I downstream signalling activity. The Lys 172 residue of RIG-I is critical for efficient TRIM25-mediated ubiquitination and for MAVS binding, as well as the ability of RIG-I to induce antiviral signal transduction. Furthermore, gene targeting demonstrates that TRIM25 is essential not only for RIG-I ubiquitination but also for RIG-I-mediated interferon-β production and antiviral activity in response to RNA virus infection. Thus, we demonstrate that TRIM25 E3 ubiquitin ligase induces the Lys 63-linked ubiquitination of RIG-I, which is crucial for the cytosolic RIG-I signalling pathway to elicit host antiviral innate immunity.

A recent series of studies has identified RIG-I and melanoma differentiation-associated gene 5 (MDA5; also called IFIH1) as cytosolic receptors for viral double-stranded RNA and 5′ triphosphate RNA[2,4,6]. RIG-I and MDA5 belong to the DExD/H box RNA helicase family, the members of which contain two caspase recruitment domains (2CARD) in the N-terminal region and a potential ATP-dependent RNA helicase activity in the C-terminal region[8,9]. To decipher the cytosolic RIG-I-mediated antiviral signalling pathway, we attempted to identify cellular proteins associated with the N-terminal 2CARD of RIG-I and MDA5 using mammalian glutathione *S*-transferase (GST) fusion constructs. Polypeptides with apparent molecular masses of 52, 60 and 68 kDa were present specifically in the GST–RIG-I(2CARD) complex but not in the GST–MDA5(2CARD) complex or with GST alone (Fig. 1a). Notably, mass spectrometry and immunoblotting showed that these polypeptides were exclusively identified as ubiquitinated forms of GST–RIG-I(2CARD) (Supplementary Fig. 1a). To confirm RIG-I ubiquitination, HEK293T cells were co-transfected with Flag-tagged full-length RIG-I or a RIG-I mutant in which the 2CARD had been deleted (RIG-I(Δ2CARD)) together with haemagglutinin (HA)-tagged ubiquitin. RIG-I, but not RIG-I(Δ2CARD), was extensively ubiquitinated (Fig. 1b and Supplementary Fig. 1b). In addition, anti-HA immunoblotting detected ubiquitinated Flag-tagged RIG-I as multiple species with apparent molecular masses of 120–150 kDa, significantly larger than unmodified Flag–RIG-I (Fig. 1c, top left panel). Furthermore, Sendai virus infection and/or interferon (IFN)-β treatment resulted in the markedly increased ubiquitination of endogenously or exogenously expressed RIG-I (Fig. 1c and Supplementary Fig. 1c). These results indicate that RIG-I undergoes robust ubiquitination at its N-terminal 2CARD and that this ubiquitination apparently increases on viral infection.

To dissect further the ubiquitination of the 2CARD of RIG-I, which contains 18 lysine residues, the *in vivo* ubiquitinated forms of N-terminal GST-fused and C-terminal Flag-tagged RIG-I(2CARD) were purified and analysed by multi-dimensional liquid chromatography coupled with tandem mass spectrometry (LC/LC-MS/MS; Fig. 1a, d, bands 1–3). Both GST–RIG-I(2CARD) and Flag–RIG-I(2CARD) carried the ubiquitin peptides at Lys 99, 169, 172, 181, 190 or 193 (Fig. 1d). Additional mass spectrometry analysis showed that band 2 and 3 fragments carried the unique, branched Gly-Gly signature peptides primarily with the ubiquitin Lys 63 linkage (Fig. 1d). Furthermore, GST–RIG-I(2CARD) and full-length RIG-I were strongly ubiquitinated when HA-tagged wild-type ubiquitin or a K48R ubiquitin mutant was expressed, whereas their ubiquitination was significantly reduced upon expression of a K63R ubiquitin mutant protein (Supplementary Fig. 2). These results indicate that the second CARD of RIG-I is the primary site for Lys 63-linked ubiquitination.

To corroborate the ubiquitination of the 2CARD of RIG-I, six lysine residues were replaced with arginine (K→R) individually and in various combinations; these mutants were then tested for their ubiquitination level. The K172R mutation (alone or together with other mutations) caused near-complete loss of ubiquitination of the 2CARD of RIG-I (Fig. 1e and Supplementary Fig. 3a). In contrast, other K→R mutations had little or no effect on ubiquitination of the RIG-I 2CARD (Fig. 1e). As previously shown[10], wild-type GST–RIG-I(2CARD) potently induced IFN-β and NF-κB promoter activity (Fig. 1f and Supplementary Fig. 3b). GST–RIG-I(2CARD) mutants containing the K172R mutation alone or together with other mutations showed markedly reduced IFN-β and NF-κB promoter activation, consistent with their lack of ubiquitination; in contrast, other GST–RIG-I(2CARD) mutants induced IFN-β and NF-κB promoter activity as strongly as wild-type GST–RIG-I(2CARD) (Fig. 1f and Supplementary Fig. 3b). These results suggest that Lys 172 is the essential site for RIG-I 2CARD ubiquitination and signalling activity

[1]Department of Microbiology and Molecular Genetics and Tumor Virology Division, New England Primate Research Center, Harvard Medical School, 1 Pine Hill Drive, Southborough, Massachusetts 01772, USA. [2]Institute for Clinical and Molecular Virology, Friedrich-Alexander University Erlangen-Nuremberg, 91054 Erlangen, Germany. [3]Department of Microbiology, University of Ulsan College of Medicine, Seoul 138-736, South Korea. [4]Department of Geriatric Medicine, Graduate School of Medicine, The University of Tokyo, 7-3-1 Hongo, Bunkyo, Tokyo 113-8655, Japan. [5]Research Center for Genomic Medicine, Saitama Medical School, Saitama 350-124-2, Japan. [6]Department of Molecular Biology, University of Texas Southwestern Medical Center, Dallas, Texas 75390-9148, USA. [7]Department of Host Defense, Japan Science and Technology Agency, Osaka 565-0871, Japan

©2007 Nature Publishing Group

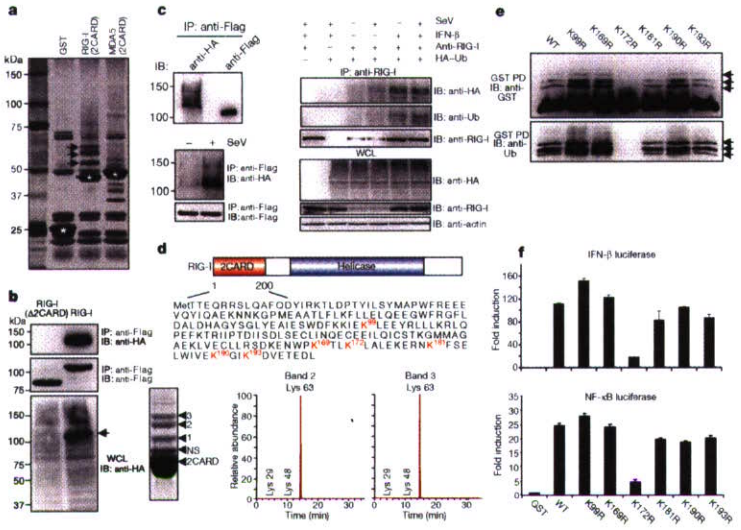

Figure 1 | The 2CARD of RIG-I undergoes robust ubiquitination. a, Silver-stained purified GST fusion complexes. Arrows, unique bands; asterisks, GST fusions. **b**, **c**, HEK293T cells transfected with Flag–RIG-I (**b**, and **c**, top-left) or Flag–RIG-I(Δ2CARD) (**b**) together with HA–ubiquitin were used for immunoprecipitation (IP) and immunoblotting (IB). WCL, whole cell lysate. **c**, Bottom-left panel: HEK293T cells transfected with Flag–RIG-I and HA–ubiquitin were mock-infected or infected with Sendai virus (SeV). Right: HEK293T cells transfected with HA–ubiquitin were treated (or not) with IFN-β and/or infected, as indicated, with Sendai virus before immunoprecipitation with anti-RIG-I antibody. **d**, The red lysine residues indicate the sites of ubiquitination. Bottom-left panel: Coomassie-blue-stained Flag–RIG-I(2CARD) complex. NS, nonspecific protein. Bottom-right panel: Lys 29/48/63-linked ubiquitination of RIG-I(2CARD)[21]. **e**, GST pull down (PD) of HEK293T cells transfected with GST–RIG-I(2CARD) or K→R mutants. Arrows indicate the ubiquitinated bands. WT, wild type. **f**, IFN-β and NF-κB promoter activity in GST–RIG-I(2CARD) or K→R mutant transfected cells. The results are expressed as means ± s.d. ($n = 3$).

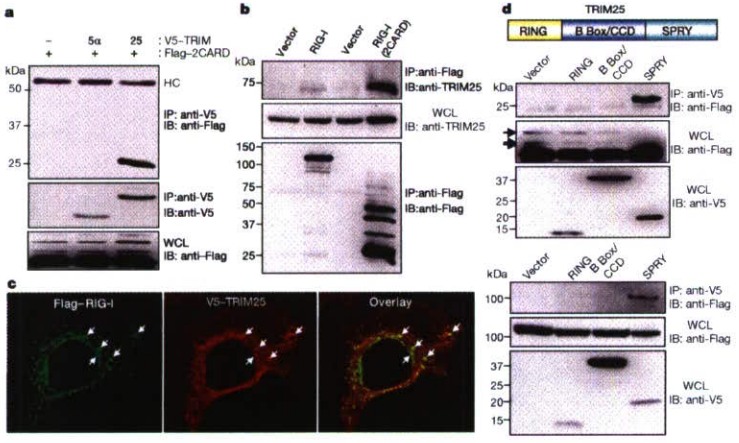

Figure 2 | Interaction between RIG-I and TRIM25. a, **b**, WCLs of HEK293T cells transfected with Flag–RIG-I(2CARD) and V5–TRIM25 or V5–TRIM5-α (**a**), or with Flag-RIG-I or Flag-RIG-I(2CARD) (**b**) were used for immunoprecipitation and immunoblotting, as indicated. **c**, Confocal images of Hela cells transiently transfected with Flag–RIG-I (green) and V5–TRIM25 (red). Arrows indicate representative co-localization between Flag–RIG-I and V5–TRIM25. Original magnification, ×100. **d**, WCLs of HEK293T cells transfected with Flag-tagged RIG-I(2CARD) (top) or full-length Flag–RIG-I (bottom) together with V5-tagged domains of TRIM25 were used for immunoprecipitation with V5 antibody, followed by immunoblotting with anti-Flag. WCLs were used for immunoblotting with anti-Flag and anti-V5 antibodies.

©2007 Nature Publishing Group

and that the extent of RIG-I 2CARD ubiquitination correlates strongly with its signal transduction activity.

Protein purification and mass spectrometry demonstrated that TRIM25 (also called oestrogen-responsive finger protein (EFP)[11]) is one of the proteins that associates with Flag–RIG-I(2CARD). TRIM25 has ubiquitin and ISG15 E3 ligase activity and downregulates 14-3-3σ through proteolysis for cell cycle regulation[12,13]. Co-immunoprecipitation revealed that RIG-I(2CARD) interacts with TRIM25 but not TRIM5-α, which has a similar structure to TRIM25 and functions as an intracellular inhibitor of retroviral replication[7] (Fig. 2a). Furthermore, interaction between Flag-tagged RIG-I or RIG-I(2CARD) and endogenous TRIM25 was readily detected in HEK293T cells (Fig. 2b). Confocal microscopy revealed that both RIG-I and TRIM25 exhibited punctate staining throughout the cytoplasm and that they co-localized extensively at cytoplasmic perinuclear bodies (Fig. 2c). As with other TRIM family members[7], TRIM25 contains a cluster of a RING-finger domain, a B box/coiled-coil domain (B Box/CCD) and a SPRY domain (Fig. 2d). Binding analysis revealed that the C-terminal SPRY domain of TRIM25 bound to both RIG-I and RIG-I(2CARD) as effectively as full-length TRIM25, whereas the RING-finger domain and B Box/CCD did not (Fig. 2d).

To test the role of TRIM25 in RIG-I ubiquitination, RIG-I or GST–RIG-I(2CARD) was co-expressed with wild-type TRIM25, E3 ligase-defective TRIM25(ΔRING) or TRIM5-α. TRIM25 expression markedly increased the ubiquitination levels of exogenous RIG-I and GST–RIG-I(2CARD), as well as endogenous RIG-I, but neither TRIM25(ΔRING) nor TRIM5-α had any effect (Fig. 3a, b; see also Supplementary Fig. 4a). In contrast, TRIM25 expression did not induce the ubiquitination of GST–MDA5(2CARD) (Supplementary Fig. 4b). TRIM25 depletion *in vivo* by a TRIM25-specific small hairpin RNA (shRNA)[13] significantly reduced the ubiquitination level of GST–RIG-I(2CARD) and RIG-I in a dose-dependent manner (Fig. 3c and Supplementary Fig. 5a), but a nonspecific scrambled-sequence shRNA had no effect on GST–RIG-I(2CARD) ubiquitination (Supplementary Fig. 5b). Finally, an *in vitro* ubiquitination assay showed that TRIM25 effectively delivered the ubiquitin moieties to maltose-binding protein (MBP)–T7-tagged RIG-I(2CARD), but not MBP–T7 alone or MBP–T7–RIG-I(2CARD(170stop)) (Fig. 3d and Supplementary Fig. 6a). Consistent with its ubiquitination level, RIG-I-mediated induction of IFN-β or NF-κB promoter activity considerably increased on TRIM25 expression in a dose-dependent manner (Fig. 3e and Supplementary Fig. 6b). Notably, expression of the TRIM25(SPRY) mutant, which was sufficient to bind to RIG-I, markedly suppressed GST–RIG-I(2CARD) ubiquitination in a dose-dependent manner (Fig. 3f) as well as endogenous RIG-I ubiquitination (Supplementary Fig. 4a). Furthermore, expression of the TRIM25(SPRY) mutant considerably decreased the RIG-I 2CARD-mediated activation of IFN-β or NF-κB promoter activity in a dose-dependent manner (Supplementary Fig. 7). This suggests that TRIM25-mediated ubiquitination has an important role in RIG-I signalling activity.

Unlike the GST–RIG-I(2CARD) K172R mutant, which showed an almost complete loss of ubiquitination and IFN-β and NF-κB promoter activation, GST–RIG-I(2CARD) K172only—containing five K→R substitutions but leaving K172 intact—demonstrated highly induced IFN-β and NF-κB promoter activity (Fig. 4a, b). Furthermore, the GST–RIG-I(2CARD) K172only mutant underwent robust ubiquitination (albeit lower than that of wild-type GST–RIG-I(2CARD)) on TRIM25 expression, whereas GST–RIG-I(2CARD) K172R was minimally ubiquitinated (Fig. 4c). However, despite a significant reduction in its level of ubiquitination, GST–RIG-I(2CARD) K172R interacted with TRIM25 as efficiently as wild-type GST–RIG-I(2CARD) and the K172only mutant (Fig. 4c). As seen with RIG-I(2CARD), full-length RIG-I K172only but not RIG-I K172R demonstrated ubiquitination at the same level as RIG-I wild type (Supplementary Fig. 8). Finally, correlated with their ubiquitination levels, expression of wild-type RIG-I and mutant RIG-I K172only in *RIG-I*$^{-/-}$ mouse embryonic fibroblasts (MEFs) induced IFN-β production on Sendai virus infection, whereas expression of mutant RIG-I K172R showed no effect on IFN-β production (Supplementary Fig. 9).

The 2CARD of RIG-I has been shown to bind to the MAVS CARD to elicit downstream signal transduction[14–17]. GST pull-down analysis showed that wild-type GST–RIG-I(2CARD) and mutant GST–RIG-I(2CARD) K172only efficiently interacted with the Flag-tagged CARD proline-rich domain of MAVS (Flag–MAVS(CARD-PRD)), whereas GST–RIG-I(2CARD) K172R and GST–RIG-I(2CARD) K99,169,172, 181,190,193R mutants poorly bound to Flag–MAVS(CARD-PRD) (Fig. 4d), indicating that Lys 172 is critical for TRIM25-mediated ubiquitination, RIG-I signalling and MAVS interaction, but not for TRIM25 binding (Fig. 4c).

Wild-type, *Trim25*$^{+/-}$ and *Trim25*$^{-/-}$ MEFs[18] were used to test the direct contribution of TRIM25 to RIG-I-mediated IFN-β expression. IFN-β promoter activity was very low in *Trim25*$^{-/-}$ MEFs and was reduced in *Trim25*$^{+/-}$ MEFs compared with wild-type MEFs

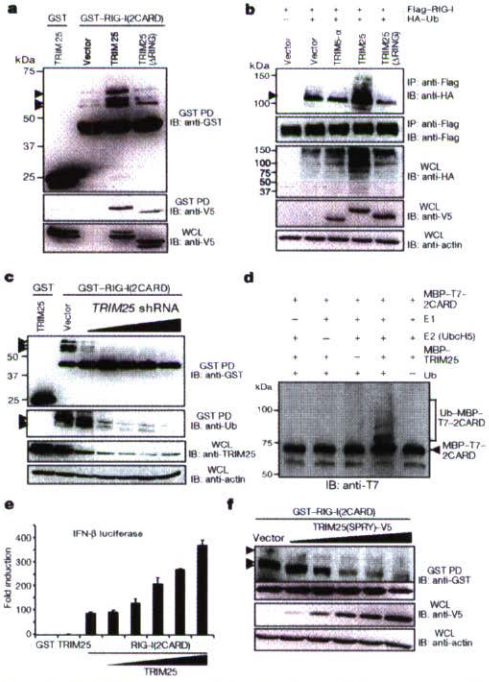

Figure 3 | TRIM25 is a primary E3 ubiquitin ligase of RIG-I. HEK293T cells transfected with GST or GST–RIG-I(2CARD) (**a**) or Flag–RIG-I and HA–ubiquitin (**b**) together with vector, TRIM25, TRIM25(ΔRING) or TRIM5-α were used for GST pull down (PD) (**a**) or immunoprecipitation with anti-Flag antibody (**b**). **c**, HEK293T cells transfected with GST or GST–RIG-I(2CARD) together with pSUPER.retro.puro or *TRIM25*-shRNA-specific pSUPER.retro.puro[13] were used for GST pull down. Arrows indicate the ubiquitinated GST–RIG-I(2CARD) and Flag–RIG-I. **d**, *In vitro* ubiquitination was detected by anti-T7 immunoblotting. **e**, IFN-β luciferase activity in HEK293T cells transfected with GST–RIG-I(2CARD) and TRIM25. The results are expressed as means ± s.d. ($n = 3$). **f**, HEK293T cells transfected with GST–RIG-I(2CARD) and V5–TRIM25(SPRY) were used for GST pull down. Arrows indicate ubiquitinated GST–RIG-I(2CARD).

©2007 Nature Publishing Group

(Supplementary Fig. 10a). Consistent with IFN-β promoter activation, virus-induced IFN-β production was virtually undetectable in *Trim25*$^{-/-}$ MEFs, whereas it was considerably high in wild-type MEFs (Fig. 4e). *Trim25*$^{+/-}$ MEFs showed a slightly reduced level of IFN-β production compared with wild-type MEFs (Fig. 4e). On vesicular stomatitis virus (VSV)–enhanced green fluorescent protein (eGFP) infection at various multiplicity of infections (MOIs), *Trim25*$^{-/-}$ MEFs showed remarkably increased levels of VSV–eGFP-positive cells (Fig. 4g and Supplementary Fig. 10b) and increased VSV yields (over 100-fold) (Fig. 4f) compared with wild-type and *Trim25*$^{+/-}$ MEFs. Similarly, *Trim25*$^{-/-}$ MEFs showed a considerable increase in the level of Newcastle disease virus (NDV)–GFP infection (Supplementary Fig. 10c). Finally, TRIM25 expression significantly suppressed VSV–eGFP replication in HEK293T cells, whereas expression of the TRIM25(SPRY) mutant detectably increased VSV–eGFP replication (Fig. 4h). Collectively, these results indicate that TRIM25 is critical for cytosolic RIG-I signal transduction that mediates the induction of the IFN response on viral infection.

Ubiquitination is a versatile post-translational modification involved in various cellular functions[19]. Our study indicates that TRIM25 E3 ubiquitin ligase induces the Lys 63-linked ubiquitination of RIG-I; that Lys 172 is the critical site for TRIM25-mediated ubiquitination; and that, as seen with the ubiquitin-dependent interaction between RIP and NEMO[20], the TRIM25-mediated ubiquitination of RIG-I may facilitate its interaction with MAVS, which ultimately leads to downstream signal transduction. Thus, the interconnection between the RIG-I cytosolic viral RNA receptor and a member of the TRIM family represents a new class of antiviral regulatory pathway involved in innate immunity.

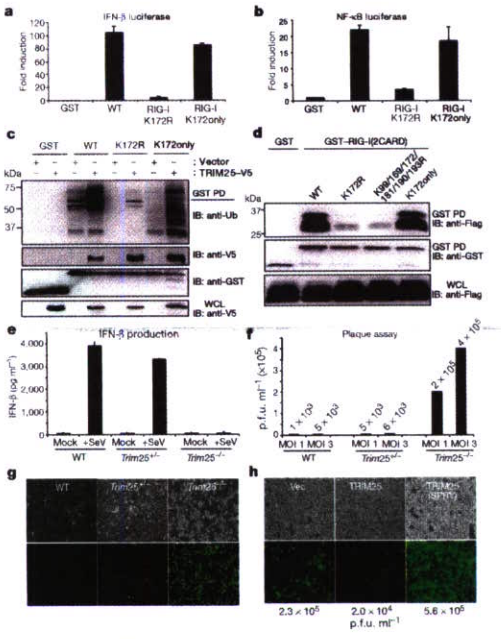

Figure 4 | Role of TRIM25-mediated ubiquitination in RIG-I antiviral activity. IFN-β (**a**) and NF-κB (**b**) promoter activity in GST–RIG-I(2CARD) or mutant transfected cells. The results are expressed as means ± s.d. ($n = 3$). **c**, HEK293T cells transfected with GST–RIG-I(2CARD), GST–RIG-I(2CARD) K172R, or GST–RIG-I(2CARD) K172only together with vector or TRIM25 were used for GST pull down. **d**, HEK293T cells transfected with GST–RIG-I(2CARD) or the indicated mutants together with Flag–MAVS(CARD-PRD) were used for GST pull down. **e**, IFN-β production in wild-type, *Trim25*$^{+/-}$ and *Trim25*$^{-/-}$ MEFs upon Sendai virus infection. The results are expressed as means ± s.d. ($n = 3$). **f–h**, VSV–eGFP replication in wild-type, *Trim25*$^{+/-}$ and *Trim25*$^{-/-}$ MEFs (**f** and **g**) or in vector-, TRIM25-, or TRIM25(SPRY)-expressing HEK293T cells (**h**) was determined by plaque assay or visualized by fluorescence microscopy.

METHODS SUMMARY

RNA interference for TRIM25. The mammalian expression vector pSUPER.retro.puro (OligoEngine), encoding shRNAs for *TRIM25* sequence, was provided by D.-E. Zhang. Details of the shRNA sequence and transfection method have been described[13].

Viruses. NDV–GFP and VSV–eGFP were provided by A. Garcia-Sastre and S. Whelan, respectively.

Measurement of IFN-β production. Cell culture supernatants were collected and analysed for IFN-β production using enzyme-linked immunosorbent assays (PBL Biomedical Laboratories).

***In vitro* ubiquitination assay.** Purified MBP–T7–RIG-I(2CARD) (20 μg ml^{-1}) and MBP–TRIM25 (20 μg ml^{-1}) derived from *Escherichia coli* were incubated in a reaction buffer (50 mM Tris-HCl, 2 mM dithiothreitol, 5 mM $MgCl_2$ and 4 mM ATP) with ubiquitin (50 μg ml^{-1}; Sigma), human recombinant E1 (1.6 μg ml^{-1}; BIOMOL) and human recombinant UbcH5a (20 μg ml^{-1}; BIOMOL) at 32 °C for 2 h and subjected to immunoblotting with anti-T7 antibody (Novagen).

Full Methods and any associated references are available in the online version of the paper at www.nature.com/nature.

Received 14 February; accepted 8 March 2007.
Published online 28 March 2007.

1. Honda, K., Takaoka, A. & Taniguchi, T. Type I interferon gene induction by the interferon regulatory factor family of transcription factors. *Immunity* **25**, 349–360 (2006); erratum **25**, 849 (2006).
2. Hornung, V. *et al.* 5′-Triphosphate RNA is the ligand for RIG-I. *Science* **314**, 994–997 (2006).
3. Meylan, E. & Tschopp, J. Toll-like receptors and RNA helicases: two parallel ways to trigger antiviral responses. *Mol. Cell* **22**, 561–569 (2006).
4. Pichlmair, A. *et al.* RIG-I-mediated antiviral responses to single-stranded RNA bearing 5′-phosphates. *Science* **314**, 997–1001 (2006).
5. Stetson, D. B. & Medzhitov, R. Antiviral defense: interferons and beyond. *J. Exp. Med.* **203**, 1837–1841 (2006).
6. Yoneyama, M. *et al.* The RNA helicase RIG-I has an essential function in double-stranded RNA-induced innate antiviral responses. *Nature Immunol.* **5**, 730–737 (2004).
7. Nisole, S., Stoye, J. P. & Saib, A. TRIM family proteins: retroviral restriction and antiviral defence. *Nature Rev. Microbiol.* **3**, 799–808 (2005).
8. Johnson, C. L. & Gale, M. Jr. CARD games between virus and host get a new player. *Trends Immunol.* **27**, 1–4 (2006).
9. Meylan, E., Tschopp, J. & Karin, M. Intracellular pattern recognition receptors in the host response. *Nature* **442**, 39–44 (2006).
10. Kato, H. *et al.* Cell type-specific involvement of RIG-I in antiviral response. *Immunity* **23**, 19–28 (2005).
11. Orimo, A., Inoue, S., Ikeda, K., Noji, S. & Muramatsu, M. Molecular cloning, structure, and expression of mouse estrogen-responsive finger protein Efp. Co-localization with estrogen receptor mRNA in target organs. *J. Biol. Chem.* **270**, 24406–24413 (1995).
12. Urano, T. *et al.* Efp targets 14-3-3σ for proteolysis and promotes breast tumour growth. *Nature* **417**, 871–875 (2002).
13. Zou, W. & Zhang, D. E. The interferon-inducible ubiquitin-protein isopeptide ligase (E3) EFP also functions as an ISG15 E3 ligase. *J. Biol. Chem.* **281**, 3989–3994 (2006).
14. Meylan, E. *et al.* Cardif is an adaptor protein in the RIG-I antiviral pathway and is targeted by hepatitis C virus. *Nature* **437**, 1167–1172 (2005).
15. Seth, R. B., Sun, L., Ea, C. K. & Chen, Z. J. Identification and characterization of MAVS, a mitochondrial antiviral signaling protein that activates NF-κB and IRF 3. *Cell* **122**, 669–682 (2005).
16. Xu, L. G. *et al.* VISA is an adapter protein required for virus-triggered IFN-β signaling. *Mol. Cell* **19**, 727–740 (2005).
17. Kawai, T. *et al.* IPS-1, an adaptor triggering RIG-I- and Mda5-mediated type I interferon induction. *Nature Immunol.* **6**, 981–988 (2005).
18. Orimo, A. *et al.* Underdeveloped uterus and reduced estrogen responsiveness in mice with disruption of the estrogen-responsive finger protein gene, which is a direct target of estrogen receptor α. *Proc. Natl Acad. Sci. USA* **96**, 12027–12032 (1999).

©2007 Nature Publishing Group

19. Haglund, K. & Dikic, I. Ubiquitylation and cell signaling. *EMBO J.* **24**, 3353–3359 (2005).
20. Ea, C. K., Deng, L., Xia, Z. P., Pineda, G. & Chen, Z. J. Activation of IKK by TNFα requires site-specific ubiquitination of RIP1 and polyubiquitin binding by NEMO. *Mol. Cell* **22**, 245–257 (2006).
21. Kirkpatrick, D. S., Denison, C. & Gygi, S. P. Weighing in on ubiquitin: the expanding role of mass-spectrometry-based proteomics. *Nature Cell Biol.* **7**, 750–757 (2005).

Supplementary Information is linked to the online version of the paper at www.nature.com/nature.

Acknowledgements This work was supported by US Public Health Service grants (J.U.J.), the exchange programme between Harvard Medical School and the graduate training programme 1071 at the Friedrich-Alexander University Erlangen-Nuremberg, Germany (M.U.G.), and a Korea Research Foundation Grant (C.-H.J.). We thank A. Garcia-Sastre, D.-E. Zhang and S. Whelan for providing reagents, and R. Tomaino and J. Nagel for mass spectrometry. We also thank all members of the Tumor Virology Division, New England Primate Research Center, for discussions.

Author Contributions M.U.G. performed all aspects of this study. Y.C.S., C.-H.J. and C.L. assisted in experimental design and in collecting the data. T.U. and S.I. performed the *in vitro* ubiquitination assay and generated *Trim25*$^{-/-}$ MEFs. L.S. and Z.C. generated the MAVS construct and RIG-I antibody. T.O. and S.A. generated the RIG-I construct and *RIG-I*$^{-/-}$ MEFs. M.U.G. and J.U.J. organized this study and wrote the paper. All authors discussed the results and commented on the manuscript.

Author Information Reprints and permissions information is available at www.nature.com/reprints. The authors declare no competing financial interests. Correspondence and requests for materials should be addressed to J.U.J. (jae_jung@hms.harvard.edu).

©2007 Nature Publishing Group

METHODS

Cell culture. HEK293T, MEF and Hela cells were cultured in Dulbecco's modified Eagle's medium supplemented with 10% fetal bovine serum, 2 mM L-glutamine and 1% penicillin-streptomycin (Gibco-BRL). Transient transfections were performed with FuGENE 6 (Roche), lipofectamine 2000 (Invitrogen), or calcium phosphate (Clontech) following the manufacturer's instructions. Wild-type, *Trim25*$^{+/-}$ and *Trim25*$^{-/-}$ MEFs were immortalized with LXSN-E6/E7 retroviral vector containing human papilloma virus 16 E6 and E7 oncogenes using a standard protocol of selection with 200 μg ml^{-1} of neomycin. *RIG-I*$^{-/-}$ MEFs were infected with pBabe-puro vector, pBabe-puro-RIG-I wild-type, pBabe-puro-RIG-I K172R, or pBabe-puro-RIG-I K172only retrovirus, followed by selection with 1 μg ml^{-1} of puromycin.

Plasmid construction. All constructs for transient and stable expression in mammalian cells were derived from the pEBG GST fusion vector and the pEF-IRES-Puro expression vector. DNA fragments corresponding to the coding sequence of the *RIG-I* and *TRIM25* genes were amplified from template DNA by polymerase chain reaction (PCR) and subcloned into plasmid pEBG between restriction sites *Kpn*I and *Not*I or pEF-IRES-puro between *Afl*II and *Not*I for selection of stable transfectants. V5-tagged TRIM25 and Flag-tagged RIG-I were expressed from a modified pIRES-puro encoding a C-terminal V5 tag and Flag tag, respectively. RIG-I mutants were generated by PCR using site-directed mutagenesis. All constructs were sequenced using an ABI PRISM 377 automatic DNA sequencer to verify 100% agreement with the original sequence.

***In vivo* GST pull down, protein purification and mass spectrometry.** At 48 h after transfection with vectors expressing GST, GST–RIG-I(2CARD) or GST–MDA5(2CARD) fusions, HEK293T cells were collected and lysed with NP40 buffer (50 mM HEPES, pH 7.4, 150 mM NaCl, 1 mM EDTA, 1% (v/v) NP40) supplemented with a complete protease inhibitor cocktail (Roche). Post-centrifuged supernatants were pre-cleared with protein A/G beads at 4 °C for 2 h. Pre-cleared lysates were mixed with a 50% slurry of glutathione-conjugated Sepharose beads (Amersham Biosciences), and the binding reaction was incubated for 4 h at 4 °C. Precipitates were washed extensively with lysis buffer. Proteins bound to glutathione beads were eluted and separated on a NuPAGE 4–12% Bis-Tris gradient gel (Invitrogen). After Coomassie or silver staining (Invitrogen), specific protein bands were excised and analysed by ion-trap mass spectrometry at the Harvard Taplin Biological Mass Spectrometry facility, and amino acid sequences were determined by tandem mass spectrometry and database searches.

Immunoblot analysis and immunoprecipitation assay. For immunoblotting, polypeptides were resolved by SDS–polyacrylamide gel electrophoresis (SDS–PAGE) and transferred to a PVDF membrane (Bio-Rad). Immunodetection was achieved with anti-V5 (1:5,000) (Invitrogen), anti-Flag (1:5,000) (Sigma), anti-HA (1:5,000), anti-GST (1:10,000) (Sigma), anti-actin (1:10,000) (Abcam), or anti-TRIM25 (1:2,000) (BD Bioscience) antibodies. The proteins were visualized by a chemiluminescence reagent (Pierce) and detected by a Fuji Phosphor Imager.

For immunoprecipitation, cells were collected after 48 h and then lysed in NP40 buffer supplemented with a complete protease inhibitor cocktail (Roche). After pre-clearing with protein A/G agarose beads for 2 h at 4 °C, whole-cell lysates were used for immunoprecipitation with the indicated antibodies. Generally, 1–2 μg of commercial antibody was added to 1 ml of cell lysate, which was incubated at 4 °C for 4–12 h. After addition of protein A/G agarose beads, the incubation was continued for 2 h. Immunoprecipitates were extensively washed with lysis buffer and eluted with SDS loading buffer by boiling for 5 min.

Confocal immunofluorescence microscopy. Eighteen to twenty-four hours after transfection, cells were fixed with 4% paraformaldehyde for 15 min, permeabilized with 0.2% (v/v) Triton X-100 for 15 min, blocked with 10% goat serum in PBS for 1 h and reacted with diluted primary antibody in 1% goat serum for up to 2 h at room temperature. After incubation, cells were washed extensively with PBS, incubated with the appropriate secondary antibody diluted in 1% goat serum for 1 h at room temperature, and washed three times with PBS. Confocal microscopy was performed using a Leica TCS SP laser-scanning microscope (Leica Microsystems) fitted with a ×100 Leica objective (PL APO, 1.4NA) and Leica imaging software. Images were collected at 512 × 512-pixel resolution. The stained cells were optically sectioned in the *z* axis, and the images in the different channels (photo multiplier tubes) were collected simultaneously. The step size in the *z* axis varied from 0.2 to 0.5 μm to obtain 16 slices per imaged file. The images were transferred to a Macintosh G4 computer (Apple Computer), and Photoshop (Adobe) was used to render the images.

©2007 Nature Publishing Group

Vitamin K_2 induces phosphorylation of protein kinase A and expression of novel target genes in osteoblastic cells

T Ichikawa[1], K Horie-Inoue[1], K Ikeda[1], B Blumberg[2] and S Inoue[1,3]

[1]Division of Gene Regulation and Signal Transduction, Research Center for Genomic Medicine, Saitama Medical University, Hidaka-shi, Saitama 350-1241, Japan

[2]Department of Developmental and Cell Biology, University of California, Irvine, California 92697-2300, USA

[3]Department of Geriatric Medicine, Graduate School of Medicine, The University of Tokyo, 7-3-1 Hongo, Bunkyo-ku, Tokyo 113-8655, Japan

(Correspondence should be addressed to S Inoue; Email: inoue-ger@h.u-tokyo.ac.jp)

Abstract

Vitamin K is known as a critical nutrient required for bone homeostasis and blood coagulation, and it is clinically used as a therapeutic agent for osteoporosis in Japan. Besides its enzymatic action as a cofactor of vitamin K-dependent γ-glutamyl carboxylase (GGCX), we have previously shown that vitamin K_2 is a transcriptional regulator of bone marker genes and extracellular matrix-related genes, by activating the steroid and xenobiotic receptor (SXR). To explore a novel action of vitamin K in osteoblastic cells, we identified genes up-regulated by a vitamin K_2 isoform menaquinone-4 (MK-4) using oligonucleotide microarray analysis. Among these up-regulated genes by MK-4, growth differentiation factor 15 (GDF15) and stanniocalcin 2 (STC2) were identified as novel *MK-4* target genes independent of GGCX and SXR pathways in human and mouse osteoblastic cells. The induction of GDF15 and STC2 is likely specific to MK-4, as it was not exerted by another vitamin K_2 isoform MK-7, vitamin K_1, or the MK-4 side chain structure geranylgeraniol. Investigation of the involved signaling pathways revealed that MK-4 enhanced the phosphorylation of protein kinase A (PKA), and the MK-4-dependent induction of both *GDF15* and *STC2* genes was reduced by the treatment with a PKA inhibitor H89 or siRNA against PKA. These results suggest that vitamin K_2 modulates its target gene expression in osteoblastic cells through the PKA-dependent mechanism, which may be distinct from the previously known vitamin K signaling pathways.

Journal of Molecular Endocrinology (2007) **39**, 239–247

Introduction

Vitamin Ks are fat-soluble 2-methyl-1,4-naphthoquinone-related compounds, including natural phylloquinone (K_1) and menaquinones (K_2). Vitamins K_1 and K_2 differ only in the substituent group. Vitamin K_1 possesses a phytyl group (partially saturated polyisoprenoid group), whereas K_2 possesses a repeating, unsaturated *trans*-polyisoprenyl group. Menaquinones include a range of related forms generally designated as menaquinone-*n* (MK-*n*), where *n* is the number of isoprenyl groups. Vitamin Ks play a role in the bone-building process as well as classic blood coagulation pathway. Indeed, clinical studies have demonstrated that vitamin K_2 is an effective treatment for osteoporosis and preventing fractures (Booth *et al.* 2000, Shiraki *et al.* 2000). Menaquinone-4 (MK-4), one of the vitamin K_2 containing four isoprene units, is frequently prescribed for osteoporosis in Japan.

One of the notable molecular functions of vitamin K is as a cofactor for vitamin K-dependent γ-glutamyl carboxylase (GGCX). GGCX catalyzes the post-translational modification of specific glutamates to γ-carboxyglutamate (Gla) in a number of proteins. Most vitamin K-dependent proteins are involved in the hemostatic process and are associated with bone metabolism. Osteocalcin (bone Gla protein), and matrix Gla protein (MGP) are two major Gla proteins in bone and γ-carboxylated proteins are important in bone metabolism. Osteocalcin serves as a good biochemical marker of the metabolic turnover of bone because osteocalcin lacking Gla residues cannot bind to hydroxyapatite, one of the major components of bone matrix (Nishimoto & Price 1985, Vergnaud *et al.* 1997). Moreover, levels of undercarboxylated osteocalcin increase during aging and significantly correlate with fracture risk (Vergnaud *et al.* 1997).

MGP is predominantly expressed and produced in chondrocytes and vascular smooth muscle cells (Luo *et al.* 1997, Shanahan & Weissberg 1998). Data from rodent studies revealed that MGP plays a key role in the inhibition of tissue calcification. Luo *et al.* (1997) reported that MGP-deficient mice showed excessive cartilage formation and growth plate mineralization, resulting in impaired growth of the long bones. Thus, vitamin K plays a significant role in bone homeostasis through γ-carboxylated proteins. On the other hand, we previously reported that vitamin K_2 has a

Journal of Molecular Endocrinology (2007) **39**, 239–247
0952–5041/07/039–239 © 2007 Society for Endocrinology *Printed in Great Britain*

DOI: 10.1677/JME-07-0048
Online version via http://www.endocrinology-journals.org

transcriptional regulatory function in addition to its role as an enzyme cofactor (Tabb *et al.* 2003). Vitamin K_2 was a ligand of the steroid and xenobiotic receptor (SXR), and both vitamin K_2 and the known SXR ligands rifampicin (RIF) up-regulated expression of the prototypical *SXR* target gene cytochrome P450 (CYP) 3A4 and bone marker genes, such as alkaline phosphatase and osteoprotegerin (Tabb *et al.* 2003). Furthermore, we identified SXR-dependent vitamin K_2 target genes that participated in extracellular matrix formation in osteoblastic cells (Ichikawa *et al.* 2006). These findings suggested an important role for vitamin K_2-dependent transcriptional regulation in bone homeostasis. Meanwhile, during our microarray analyses that identify the *SXR* target genes using osteoblastic cells treated with RIF or vitamin K_2, we found that a number of genes were specifically up-regulated by vitamin K_2 but not RIF. This observation suggested that potentially novel mechanism could be associated with the up-regulation of these genes by vitamin K_2.

In the present study, we screened for genes induced by MK-4 in osteoblastic MG63 cells using microarray analysis, and identified several vitamin K_2-target genes. Here, we focused on the growth differentiation factor 15 (GDF15) and stanniocalcin 2 (*STC2*) genes as MK-4 targets. We found that other vitamin Ks, geranylgeraniol (GGO), and SXR agonists failed to induce the expression of *GDF15* and *STC2* genes, although a protein kinase A (PKA) activator forskolin (FSK) induced the expression of both genes. Our findings indicate that GDF15 and STC2 are regulated by a PKA-dependent, GGCX- and SXR-independent pathways.

Materials and methods

Materials

RIF was purchased from Nacalai Tesque (Kyoto, Japan). Vitamin K_1, GGO, and FSK were purchased from Sigma. MK-4 and MK-7 were gifts of Eisai Co. Ltd (Tokyo, Japan). H89 was obtained from BioMol (Plymouth Meeting, PA, USA).

Cell culture and generation of stable cell lines expressing SXR

MG63 human osteosarcoma cells were grown in Dulbecco's modified Eagle's medium supplemented with 10% fetal bovine serum (FBS), 50 U/ml penicillin, and 50 μg/ml streptomycin. Mouse MC3T3-E1 osteoblastic cells were maintained in α-minimum essential medium (MEM) supplemented with 10% FBS, 50 U/ml penicillin, and 50 μg/ml streptomycin. Prior to vitamin K treatment, cells were cultured in phenol red-free media containing 10% dextran–charcoal stripped FBS (dcc-FBS). N-terminally Flag-tagged pcDNA3 (Invitrogen) plasmids containing VP16C-SXR (pcDNA3-Flag-VP16C-SXR) were previously described (Ichikawa *et al.* 2006). VP16C-SXR contained 20 amino acids from the C-terminus of VP16 activation domain upstream of SXR. Generation of MG63 cell lines stably expressing pcDNA3-Flag-VP16C-SXR (MG63/Flag-VP16C-SXR) or the empty vector Flag-tagged pcDNA3 (MG63/vector) were previously described (Ichikawa *et al.* 2006).

Table 1 Common up-regulated genes by 48-h treatment with menaquinone-4 (MK-4; 10 μM) in both MG63/vector and MG63/Flag-VP16C-SXR stable cell lines identified by GeneChip analysis

	Ensemble gene ID	Gene symbol	Description	Fold change	
				MG63/vector	MG63/Flag-VP16C-SXR
Probe set ID					
221577_x_at	ENSG00000130513	*GDF15*	Growth differentiation factor 15	8·00	5·66
218145_at	ENSG00000101255	*TRIB3*	Tribbles homolog 3 (*Drosophila*)	6·50	4·29
207145_at	ENSG00000138379	*GDF8*	Growth differentiation factor 8	4·29	2·00
219270_at	ENSG00000128965	*MGC4504*	Hypothetical protein MGC4504	3·03	3·48
202847_at	ENSG00000100889	*PCK2*	Phosphoenolpyruvate carboxykinase 2 (mitochondrial)	2·46	2·00
205047_s_at	ENSG00000070669	*ASNS*	Asparagine synthetase	2·46	3·25
203665_at	ENSG00000100292	*HMOX1*	Heme oxygenase (decycling) 1	2·30	2·46
206026_s_at	ENSG00000123610	*TNFAIP6*	Tumor necrosis factor, α-induced protein 6	2·30	2·00
203438_at	ENSG00000113739	*STC2*	Stanniocalcin 2	2·14	2·00
203477_at	ENSG00000204291	*COL15A1*	Collagen, type XV, α 1	2·14	2·14
206025_s_at	ENSG00000123610	*TNFAIP6*	Tumor necrosis factor, α-induced protein 6	2·14	2·46
209921_at	ENSG00000151012	*SLC7A11*	Solute carrier family 7, member 11	2·14	2·64
202887_s_at	ENSG00000168209	*DDIT4*	DNA-damage-inducible transcript 4	2·00	2·64
204422_s_at	ENSG00000138685	*FGF2*	Fibroblast growth factor 2 (basic)	2·00	2·30
220892_s_at	ENSG00000135069	*PSAT1*	Phosphoserine aminotransferase 1	2·00	2·00

MG63/vector and MG63/Flag-VP16C-SXR cells are stably expressing Flag-pcDNA3 vector and pcDNA3-Flag-VP16C-SXR respectively. Twofold or more up-regulated genes by MK-4 over vehicle in both cells were selected, except SXR-dependent up-regulated ones with the ratios of fold change in MG63/Flag-VP16C-SXR versus MG63/vector by ≥1·5-fold. Gene annotation was determined based on the probe set ID by the Array Finder on the Affymetrix web site (http://www.affymetrix.com).

Western blot analysis

Whole cell lysates were prepared using a lysis buffer (50 mM HEPES (pH 7·5), 150 mM NaCl, 10% glycerol, 1% Triton X-100, 1·5 mM $MgCl_2$, 1 mM sodium orthovanadate, 10 μg/ml aprotinin, and 10 μg/ml leupeptin). Protein concentrations were analyzed using the BCA protein assay kit (Pierce Biotechnology, Rockford, IL, USA). Proteins were resolved by SDS-PAGE and electroblotted onto Immobilon-P Transfer Membrane (Millipore, Billerica, MA, USA). The antibody–antigen complexes were detected using the Western Blotting Chemiluminescence Luminol Reagent (Santa Cruz Biotechnology, Santa Cruz, CA, USA). Antibodies used included anti-phospho PKA and anti-PKA (Cell Signaling Technology, Danvers, MA, USA).

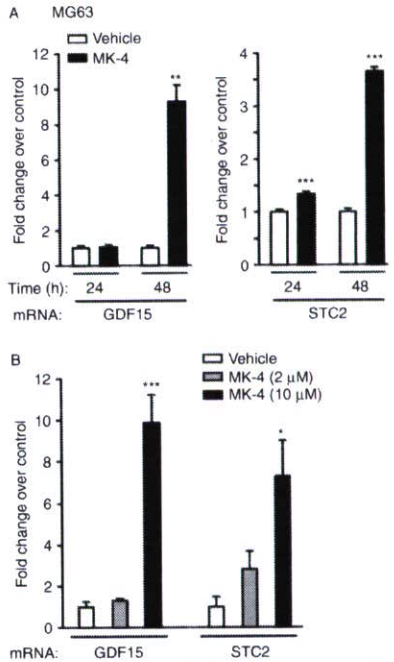

Figure 1 Up-regulation of growth differentiation factor 15 (GDF15) and stanniocalcin-2 (STC2) mRNA levels by a vitamin K_2 isoform menaquinone-4 (MK-4) in osteoblastic cells. Human osteoblastic MG63 cells were treated with MK-4 (10 μM) or vehicle for the indicated times (A), and mouse osteoblastic MC3T3-E1 cells were treated with MK-4 (2 or 10 μM) or vehicle for 48 h (B). mRNA levels for GDF15 and STC2 were determined by quantitative RT-PCR (qRT-PCR). Data are representative of experiments with similar results, each performed in triplicate. $^*P<0·05$, $^{**}P<0·01$, $^{***}P<0·001$ when compared with control cells treated with vehicle.

Preparation of cRNA and oligonucleotide array hybridization

Total RNA was extracted from MG63/vector and MG63/Flag-VP16C-SXR cells treated with vehicle (0·1% ethanol) and MK-4 (10 μM) for 48 h. The methods for preparation of cRNA and subsequent steps leading to hybridization and scanning of the U133A GeneChip Arrays Station (Affymetrix, Santa Clara, CA, USA) were performed as described previously (Ichikawa *et al.* 2006). Data analysis was performed using Affymetrix Microarray Suite software. For comparing arrays, normalization was performed using data from all probe sets.

Quantitative reverse transcription PCR analysis

Osteoblastic cells were treated with RIF, MK-4, MK-7, vitamin K_1, GGO, FSK, or vehicle for indicated times. Total RNA was isolated using the ISOGEN reagent (Nippon gene, Tokyo, Japan). First, strand cDNA was generated from RNase-free DNase I-treated total RNA using the SuperScript II Reverse Transcriptase (Invitrogen) and oligo-dT_{20} primer. For PCR amplification, the primer sequences were: human GDF15, 5′-GAAACGCTACGAGGACCTGCTA-3′ and 5′-ACGAGGTCGGTGTTCGAATC-3′; human STC2, 5′-TGGGATTTGCATGACTTTTCTG-3′ and 5′-GGCGTCTTTGATGAATGACTTG-3′; human GGCX, 5′-CTTGAGACCCTTTGAGGCAGTT-3′ and 5′-GGATTTGACTCAGGAGGATTAGAATG-3′; human CYP3A4, 5′-TTCAGCCCATCTCCTTTCATATTT-3′ and 5′-CAGTTGGGTGTTGAGGATGGA-3′; human α-catalytic subunit of PKA (PRKACA), 5′-CAACTTTCCGTTCCTCGTCAA-3′ and 5′-CGCCGGGCACGTACTC-3′; human glyceraldehyde-3-phosphate dehydrogenase (GAPDH), 5′-GCCTGCCTGACCAAATGC-3′ and 5′-GTGGTCGTTGAGGGCAATG-3′; mouse GDF15, 5′-AGACTGTGCAGGCAACTCTTGA-3′ and 5′-ACACTCGCCCACGCACAT-3′; mouse STC2, 5′-CAACTCTTGTGAAATCCAGGGTTT-3′ and 5′-CATCGAATTTTCCAGCGTTGT-3′; and mouse GAPDH, 5′-GCATGGCCTTCCGTGTTC-3′ and 5′-TGTCATCAT-

132# ACTTGGCAGGTTTCT-3′. mRNAs were quantified by real-time PCR using SYBR green PCR master mix (Applied Biosystems, Foster City, CA, USA) and the ABI Prism 7000 system (Applied Biosystems) as previously described (Ichikawa *et al.* 2006).

RNA interference

Small interfering RNA (siRNA) duplexes to target human GGCX (D-009856-02) and PRKACA (D-004649-01) were purchased from Dharmacon Research Inc. (Lafayette, CO, USA). An siRNA specific to luciferase gene (Luciferase GL2 Duplex, Dharmacon) was used as a control. Cells were transfected with siRNA using GeneSilencer reagent (Genlantis, San Diego, CA, USA) for indicated times in the culture medium containing 10% dcc-FBS in the presence or absence of MK-4.

Statistical analysis

Differences between two groups were analyzed using two-sample, two-tailed Student's *t*-test. A P value $<0{\cdot}05$ was considered to be significant. All data are presented in the text and figures as the mean ± S.D.

Results

Identification of genes up-regulated by MK-4 in osteoblastic cells by microarray analysis

To identify up-regulated genes by MK-4 treatment in osteoblastic cells, we prepared biotin-labeled cRNA samples from MG63 cells expressing empty Flag-pcDNA3 (MG63/vector) or Flag-VP16C-SXR (MG63/Flag-VP16C-SXR) treated with vehicle (0·1% ethanol) or MK-4 (10 μM). The Affymetrix U133A GeneChip array represents more than 18 000 human transcripts from ~14 000 genes. Gene expression analysis for the MG63 samples was performed by hybridizing aliquots of cRNA (10 μg each) to the GeneChip arrays. Eighty-five transcripts were induced twofold or greater by MK-4 in MG63/vector cells, whereas 77 transcripts were induced in MG63/Flag-VP16C-SXR cells. In the present study, we focused on the SXR-independent gene expression in osteoblastic cells, by screening the common up-regulated genes (greater than or equal to twofold) in both vector and Flag-VP16C-SXR-transfected MG63 cells. In this population, we excluded genes up-regulated with the ratios of fold change in Flag-VP16C-SXR cells versus vector cells by ≥1·5-fold, as we considered that such genes were SXR dependent.

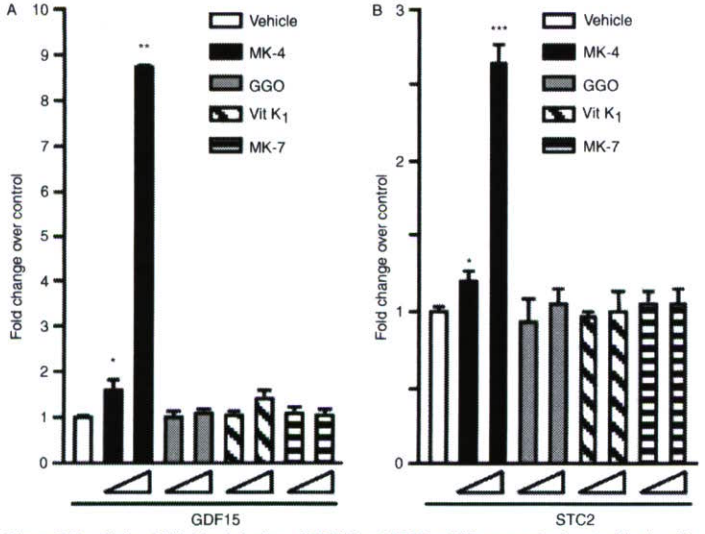

Figure 2 Specificity of MK-4 for induction of GDF15 and STC2 mRNA expression in osteoblastic cells. MG63 cells were treated with 5 or 10 μM of vitamin K_1, MK-4, MK-7, or geranylgeraniol (GGO) for 72 h. mRNA levels for GDF15 (A) and STC2 (B) were determined by qRT-PCR. Data are representative of experiments with similar results, each performed in triplicate. *$P<0{\cdot}05$, **$P<0{\cdot}01$, ***$P<0{\cdot}001$ when compared with control cells treated with vehicle.

Flag-VP16C-SXR was constructed previously that could provide more intense SXR ligand-dependent signals when compared with the original SXR plasmid (Ichikawa *et al.* 2006). We used Flag-VP16C-SXR as it was useful to exclude SXR-dependent genes from the SXR-independent gene group. Through this procedure, 15 transcripts from 14 distinct genes were selected as MK-4 targets that were potentially independent of SXR pathways (Table 1). We focused on GDF15 and a secreted peptide hormone STC2 as putative bone-related genes for further experiments.

Induction of GDF15 and STC2 specifically by MK-4 in osteoblastic cells

We validated whether mRNA expression levels for these two genes could be modulated by MK-4 in parental MG63 cells using quantitative RT-PCR (qRT-PCR) analysis. In proliferating culture of MG63 cells, the significant induction of both GDF15 and STC2 was detected after 48-h treatment with MK-4 (Fig. 1A). GDF15 and STC2 were also induced in mouse osteoblastic MC3T3-E1 cells after 48-h treatment with MK-4 (Fig. 1B).

We next investigated whether GDF15 and STC2 were induced by other vitamin Ks or the MK-4 side chain structure GGO. Induction of GDF15 and STC2 mRNA by vitamin K_1, MK-7, or GGO was compared with that by MK-4. MK-4 of 5 and 10 μM significantly up-regulated the *MK-4* target genes, whereas the others had no effect (Fig. 2).

Up-regulation of *MK-4* target genes in a GGCX and SXR-independent manner

Since *MK-4* target genes were not induced by vitamin K_1 or MK-7, we next sought to verify that a GGCX-mediated pathway does not participate in the induction of these *MK-4* target genes. We investigated the effects of a siRNA against GGCX on the ligand-dependent induction of gene expression. Ninety-six-hour treatment with the specific siRNA duplex against GGCX (70 nM), but not with a control siRNA directed against luciferase, reduced the GGCX mRNA level by more than 80% in MG63 cells (Fig. 3A). In that cell system, the GGCX siRNA had no effects in MK-4-activated mRNA expression for GDF15 and STC2 (Fig. 3B). We next examined whether the SXR pathway was involved in the regulation of GDF15 and STC2 mRNA expression using MG63/Flag-VP16C-SXR cells. In cells stably expressing SXR, mRNA encoding the *SXR* target gene *CYP3A4* was induced in 24 h by treatment with MK-4 or the SXR agonist RIF. In contrast, GDF15 and STC2 were up-regulated after 48-h treatment with MK-4 but not with RIF (Fig. 4A and B).

PKA is an activator for the induction of *MK-4* target genes in osteoblastic cells

It has been shown that the modulation of transcriptional activities by PKA phosphorylation is one of the key events in osteoblasts, such as through parathyroid hormone or β2-adrenergic receptor pathways (Selvamurugan *et al.* 2000, Elefteriou *et al.* 2005). There is a report that MK-4 might modulate gene expression and activate transcriptional factor activities in a PKA-dependent manner in a hepatocellular carcinoma cell line (Otsuka *et al.* 2004). Thus, we questioned whether PKA activity was responsible for the up-regulation of GDF15 and STC2 by MK-4 in osteoblastic cells. MK-4 (10 μM) markedly induced phosphorylation of PKA in MG63 cells from 2 to 24 h after the stimulation (Fig. 5A). In experiments of PKA activation by FSK (10 nM), the mRNA expression of GDF15 and STC2 was significantly up-regulated after 48-h treatment (Fig. 5B).

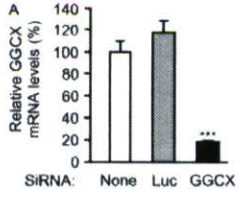

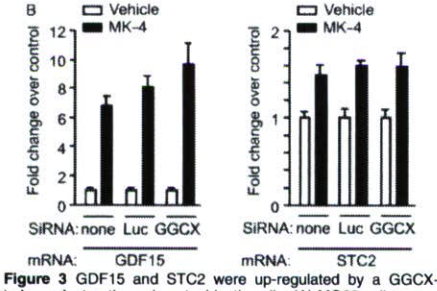

Figure 3 GDF15 and STC2 were up-regulated by a GGCX-independent pathway in osteoblastic cells. (A) MG63 cells were transfected with GGCX siRNA (70 nM) for 96 h, and mRNA expression of GGCX was determined by qRT-PCR. Data represent percentages of mRNA levels using the value with Luc siRNA treatment as 100%. (B) Effects of GGCX siRNA on MK-4-induced up-regulation of GDF15 and STC2. At 24 h after transfection of GGCX siRNA, MG63 cells were treated with MK-4 (10 μM) for 72 h and mRNA expression was determined by qRT-PCR. Data represent fold changes in mRNA over vehicle treatment. ***$P<0{\cdot}001$ when compared with control cells with no siRNA treatment.

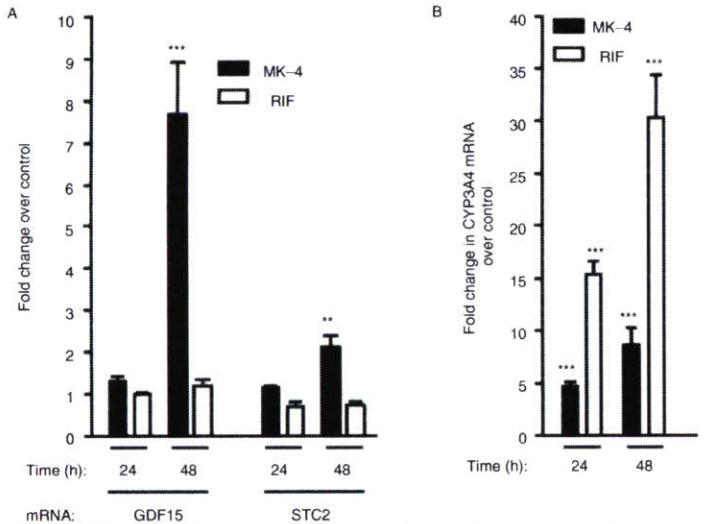

Figure 4 GDF15 and STC2 were up-regulated in an SXR-independent manner in osteoblastic cells. MG63/Flag-VP16C-SXR cells were treated with MK-4 (10 μM), rifampicin (RIF, 10 μM), or vehicle for 24 or 48 h, and mRNA expression was determined by qRT-PCR. (A) GDF15 and STC2 mRNA levels. (B) CYP3A4 mRNA levels. Data are representative of experiments with similar results, each performed in triplicate. $^{**}P<0.01$, $^{***}P<0.001$ when compared with control cells treated with vehicle.

Because it was likely that PKA activity was related to the transcriptional regulation of GDF15 and STC2, we further investigated whether the loss of function of PKA might affect the expression of GDF15 and STC2. Using a specific PKA inhibitor H89 (10 μM) for 72 h, MK-4-dependent up-regulation of these two genes was reduced by ~30% (Fig. 6A). We also performed the knockdown study of PRKACA in MG63 cells using a specific siRNA duplex (Fig. 6B and C). In a condition of >60% reduction of PRKACA mRNA levels by siPKA compared with the control siRNA against luciferase, MK-4-dependent up-regulation of GDF15 and STC2 was reduced by 45 and 30% respectively.

Discussion

We previously reported that SXR mediated the transcriptional regulation of several osteoblastic marker genes by the vitamin K_2 congener MK-4 (Tabb *et al.* 2003). In the present study, we identified GDF15 and STC2 as novel vitamin K_2 target genes up-regulated only by MK-4 in an SXR-independent manner in osteoblastic cells. The expression of both *GDF15* and *STC2* genes was markedly induced by MK-4 after 48-h treatment, whereas vitamin K_1, MK-7, GGO, and the SXR agonist RIF were not effective in inducing the expression of the genes. Furthermore, siRNA against GGCX did not affect the up-regulation of *GDF15* and *STC2* gene expression by MK-4. These results suggested that induction of GDF15 and STC2 was specific for MK-4 in osteoblastic cells, and that this induction was mediated by SXR- and GGCX-independent pathway(s).

GDF15 belongs to the superfamily of transforming growth factor-β, and it is generated as a 40 kDa propeptide from which the N-terminus is cleaved and a 30 kDa disulfide-linked dimeric protein is secreted as the active form (Bootcov *et al.* 1997). It was first named macrophage-inhibiting cytokine 1 (Bootcov *et al.* 1997) or placental bone morphogenetic protein (Hromas *et al.* 1997), and also later named prostate-derived factor (Paralkar *et al.* 1998) or non-steroidal anti-inflammatory drug-activated gene (Baek *et al.* 2001). GDF15 is abundantly expressed in placenta and mildly expressed in liver and prostate at baseline, but many tissues show the dramatic induction of expression following various stimuli such as cytokine, growth factor, or hypoxia (Bootcov *et al.* 1997, Albertoni *et al.* 2002, Nazarova *et al.* 2004, Schlittenhardt *et al.* 2004). It has been shown that several kinases and transcriptional factors may contribute to the regulation of GDF15

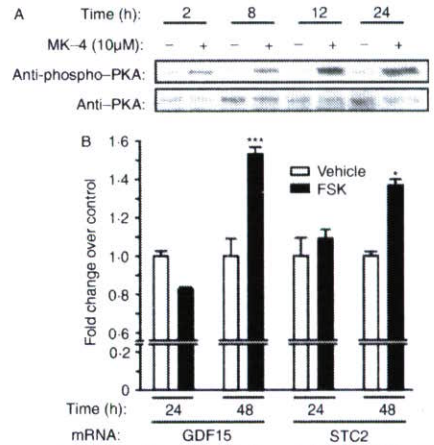

Figure 5 Phosphorylation of protein kinase A (PKA) by MK-4 and induction of GDF15 and STC2 mRNA by a PKA activator. (A) MG63 cells were treated with MK-4 (10 μM) or vehicle (MK-4,) for the indicated times. Whole cell lysates were separated by SDS-PAGE, and phosphorylated PKA was detected by immunoblot analysis using anti-phospho-PKA antibody. The identical membrane was re-probed with whole PKA antibody (anti-PKA). (B) MG63 cells were treated with forskolin (FSK, 10 nM) or vehicle (0·1% DMSO) for the indicated times. mRNA levels for GDF15 and STC2 were determined by qRT-PCR. Data are representative of experiments with similar results, each performed in triplicate. $^{*}P<0.05$, $^{***}P<0.001$ when compared with control cells treated with vehicle.

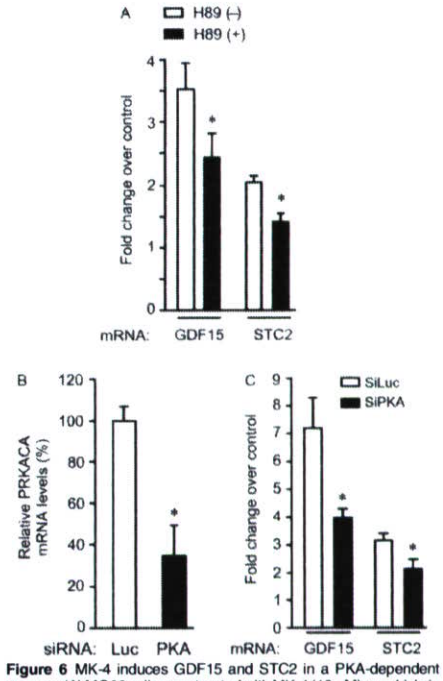

Figure 6 MK-4 induces GDF15 and STC2 in a PKA-dependent manner. (A) MG63 cells were treated with MK-4 (10 μM) or vehicle in the presence or absence of H89 (10 μM) for 72 h. mRNA levels for GDF15 and STC2 were determined by qRT-PCR. (B) MG63 cells were transfected with siRNAs (14 nM) that target either α-catalytic subunit of PKA, PRKACA (siPKA), or luciferase (siLuc) for 72 h. PRKACA mRNA expression was determined by qRT-PCR. (C) Effects of siPKA on MK-4-dependent up-regulation of GDF15 and STC2. Cells were transfected with siRNAs (14 nM) and incubated with MK-4 (10 μM) or vehicle for 72 h. Data are representative of experiments with similar results, each performed in triplicate. $^{*}P<0.05$ when compared with control cells treated with vehicle test.

expression, including p53 (Li *et al.* 2000, Tan *et al.* 2000), protein kinase C (Shim & Eling 2005), phosphatidylinositol 3-kinase/AKT (Yamaguchi *et al.* 2004), or early growth response 1 (EGR-1; Baek *et al.* 2005). The transcriptional regulation by PKA has not been definitely shown previously, yet it is likely that PKA is involved in GDF15 regulation as the gene expression was induced by dibutyryl cAMP in murine preadipocytes (Uldry *et al.* 2006). Although PKA sometimes phosphorylates p53, it is unlikely that p53 is responsible for the modulation of GDF15 expression in MG63 cells as the cell line has been shown to lack p53 (Masuda *et al.* 1987, Diller *et al.* 1990).

Regarding the physiological significance of GDF15 in bone-related tissues, the gene may play a role in the developmental stage as it has been shown to be expressed in the skin and in the cartilaginous tissue in the 18-dpc rat embryos (Paralkar *et al.* 1998). Similar to the function of bone morphogenic proteins, s.c. implantation of recombinant GDF15 protein ectopically induced the cartilage and immature endochondral bone formation (Paralkar *et al.* 1998). In prostate cancer, GDF15 expression was expressed only in osseous metastatic lesions, while it was reduced or absent in primary tumor, suggesting that GDF15 expression might be linked to the osteoblastic phenomena associated with bone metastasis (Thomas *et al.* 2001). GDF15 also has modulating effects on cell adhesion or proliferation (Li *et al.* 2000, Tan *et al.* 2000, Nazarova *et al.* 2004). As MK-4 has been known as a modulator of cell proliferation in osteoblastic cells (Akedo *et al.* 1992) and hepatocellular carcinoma cells (Otsuka *et al.* 2004), GDF15 might be also involved in this growth-regulatory function of MK-4.

STCs represent a small family of secreted glycoprotein hormones, consisting of STC1 and STC2, which has been conserved from fish to mammals. It was assumed that mammalian STC would mimic the function of fish STC-1 in mineral homeostasis (Olsen

et al. 1996, Wagner *et al.* 1997, Madsen *et al.* 1998). STC1 is expressed in osteoblastic cells and could be induced during osteoblastic differentiation of rat fetal calvaria cells (Yoshiko *et al.* 1999, 2003). Overexpression and knockdown study of STC1 led to the acceleration and retardation of osteogenic development respectively (Yoshiko *et al.* 2003). STC1 is also expressed in chondrocytes and may also stimulate chondrocyte proliferation in cartilage matrix (Jiang *et al.* 2000, Filvaroff *et al.* 2002). In transgenic mice expressing human STC2, growth restriction and developmental retardation were observed in both prenatal and postnatal stages, and ossification was reduced in different endochondral skeletal elements (Gagliardi *et al.* 2005). Systemic overexpression of human STC1 in transgenic mice, however, also exhibited postnatal growth retardation (Varghese *et al.* 2002) and reduced ossification in cranial bones (Gagliardi *et al.* 2005), suggesting the discrepancy between animal models and culture cells. More specific studies targeting osteoblast and chondrocyte lineage will be required for better understanding of the STC physiology in bone development and formation, yet STC could be one of the key factors for the regulation of bone homeostasis. Interestingly, it has been shown that STC2 is closely related to steroid hormone physiology, as its expression is induced by estrogen (Charpentier *et al.* 2000, Bouras *et al.* 2002), or it has an inhibitory effect on FSH-induced progesterone production in rat ovary granulose cells (Luo *et al.* 2005). It is likely that STC2 could play a paracrine role also in bone formation.

In this study, we investigated the effects of PKA on GDF15 and STC2 expression in osteoblastic cells and demonstrated that PKA was responsible, at least in part, for the MK-4-dependent up-regulation of these two genes. It has been reported that MK-4 activated transcriptional factors activating enhancer-binding protein 2α (AP-2), upstream stimulatory factor (USF), and cyclic adenosine monophosphate response element-binding protein (CREB), and PKA activity might be stimulated by MK-4 in hepatocellular carcinoma cell line HepG2 (Otsuka *et al.* 2004). The activation of PKA by FSK in the present study mimicked the MK-4-induced up-regulation of GDF15 and STC2 in osteoblastic cells, although it is not clear whether MK-4 directly increases cyclic AMP production. It is also possible that PKA is phosphorylated by MK-4 through a cAMP-independent pathway, such as the one mediated by sphingosine (Ma *et al.* 2005). Future study will reveal the molecular details of MK-4-induced PKA activity in osteoblastic cells. It might be also interesting to investigate whether the MK-4-dependent PKA activation is important in other non-osteoblastic cells.

Here, we have shown that the PKA-dependent pathway is involved in the regulation of *MK-4* target genes in osteoblastic cells in an SXR- and GGCX-independent manner. Our data suggest that GDF15 and STC2 are novel *MK-4* target genes up-regulated by the PKA-dependent pathway. Induction of GDF15 and STC2 at proliferation stage and post-confluent phase in osteoblastic cells might affect osteogenesis and chondrogenesis via autocrine or paracrine mechanisms.

Acknowledgements

We thank T Suzuki and R Nozawa for their technical assistance. This work was supported in part by grants-in-aid from the Ministry of Health, Labor and Welfare, the Promotion and Mutual Aid Corporation for Private Schools of Japan, the Japan Society for the Promotion of Science, and the NIH (GM-60572 to BB). This work was supported in part by a grant of the Genome Network Project from the Ministry of Education, Culture, Sports, Science and Technology of Japan. The authors declare that there is no conflict of interest that would prejudice the impartiality of this scientific work.

Disclosure

The authors have nothing to declare.

References

Akedo Y, Hosoi T, Inoue S, Ikegami A, Mizuno Y, Kaneki M, Nakamura T, Ouchi Y & Orimo H 1992 Vitamin K_2 modulates proliferation and function of osteoblastic cells in vitro. *Biochemical and Biophysical Research Communications* **187** 814–820.

Albertoni M, Shaw PH, Nozaki M, Godard S, Tenan M, Hamou MF, Fairlie DW, Breit SN, Paralkar VM, de Tribolet N *et al.* 2002 Anoxia induces macrophage inhibitory cytokine-1 (MIC-1) in glioblastoma cells independently of p53 and HIF-1. *Oncogene* **21** 4212–4219.

Baek SJ, Kim KS, Nixon JB, Wilson LC & Eling TE 2001 Cyclooxygenase inhibitors regulate the expression of a TGF-β superfamily member that has proapoptotic and antitumorigenic activities. *Molecular Pharmacology* **59** 901–908.

Baek SJ, Kim JS, Moore SM, Lee SH, Martinez J & Eling TE 2005 Cyclooxygenase inhibitors induce the expression of the tumor suppressor gene *EGR-1*, which results in the up-regulation of NAG-1, an antitumorigenic protein. *Molecular Pharmacology* **67** 356–364.

Bootcov MR, Bauskin AR, Valenzuela SM, Moore AG, Bansal M, He XY, Zhang HP, Donnellan M, Mahler S, Pryor K *et al.* 1997 MIC-1, a novel macrophage inhibitory cytokine, is a divergent member of the TGF-β superfamily. *PNAS* **94** 11514–11519.

Booth SL, Tucker KL, Chen H, Hannan MT, Gagnon DR, Cupples LA, Wilson PW, Ordovas J, Schaefer EJ, Dawson-Hughes B *et al.* 2000 Dietary vitamin K intakes are associated with hip fracture but not with bone mineral density in elderly men and women. *American Journal of Clinical Nutrition* **71** 1201–1208.

Bouras T, Southey MC, Chang AC, Reddel RR, Willhite D, Glynne R, Henderson MA, Armes JE & Venter DJ 2002 *Stanniocalcin 2* is an estrogen-responsive gene coexpressed with the estrogen receptor in human breast cancer. *Cancer Research* **62** 1289–1295.

Charpentier AH, Bednarek AK, Daniel RL, Hawkins KA, Laflin KJ, Gaddis S, MacLeod MC & Aldaz CM 2000 Effects of estrogen on global gene expression: identification of novel targets of estrogen action. *Cancer Research* **60** 5977–5983.

Diller L, Kassel J, Nelson CE, Gryka MA, Litwak G, Gebhardt M, Bressac B, Ozturk M, Baker SJ, Vogelstein B *et al.* 1990 p53 functions as a cell cycle control protein in osteosarcomas. *Molecular and Cellular Biology* **10** 5772–5781.

Elefteriou F, Ahn JD, Takeda S, Starbuck M, Yang X, Liu X, Kondo H, Richards WG, Bannon TW, Noda M *et al.* 2005 Leptin regulation of bone resorption by the sympathetic nervous system and CART. *Nature* **434** 514–520.

Filvaroff EH, Guillet S, Zlot C, Bao M, Ingle G, Steinmetz H, Hoeffel J, Bunting S, Ross J, Carano RA *et al.* 2002 Stanniocalcin 1 alters muscle and bone structure and function in transgenic mice. *Endocrinology* **143** 3681–3690.

Gagliardi AD, Kuo EY, Raulic S, Wagner GF & DiMattia GE 2005 Human stanniocalcin-2 exhibits potent growth-suppressive properties in transgenic mice independently of growth hormone and IGFs. *American Journal of Physiology. Endocrinology and Metabolism* **288** E92–E105.

Hromas R, Hufford M, Sutton J, Xu D, Li Y & Lu L 1997 PLAB, a novel placental bone morphogenetic protein. *Biochimica et Biophysica Acta* **1354** 40–44.

Ichikawa T, Horie-Inoue K, Ikeda K, Blumberg B & Inoue S 2006 Steroid and xenobiotic receptor SXR mediates vitamin K_2-activated transcription of extracellular matrix-related genes and collagen accumulation in osteoblastic cells. *Journal of Biological Chemistry* **281** 16927–16934.

Jiang WQ, Chang AC, Satoh M, Furuichi Y, Tam PP & Reddel RR 2000 The distribution of stanniocalcin 1 protein in fetal mouse tissues suggests a role in bone and muscle development. *Journal of Endocrinology* **165** 457–466.

Li PX, Wong J, Ayed A, Ngo D, Brade AM, Arrowsmith C, Austin RC & Klamut HJ 2000 Placental transforming growth factor-beta is a downstream mediator of the growth arrest and apoptotic response of tumor cells to DNA damage and p53 overexpression. *Journal of Biological Chemistry* **275** 20127–20135.

Luo G, Ducy P, McKee MD, Pinero GJ, Loyer E, Behringer RR & Karsenty G 1997 Spontaneous calcification of arteries and cartilage in mice lacking matrix GLA protein. *Nature* **386** 78–81.

Luo CW, Pisarska MD & Hsueh AJ 2005 Identification of a stanniocalcin paralog, stanniocalcin-2, in fish and the paracrine actions of stanniocalcin-2 in the mammalian ovary. *Endocrinology* **146** 469–476.

Ma Y, Pitson S, Hercus T, Murphy J, Lopez A & Woodcock J 2005 Sphingosine activates protein kinase A type II by a novel cAMP-independent mechanism. *Journal of Biological Chemistry* **280** 26011–26017.

Madsen KL, Tavernini MM, Yachimec C, Mendrick DL, Alfonso PJ, Buergin M, Olsen HS, Antonaccio MJ, Thomson AB & Fedorak RN 1998 Stanniocalcin: a novel protein regulating calcium and phosphate transport across mammalian intestine. *American Journal of Physiology* **274** G96–G102.

Masuda H, Miller C, Koeffler HP, Battifora H & Cline MJ 1987 Rearrangement of the *p53* gene in human osteogenic sarcomas. *PNAS* **84** 7716–7719.

Nazarova N, Qiao S, Golovko O, Lou YR & Tuohimaa P 2004 Calcitriol-induced prostate-derived factor: autocrine control of prostate cancer cell growth. *International Journal of Cancer* **112** 951–958.

Nishimoto SK & Price PA 1985 The vitamin K-dependent bone protein is accumulated within cultured osteosarcoma cells in the presence of the vitamin K antagonist warfarin. *Journal of Biological Chemistry* **260** 2832–2836.

Olsen HS, Cepeda MA, Zhang QQ, Rosen CA & Vozzolo BL 1996 Human stanniocalcin: a possible hormonal regulator of mineral metabolism. *PNAS* **93** 1792–1796.

Otsuka M, Kato N, Shao RX, Hoshida Y, Ijichi H, Koike Y, Taniguchi H, Moriyama M, Shiratori Y, Kawabe T *et al.* 2004 Vitamin K_2 inhibits the growth and invasiveness of hepatocellular carcinoma cells via protein kinase A activation. *Hepatology* **40** 243–251.

Paralkar VM, Vail AL, Grasser WA, Brown TA, Xu H, Vukicevic S, Ke HZ, Qi H, Owen TA & Thompson DD 1998 Cloning and characterization of a novel member of the transforming growth factor-β/bone morphogenetic protein family. *Journal of Biological Chemistry* **273** 13760–13767.

Schlittenhardt D, Schober A, Strelau J, Bonaterra GA, Schmiedt W, Unsicker K, Metz J & Kinscherf R 2004 Involvement of growth differentiation factor-15/macrophage inhibitory cytokine-1 (GDF-15/MIC-1) in oxLDL-induced apoptosis of human macrophages *in vitro* and in arteriosclerotic lesions. *Cell and Tissue Research* **318** 325–333.

Selvamurugan N, Pulumati MR, Tyson DR & Partridge NC 2000 Parathyroid hormone regulation of the rat collagenase-3 promoter by protein kinase A-dependent transactivation of core binding factor α1. *Journal of Biological Chemistry* **275** 5037–5042.

Shanahan CM & Weissberg PL 1998 Smooth muscle cell heterogeneity: patterns of gene expression in vascular smooth muscle cells *in vitro* and *in vivo*. *Arteriosclerosis, Thrombosis, and Vascular Biology* **18** 333–338.

Shim M & Eling TE 2005 Protein kinase C-dependent regulation of NAG-1/placental bone morphogenic protein/MIC-1 expression in LNCaP prostate carcinoma cells. *Journal of Biological Chemistry* **280** 18636–18642.

Shiraki M, Shiraki Y, Aoki C & Miura M 2000 Vitamin K_2 (menatetrenone) effectively prevents fractures and sustains lumbar bone mineral density in osteoporosis. *Journal of Bone and Mineral Research* **15** 515–521.

Tabb MM, Sun A, Zhou C, Grun F, Errandi J, Romero K, Pham H, Inoue S, Mallick S, Lin M *et al.* 2003 Vitamin K_2 regulation of bone homeostasis is mediated by the steroid and xenobiotic receptor SXR. *Journal of Biological Chemistry* **278** 43919–43927.

Tan M, Wang Y, Guan K & Sun Y 2000 PTGF-β, a type β transforming growth factor (TGF-β) superfamily member, is a *p53* target gene that inhibits tumor cell growth via TGF-β signaling pathway. *PNAS* **97** 109–114.

Thomas R, True LD, Lange PH & Vessella RL 2001 Placental bone morphogenetic protein (*PLAB*) gene expression in normal, pre-malignant and malignant human prostate: relation to tumor development and progression. *International Journal of Cancer* **93** 47–52.

Uldry M, Yang W, St-Pierre J, Lin J, Seale P & Spiegelman BM 2006 Complementary action of the PGC-1 coactivators in mitochondrial biogenesis and brown fat differentiation. *Cell Metabolism* **3** 333–341.

Varghese R, Gagliardi AD, Bialek PE, Yee SP, Wagner GF & Dimattia GE 2002 Overexpression of human stanniocalcin affects growth and reproduction in transgenic mice. *Endocrinology* **143** 868–876.

Vergnaud P, Garnero P, Meunier PJ, Breart G, Kamihagi K & Delmas PD 1997 Undercarboxylated osteocalcin measured with a specific immunoassay predicts hip fracture in elderly women: the EPIDOS Study. *Journal of Clinical Endocrinology and Metabolism* **82** 719–724.

Wagner GF, Vozzolo BL, Jaworski E, Haddad M, Kline RL, Olsen HS, Rosen CA, Davidson MB & Renfro JL 1997 Human stanniocalcin inhibits renal phosphate excretion in the rat. *Journal of Bone and Mineral Research* **12** 165–171.

Yamaguchi K, Lee SH, Eling TE & Baek SJ 2004 Identification of nonsteroidal anti-inflammatory drug-activated gene (*NAG-1*) as a novel downstream target of phosphatidylinositol 3-kinase/AKT/GSK-3beta pathway. *Journal of Biological Chemistry* **279** 49617–49623.

Yoshiko Y, Son A, Maeda S, Igarashi A, Takano S, Hu J & Maeda N 1999 Evidence for stanniocalcin gene expression in mammalian bone. *Endocrinology* **140** 1869–1874.

Yoshiko Y, Maeda N & Aubin JE 2003 Stanniocalcin 1 stimulates osteoblast differentiation in rat calvaria cell cultures. *Endocrinology* **144** 4134–4143.

Received in final form 28 June 2007
Accepted 30 July 2007
Made available online as an Accepted Preprint 2 August 2007

SPINE Volume 32, Number 1, pp 25–29
©2007, Lippincott Williams & Wilkins, Inc.

Q89R Polymorphism in the LDL Receptor-Related Protein 5 Gene Is Associated With Spinal Osteoarthritis in Postmenopausal Japanese Women

Tomohiko Urano, MD, PhD,* Masataka Shiraki, MD, PhD,† Ken'ichiro Narusawa, MD, PhD,‡ Takahiko Usui, MD,* Noriko Sasaki, BS,* Takayuki Hosoi, MD, PhD,§ Yasuyoshi Ouchi, MD, PhD,* Toshitaka Nakamura, MD, PhD,‡ and Satoshi Inoue, MD, PhD,*‖

Study Design. An association study investigating the genetic etiology for spinal osteoarthritis.

Objective. To determine the association of single-nucleotide polymorphism (SNP) causing an amino-acid change (Q89R) in the low-density lipoprotein receptor-related protein 5 (LRP5) coding region with spinal osteoarthritis.

Summary of Background Data. Wnt/β-catenin signaling pathway regulates bone density through a Wnt coreceptor LRP5. This pathway is also involved in cartilage development and homeostasis, suggesting that genetic variation in LRP5 gene may affect the pathogenesis of cartilage-related diseases, such as osteoarthritis.

Methods. We evaluated the presence of osteophytes, endplate sclerosis, and narrowing of disc spaces in 357 Japanese postmenopausal women. Missense coding SNP for Q89R of LRP5 gene was determined using TaqMan polymerase chain reaction (PCR) method.

Results. We found that subjects without the R allele (QQ; n = 321) had a significantly lower osteophyte formation score than did subjects bearing at least one R allele (QR + RR; n = 36) (7.80 *vs.* 10.89, $P = 0.0019$ by analysis of covariance).

Conclusions. We suggest that a genetic variation at the LRP5 gene locus is associated with spinal osteoarthritis, in line with the involvement of the LRP5 gene in the bone and cartilage metabolism.

Key words: single-nucleotide polymorphism (SNP), low-density lipoprotein receptor-related protein 5 (LRP5), spinal osteoarthritis, osteophytosis. **Spine 2007;32:25–29**

Osteoarthritis of the spine is a very common condition in the axial skeletons of aged people.[1] Vertebral osteophytes, endplate sclerosis, and intervertebral disc narrowing are recognized as characteristic features of spinal degeneration. Recent studies indicate that the appearance of these radiographic features is influenced by genetic factors, physical loading, and other environmental factors.[2,3] Association studies in using various definitions of osteoarthritis have been performed, mainly investigating genes encoding structural proteins of the extracellular matrix of cartilage (*e.g.*, collagen Type II α1, cartilage matrix protein, and aminoguanidine) or genes playing a role in the regulation of bone density and mass (*e.g.*, vitamin D receptor, insulin-like growth factor-I, and estrogen receptor α).[4,5]

The Wnt (wingless-type MMTV integration site family) represents a large group of secreted signaling proteins that are involved in cell proliferation, differentiation, and morphogenesis.[6] The name of "Wnt" is derived from wingless gene in *Drosophila melanogaster*[7] and murine int-1 oncogene identified in tumors induced by mouse mammary tumor virus.[8] It is also known that Wnt and bone morphogenetic protein (BMP) signals control apical ectodermal ridge formation and dorsal-ventral patterning during limb development.[9,10] Wnt proteins activate signal transduction through Frizzled, which act as receptors for Wnt proteins[11] and induce stabilization of cytoplasmic β-catenin protein, which also regulates target gene expression as a transcriptional coactivator. The physiologic role of Wnt in the regulation of osteoblastogenesis has been studied in experimental models, in embryonic mesenchymal progenitor cells expressing Wnt3a[12] or in mice expressing Wnt10b transgene in bone marrow.[13] It is also shown that activated β-catenin modulate osteoblast and chondrocyte differentiation.[14,15] Meanwhile, LDL receptor-related protein 5 and 6 (LRP5/6) were also found to be required for Wnt coreceptors.[16,17] Recent reports demonstrated that the Wnt/β-catenin signaling pathway regulates bone density through LRP5.[18–21] These findings indicate that Wnt-β-catenin signaling pathway plays important roles in the skeletal biology.

In addition to the regulation of limb development and bone metabolism, Wnt/β-catenin signaling may be involved in maintenance and pathophysiology of cartilage. This possibility is indirectly supported by the observation that several Wnt proteins and Frizzled receptors are expressed in synovial tissue of arthritic cartilage.[22] In addition, a secreted Frizzled-related protein (FrzB-2) that act as an antagonist for Frizzled receptor is strongly expressed in osteoarthritic cartilage and may regulate chondrocyte apoptosis.[23] It is also reported that chondrocytes express β-catenin at a low level and accumulation of β-catenin is sufficient to cause dedifferentiation of chondrocytes, suggesting that Wnt signaling is involved in cartilage metabolism.[24] Thus, it is assumed that LRP5 modulates Wnt/β-catenin signaling pathway in the bone and cartilage homeostasis. In the present study, we examine an association between a polymorphism in LRP5 gene and radiographic features of spinal osteoarthritis, including osteophyte formation, endplate sclerosis, and disc space narrowing number to investigate a possible contribution of LRP5 to human bone and cartilage metabolism.

From the *Department of Geriatric Medicine, Graduate School of Medicine, The University of Tokyo, Tokyo, Japan; †Research Institute and Practice for Involutional Diseases, Nagano, Japan; ‡Department of Orthopedic Surgery, University of Occupational and Environmental Health, School of Medicine, Kitakyushu, Japan; §Department of Advanced Medicine, National Center for Geriatrics and Gerontology, Aichi, Japan; and ‖Research Center for Genomic Medicine, Saitama Medical School, Saitama, Japan.

Acknowledgment date: October 28, 2005. First revision date: February 23, 2006. Acceptance date: March 2, 2006.

Supported in part by grants from the Japanese Ministry of Health, Labor, Welfare and Japan Society for the Promotion of Science and by a grant of the Genome Network Project from the Ministry of Culture, Education, Sports, Science and Technology of Japan.

The manuscript submitted does not contain information about medical device(s)/drug(s).

No funds were received in support of this work. No benefits in any form have been or will be received from a commercial party related directly or indirectly to the subject of this manuscript.

Address correspondence and reprint requests to Satoshi Inoue, MD, PhD, Department of Geriatric Medicine, Graduate School of Medicine, University of Tokyo, 7-3-1, Hongo, Bumkyo-ku, Tokyo, Japan; E-mail: INOUE-GER@h.u-tokyo.ac.jp

Copyright © Lippincott Williams & Wilkins. Unauthorized reproduction of this article is prohibited.

Materials and Methods

Subjects. Genotypes were analyzed in DNA sample obtained from 357 healthy postmenopausal Japanese women (mean age ± SD; 65.22 ± 8.20 years) living in central area of Japan. Exclusion criteria included endocrine disorders such as hyperthyroidism, hyperparathyroidism, diabetes mellitus, liver disease, renal disease, use of medications known to affect bone metabolism (*e.g.*, corticosteroids, anticonvulsants, heparin sodium), or unusual gynecologic history. Patients with severe hip and knee arthritis were excluded from the present study. The eligibility of subjects was determined by taking history-physical examination. All were nonrelated volunteers and provided informed consent before this study. Ethical approval for the study was obtained from appropriate ethics committees.

Radiographic Grading of Osteoarthritis of the Spine. Conventional thoracic and lumbar spinal plain roentgenograms in lateral and anteroposterior projection were obtained from all participants. The severities of spinal degeneration, including osteophyte formation, endplate sclerosis, and disc space narrowing, were assessed semiquantitatively from T4–T5 to L4–L5 disc level or from T4 to L5 vertebrae by using the grading scale of Yu *et al.*[25] Briefly, osteophyte formation at a given disc was graded 0° to 3°, endplate sclerosis at given vertebra was graded 0° to 2°, and disc space narrowing was graded 0° to 1°. Then we defined sum of each degree from T4–T5 to L4–L5 disc level for osteophyte formation on anteroposterior radiographs as a score of osteophyte formation. We also defined sum of each degree from T4 to L4 vertebra for endplate sclerosis and that from T4–T5 to L4–L5 disc level for disc space narrowing on lateral radiographs as a score of endplate sclerosis and disc narrowing, respectively. Then we defined sum of each 13 grade for osteophyte formation on anteroposterior radiographs as a score of osteophyte formation. We also defined sum of 13 grade for endplate sclerosis and disc space narrowing on lateral radiographs as a score of endplate sclerosis and disc narrowing, respectively.

Measurement of Bone Mineral Density (BMD) and Biochemical Markers. The lumbar spine BMD and total body BMD (in g/cm^2) of each participant were measured by dual-energy radiograph absorptiometry using fast-scan mode (DPX-L; Lunar, Madison, WI). The BMD data were recorded as "Z scores," that is, deviation from the weight-adjusted average BMD for each age. Z scores were calculated using installed software (Lunar DPX-L) on the basis of data from 20,000 Japanese women.

We measured serum concentration of calcium (Ca), phosphate (P), alkaline phosphatase (ALP), intact-osteocalcin (I-OC, ELISA; Teijin, Tokyo, Japan), intact parathyroid hormone (PTH), calcitonin (CT), and 1, 25(OH)2D3. We also measured urinary ratios of urinary deoxypyridinoline (DPD, HPLC method) to creatinine.

Determination of a Single Nucleotide Polymorphism in the LRP5 Gene. DNA was extracted from peripheral leukocytes by standard techniques. Missense coding SNP for Q89R (c. 266A>G) of the LRP5 gene was determined using Assays by Design SNP Genotyping Products (Applied BioSystems) that based on the TaqMan PCR method.[26] Missense coding means that the alteration of a codon (an array of three consecutive bases in mRNA) that encodes a different amino acid. TaqMan PCR method uses two kinds of TaqMan probes that correspond to a DNA fragment including the target SNP site with different alleles and the 5′–3′ nuclease activity of Taq polymerase that is essential for PCR. TaqMan probes include fluorescence dyes at their 5′ ends and a quencher at their 3′ ends. During PCR cycles, TaqMan probes will anneal to target DNA and will be excised by the 5′–3′ nuclease activity of Taq polymerase if there is no mismatch between the probes and target sequences. Then the fluorescence dyes will be released from the probes and the intensity of fluorescence can be monitored by using ABI PRISM 7000 (Applied Biosystems) as a fluorescence detector. The allele frequencies of Q89R polymorphism were confirmed as they were not significantly deviated from Hardy-Weinberg equilibrium. Since Hardy-Weinberg equilibrium is based on the following assumptions including no genetic drift, no gene flow, no natural selection, negligible mutations, and random mating, the population under the equilibrium is not evolving and its genotype and allele frequencies are predicted to remain unchanged over successive generations. Thus, we considered that our subjects were eligible for the correlation study.

Statistical Analysis. We divided subjects into those having one or two chromosomes of the minor G-allele (QR + RR) and those with only the major A-allele (QQ) encoded at the same locus. Comparisons of Z scores of lumbar spine and biochemical markers between these two groups were subjected to statistical analysis (unpaired *t* test; StatView-J 4.5, SAS Institute Inc.). The association between these two groups and osteoarthritis parameters (number of osteophyte, endoplate sclerosis, and disc narrowing) was assessed by unpaired *t* test and by analysis of covariance (ANCOVA) with adjustment of confounding clinical variables (age, body weight, and height). A P value less than 0.05 was considered statistically significant.

Results

We analyzed the genotypes for the SNP of LRP5 at Q89R (c.266 A>G) in subjects, using TaqMan methods. Among 357 postmenopausal Japanese women, 321 were QQ homozygotes, 35 were QR heterozygotes, and 1 was RR homozygote. The allelic frequencies of this SNP in the present study were in Hardy-Weinberg equilibrium.

Because only 1 of these subjects carried the RR genotype of the Q89R polymorphism, we compared those who carried the R allele (QR or RR) with those who did

Copyright © Lippincott Williams & Wilkins. Unauthorized reproduction of this article is prohibited.

Table 1. Comparison of Background, Clinical Characteristics Between Subjects Bearing at Least 1 R allele (QR + RR) and Subjects With No R allele (QQ) in the *LRP5 Gene Coding Region* (Q89R)

Item	Genotype (mean ± SD) QQ	QR + RR	P
No. of subjects	321	36	
Age (yr)	65.0 ± 8.2	67.3 ± 8.0	NS
Height (cm)	150.7 ± 5.7	151.1 ± 7.1	NS
Body weight (kg)	50.5 ± 7.6	51.3 ± 7.9	NS
Lumber spine BMD (Z score)	−0.28 ± 1.40	−0.17 ± 1.89	NS
ALP (IU/L)	190.8 ± 61.3	194.8 ± 81.1	NS
I-OC (ng/mL)	8.2 ± 4.0	7.4 ± 3.0	NS
DPD (pmol/μmol of Cr)	7.6 ± 4.0	7.6 ± 2.3	NS
Intact PTH (pg/mL)	35.6 ± 16.7	34.6 ± 14.1	NS
1,25 $(OH)_2D_3$ (pg/mL)	36.1 ± 10.8	37.3 ± 14.6	NS
BMI	22.1 ± 3.0	22.8 ± 3.1	NS

BMD indicates bone mineral density; ALP, alkaline phosphatase; I-OC, intact-osteocalcin; DPD, deoxypyridinoline; PTH, parathyroid hormone; BMI, body mass index; NS, not significant. Statistical analysis was performed according to the method described in the text.

not (QQ). The lumbar BMD was not statistically different between these groups (Table 1). The background and biochemical data were not statistically different between these groups (Table 1). On ANCOVA analysis, we found significant associations between LRP5 Q89R genotype and osteophyte formation score after controlling for age, weight, and height. Women without the R allele (QQ; n = 321) had a significantly lower osteophyte formation score than did subjects bearing at least one R allele (QR + RR; n = 36) (7.80 ± 6.51 *vs.* 10.89 ± 7.6, $P = 0.0019$, Figure 1A; Table 2). We also found significant association between them on unpaired *t* test ($P = 0.0083$, Table 1). On the other hand, the occurrence of disc narrowing and endplate sclerosis did not significantly differ in those with and without at least one R allele (Figure 1B, C; Table 2).

Table 2. Association of the *LRP5* SNP Genotype

Item	Genotype (mean ± SD) QQ	QR + RR	P (unpaired *t* test)	P (ANCOVA)
No. of subjects	321	36		
Osteophyte formation score	7.80 ± 6.51	10.89 ± 7.6	0.0083	0.0019
Endoplate sclerosis score	0.368 ± 0.845	0.389 ± 0.994	NS	NS
Disc space narrowing score	2.03 ± 1.88	2.06 ± 1.84	NS	NS

ANCOVA indicates analysis of covariance; NS, not significant.

■ Discussion

The present study is the first report that shows the influence of a single-nucleotide polymorphism of LRP5 gene on spinal osteoarthritis as far as we know. Targeting the pathogenesis of low back pain, we have previously investigated associations of genetic factors with osteoporosis. LRP5 has been shown as one of the correlated genes in Japanese postmenopausal women.[27] Because spinal osteoarthritis is another major reason for low back pain, we have extended our association study of LRP5 polymorphism with spinal osteoarthritis. We demonstrated that the Japanese postmenopausal women who had one or two allele(s) of a nonsynonymous change (Q89R) in LRP5 gene showed significantly higher osteophyte formation score of spine. Our finding may also be supported by genome-wide scan for osteoarthritis-susceptibility loci that showed a linkage to chromosome 11q12-13,[28,29] which includes the LRP5 gene locus on 11q13.4. It has been recently shown that single-nucleotide polymorphisms in LRP5 gene provided no correlation with knee osteoarthritis status while haplotype analysis revealed that there was a common haplotype that provided a 1.6-fold increased risk,[30] suggesting that LRP5 might be involved in the pathogenesis of osteoarthritis also in other joints. It is also reported that there was a significant association of a functional gene variant of secreted frizzled-related protein 3 (sFRP3), which antagonizes Wnt signaling, with hip osteoarthritis in women.[31] Taken together, our results and the recent evidence suggest that the canonical Wnt signaling pathway including LRP5 is critical in the pathogenesis of skeletal abnormality, including osteoarthritis and osteoporosis.

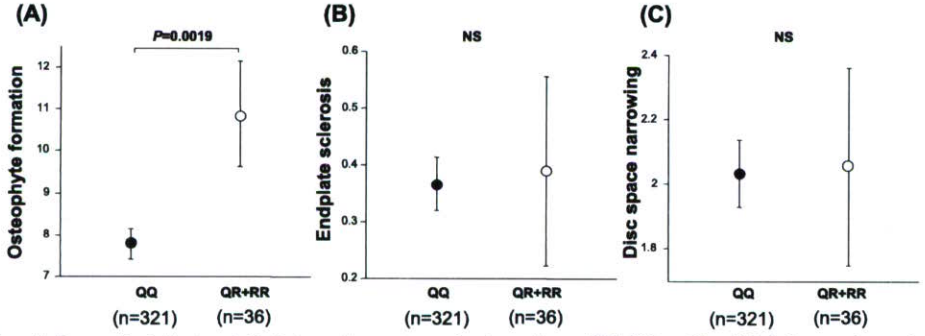

Figure 1. Scores of spinal osteoarthritis between the genotypes of polymorphism at Q89R (QQ *vs.* QR + RR). **A**, Scores of osteophyte formation are shown for genotype QQ and for genotype QR + RR. Scores are expressed as mean ± SE. Numbers of subjects are shown in parentheses. **B**, Scores of endplate sclerosis. **C**, Disc space narrowing scores. The association of the two genotype groups with osteoarthritis parameters was determined by ANCOVA, a type of multifactorial analysis, with adjustment of confounding clinical variables (age, body weight, and height).

Copyright © Lippincott Williams & Wilkins. Unauthorized reproduction of this article is prohibited.

Recently, mutations of the LRP5 gene have been described to be associated with both osteoporosis-pseudoglioma syndrome and the high bone mass phenotype.[18–21] It was found that loss-of-function of LRP5 in both human[18] and mice[19] yielded a decrease in bone formation, or an active mutation of LRP5 that cannot bind to a Wnt inhibitor Dickkopf-1 resulted in a high bone mass trait.[20,21] Moreover, our group and several other groups have reported that single-nucleotide polymorphisms in LRP5 gene predicted the bone mass.[27,32–36] These SNPs included three of different missense variations; Q89R,[33,34] V667 M,[35] and A1330V.[36] In the present study, we investigated a possible contribution of Q89R LRP5 polymorphism to spinal osteoarthritis in Japanese women. V667 M polymorphism was not detected in our Japanese population. Regarding A1330V polymorphism, we could not detect an association of the SNP with spinal osteoarthritis (data not shown).

Two groups reported consistent association of Q89R with Ward's triangle BMD but not with lumbar BMD in Korean young men[33] and Chinese premenopausal women.[34] In our Japanese population, we did not find an association of Q89R polymorphism with lumbar spine. The present data together with published data related to osteoporosis suggest that Q89R polymorphism may be involved in the pathogenesis of both osteoporosis and spinal osteoarthritis and QQ genotype in LRP5 might be preventive for both diseases. Meanwhile, there are other cases in which genetic factors contribute to the pathogenesis of osteoporosis and osteoarthritis in an opposite way. For example, it has been reported that transforming growth factor-β1 (TGF-β1) gene polymorphism T869C, which gives Leu>Pro substitution contributes differentially to osteoporosis and osteoarthritis; people with CC genotype had significantly higher BMD than those with TC or TT, whereas this CC genotype was related to significantly greater osteophytes than TT or TC.[37]

Osteoarthritis occurs as result of both mechanical and biologic events that destabilize the normal coupling of degradation and synthesis of articular cartilage chondrocytes and extracellular matrix as well as subchondral bone.[1,38] Cartilage destruction during osteoarthritis involves the loss of differentiated phenotype and apoptotic death of chondrocytes,[39] Wnt proteins were shown to regulate dedifferentiation of apoptosis of chondrocytes.[40] It is also demonstrated the interaction of β-catenin with SOX9, a transcriptional factor that is required in successive steps of chondrogenesis, controls chondrocyte differentiation.[41] These data suggest Wnt/β-catenin may participate in the pathogenesis of cartilage diseases, such as osteoarthritis. Further studies will be required to clarify the role of Q89R missense variant of the LRP5 in the pathogenesis of osteophyte formation and osteoporosis.

■ Conclusion

We have shown an association of the Q89R polymorphism in the LRP5 gene with a radiographic feature of spinal osteophytosis in postmenopausal Japanese women. The women with QQ genotypes had significantly lower osteophyte formation scores. The LRP5 genotyping might be beneficial in the prevention and management of spinal osteophytosis as well as osteoporosis. The present findings regarding the correlation of LRP5 polymorphism with spinal osteoarthritis provide a new promising direction for the clinical medicine of the spine disease, which leads us to the development of new diagnostic markers as well as therapeutic options based on the molecular target.

■ Key Points

- **Wnt/β-catenin signaling pathway regulates bone and cartilage metabolism.**
- **The single-nucleotide polymorphism, causing an amino-acid change (Q89R) in LRP5 gene that encodes a Wnt coreceptor, was associated with spinal osteophytosis in Japanese postmenopausal women.**
- **We suggest that a genetic variation at the LRP5 gene locus is associated with spinal osteoarthritis.**

References

1. Creamer P, Hochberg MC. Osteoarthritis. *Lancet* 1997;350:503–8.
2. Lane NE, Nevitt MC, Hochberg MC, et al. Reliability of new indices of radiographic osteoarthritis of the hand and hip and lumbar disc degeneration. *J Rheumatol* 1993;20:1911–8.
3. O'Neill TW, McCloskey EV, Silman AJ, et al. The distribution, determinants, and clinical correlates of vertebral osteophytosis: a population based survey. *J Rheumatol* 1999;26:842–8.
4. Spector TD, MacGregor AJ. Risk factors for osteoarthritis: genetics. *Osteoarthritis Cartilage* 2004;12(suppl):39–44.
5. Loughlin J. Genetics of osteoarthritis and potential for drug development. *Curr Opin Pharmacol* 2003;3:295–9.
6. Nusse R, Varmus HE. Wnt genes. *Cell* 1992;69:1073–87.
7. Rijsewijk F, Schuermann M, Wagenaar E, et al. The Drosophila homolog of the mouse mammary oncogene int-1 is identical to the segment polarity gene wingless. *Cell* 1987;50:649–57.
8. Nusse R, Varmus HE. Many tumors induced by the mouse mammary tumor virus contain a provirus integrated in the same region of the host genome. *Cell* 1982;31:99–109.
9. Barrow JR, Thomas KR, Boussadia-Zahui O, et al. Ectodermal Wnt3/beta-catenin signaling is required for the establishment and maintenance of the apical ectodermal ridge. *Genes Dev* 2003;17:394–409.
10. Soshnikova N, Zechner D, Huelsken J, et al. Genetic interaction between Wnt/beta-catenin and BMP receptor signaling during formation of the AER and the dorsal-ventral axis in the limb. *Genes Dev* 2003;17:1963–8.
11. Cadigan KM, Nusse R. Wnt signaling: a common theme in animal development. *Genes Dev* 1999;11:3286–305.
12. Derfoul A, Carlberg AL, Tuan RS, et al. Differential regulation of osteogenic marker gene expression by Wnt-3a in embryonic mesenchymal multipotential progenitor cells. *Differentiation* 2004;72:209–23.

Copyright © Lippincott Williams & Wilkins. Unauthorized reproduction of this article is prohibited.